

QCD for (future) hadron colliders

ICTP Summer School

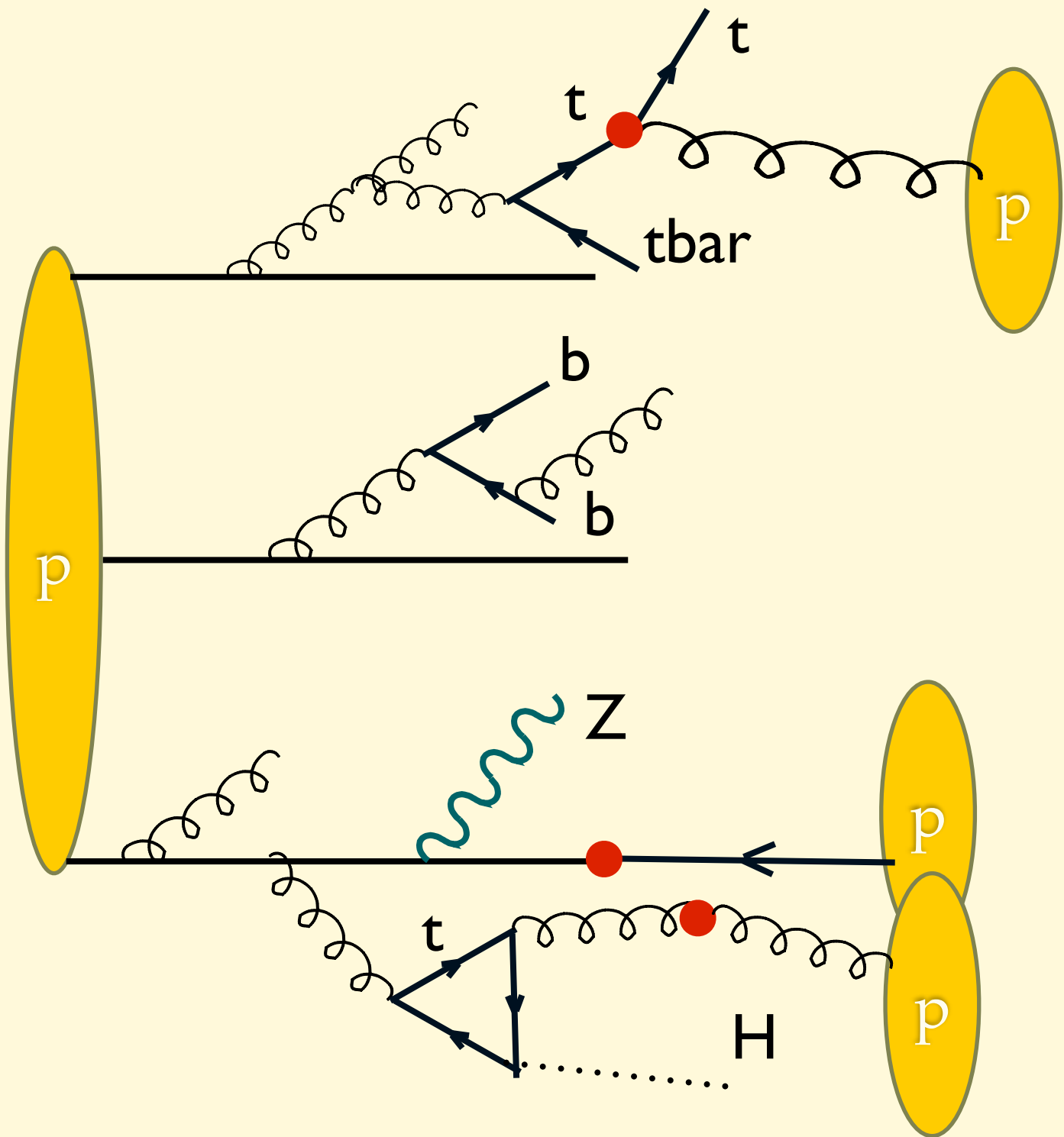
June 15- 26 2015

Lecture 3

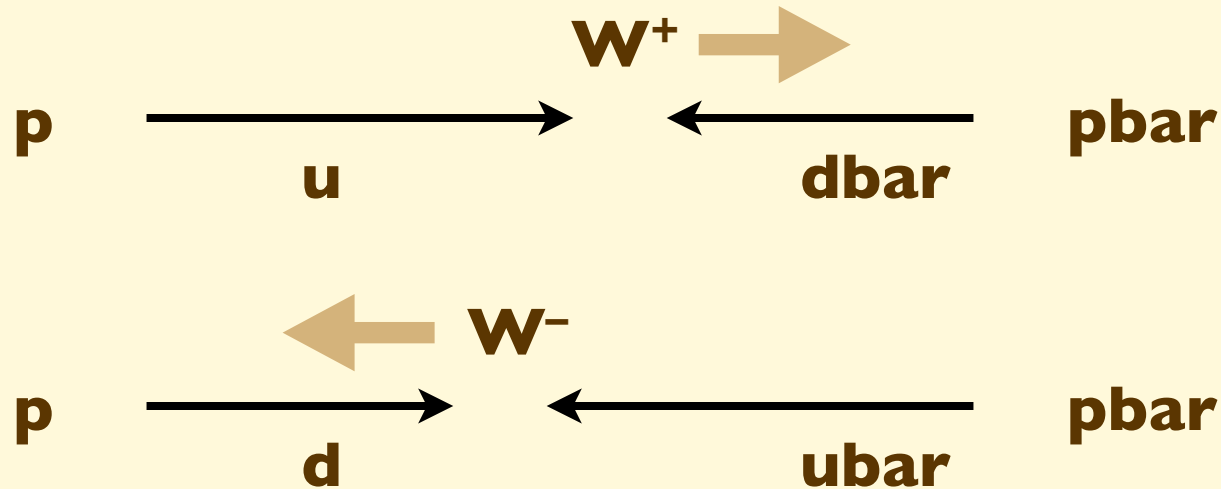
Michelangelo L. Mangano

TH Unit, Physics Department, CERN

michelangelo.mangano@cern.ch



W rapidity asymmetry in p-pbar



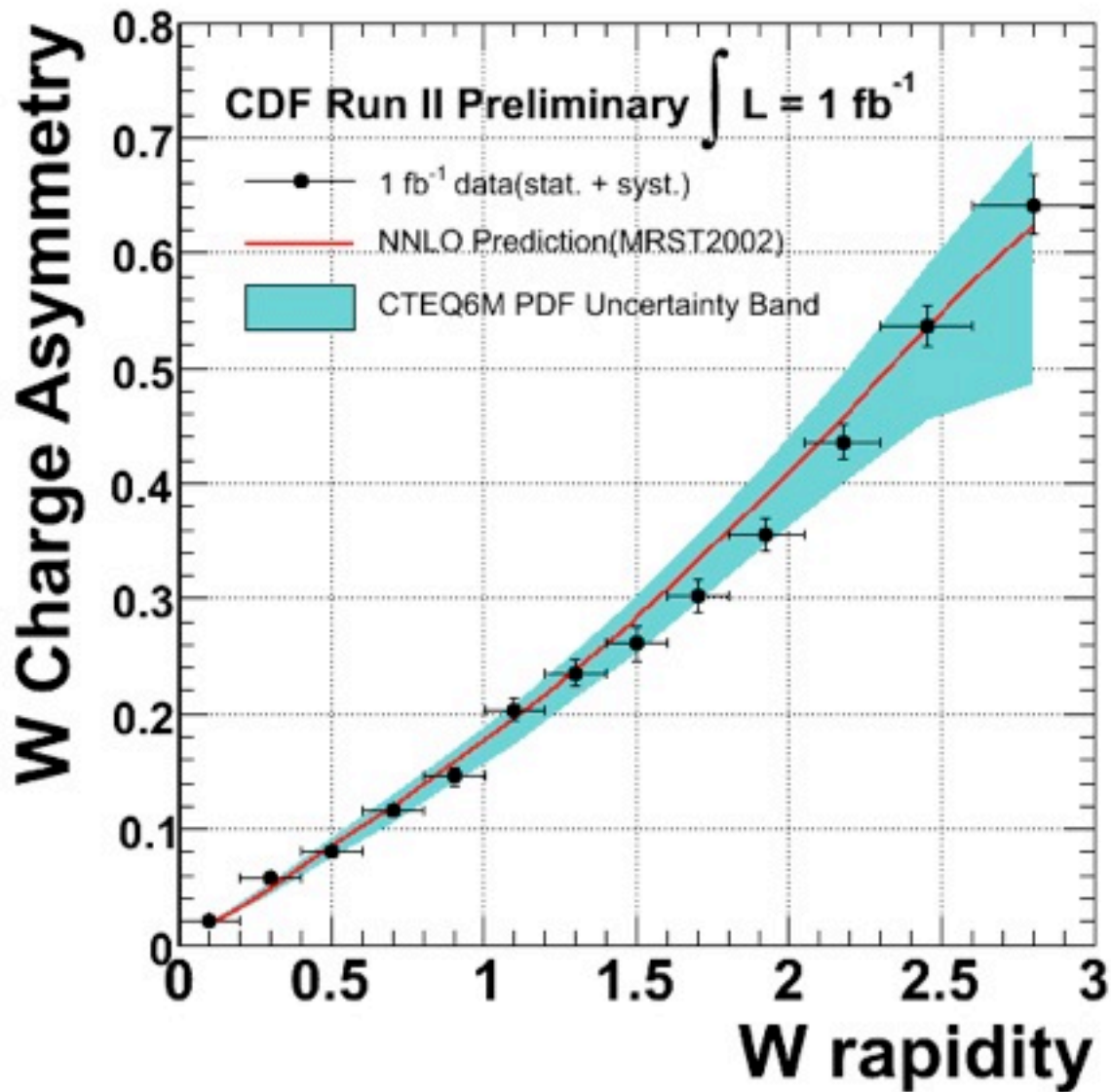
$$\frac{d\sigma_{W^+}}{dy} \propto f_u^P(x_1) f_{\bar{d}}^{\bar{P}}(x_2) + f_{\bar{d}}^P(x_1) f_u^{\bar{P}}(x_2)$$

$$\frac{d\sigma_{W^-}}{dy} \propto f_{\bar{u}}^P(x_1) f_d^{\bar{P}}(x_2) + f_d^P(x_1) f_{\bar{u}}^{\bar{P}}(x_2)$$

(Assuming dominance of valence contributions)

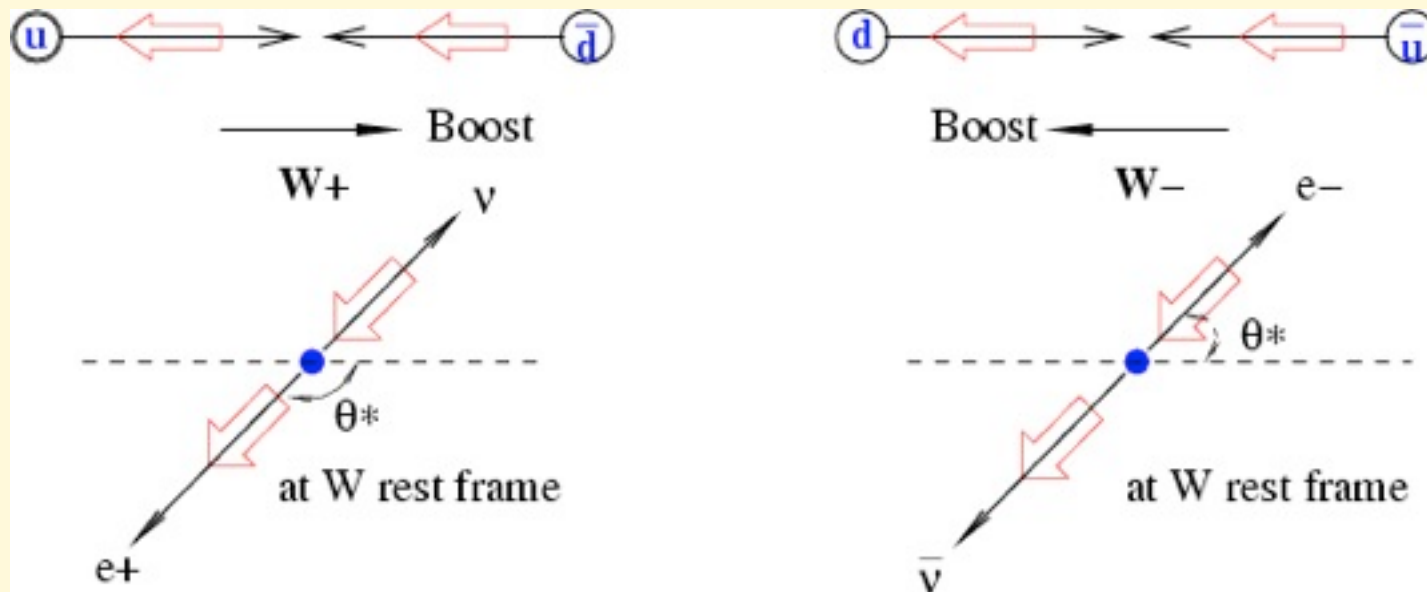
$$f_d(x) = f_u(x) R(x)$$

$$A(y) = \frac{\frac{d\sigma_{W^+}}{dy} - \frac{d\sigma_{W^-}}{dy}}{\frac{d\sigma_{W^+}}{dy} + \frac{d\sigma_{W^-}}{dy}} = \frac{f_u^P(x_1) f_d^P(x_2) - f_d^P(x_1) f_u^P(x_2)}{f_u^P(x_1) f_d^P(x_2) + f_d^P(x_1) f_u^P(x_2)} = \frac{R(x_2) - R(x_1)}{R(x_2) + R(x_1)}$$



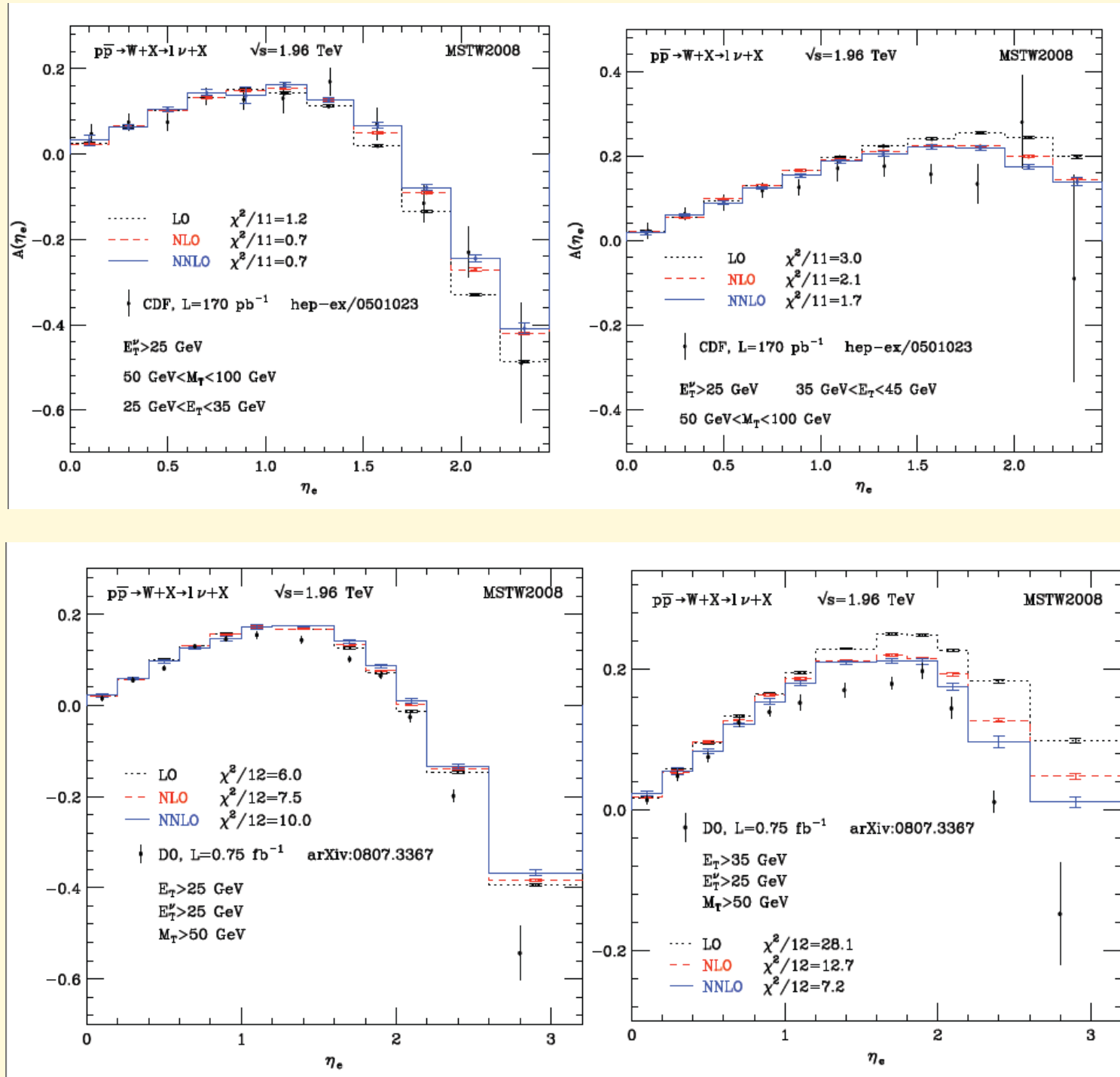
Run II comparison of W charge asymmetry with current PDF parameterizations

Lepton charge asymmetry in W production

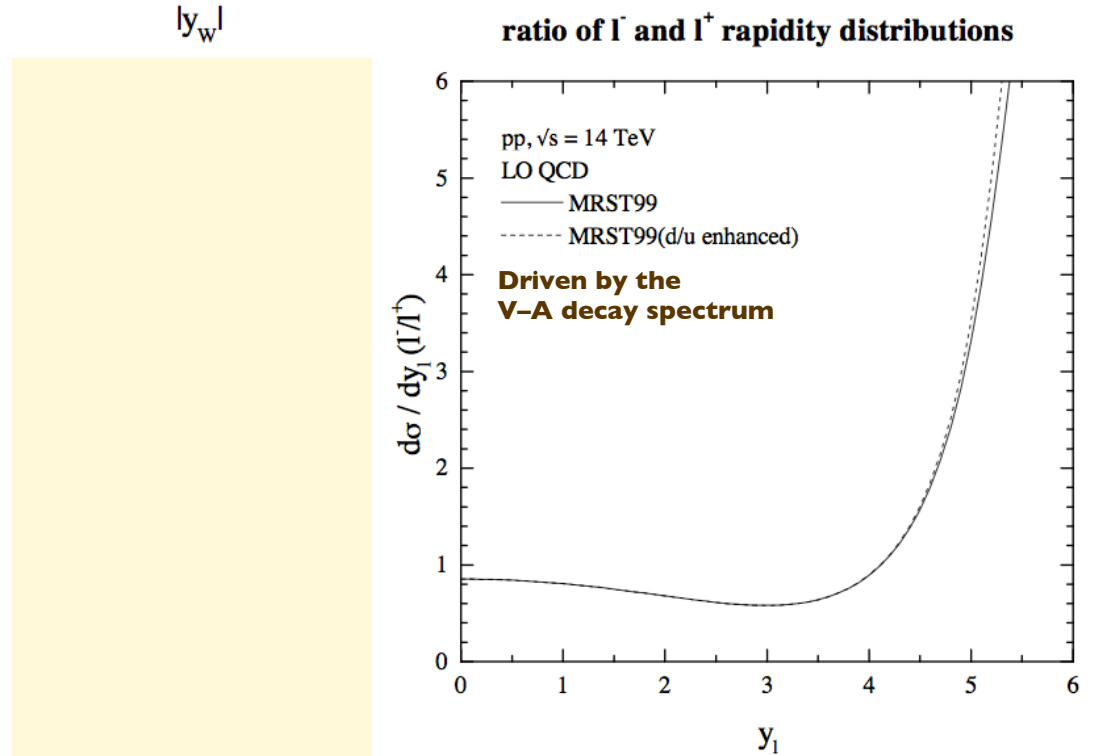
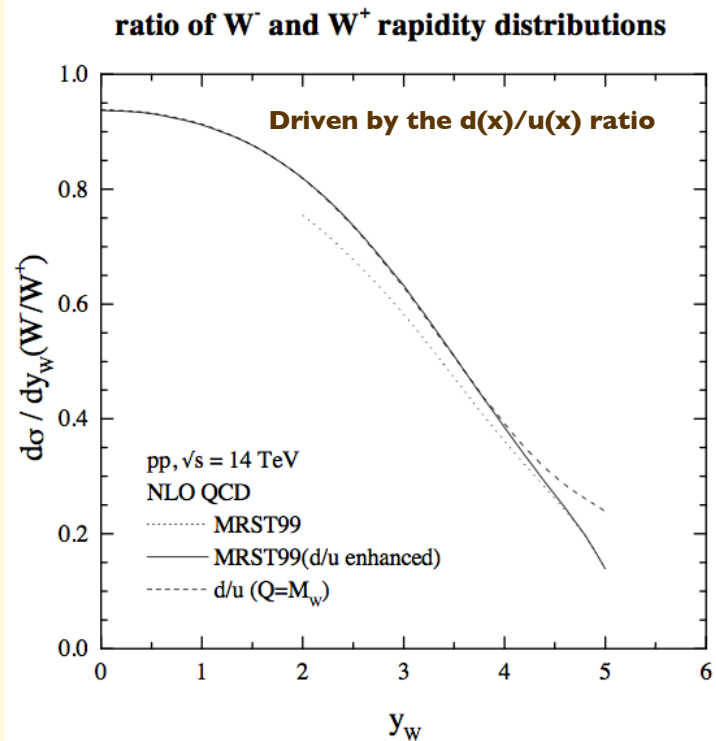
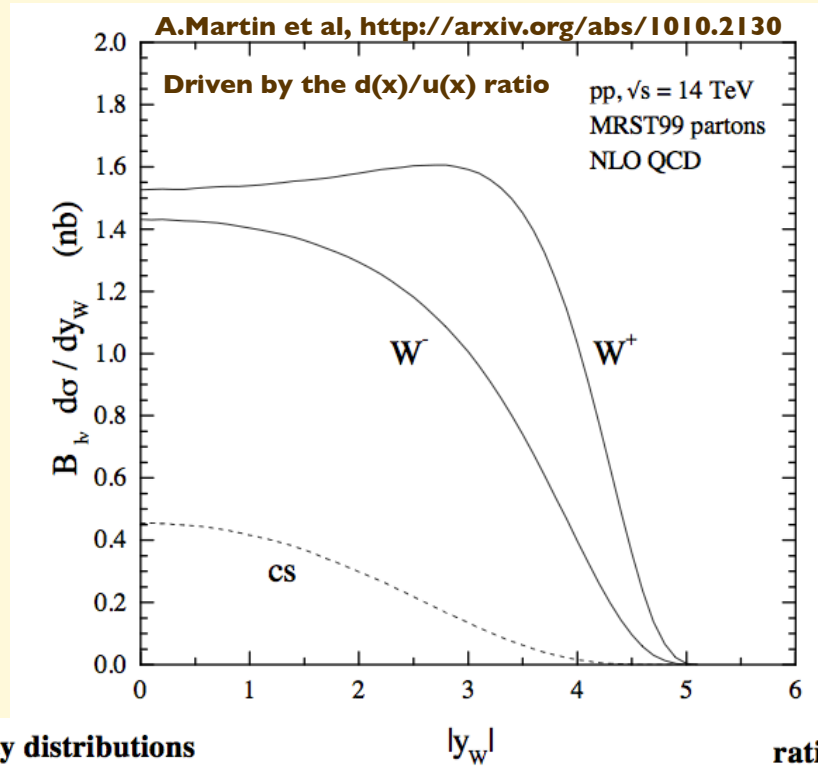


While the W^+ prefers to go in the u -quark direction, the emerging e^+ prefers to go backward. The competition between these two effects leads to a non-trivial structure in the lepton charge asymmetry distribution!

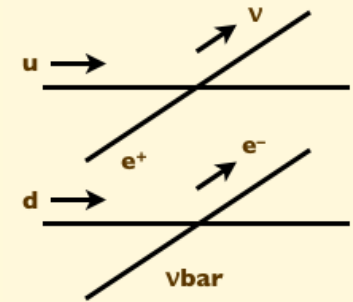
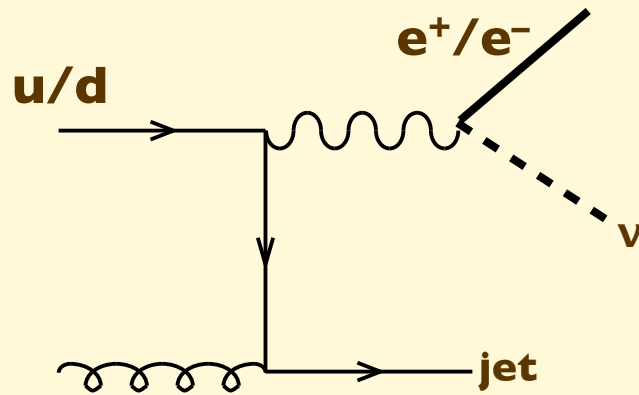
Lepton rapidity charge-asymmetry in W production at the Tevatron



W+ / W- production asymmetries in pp collisions

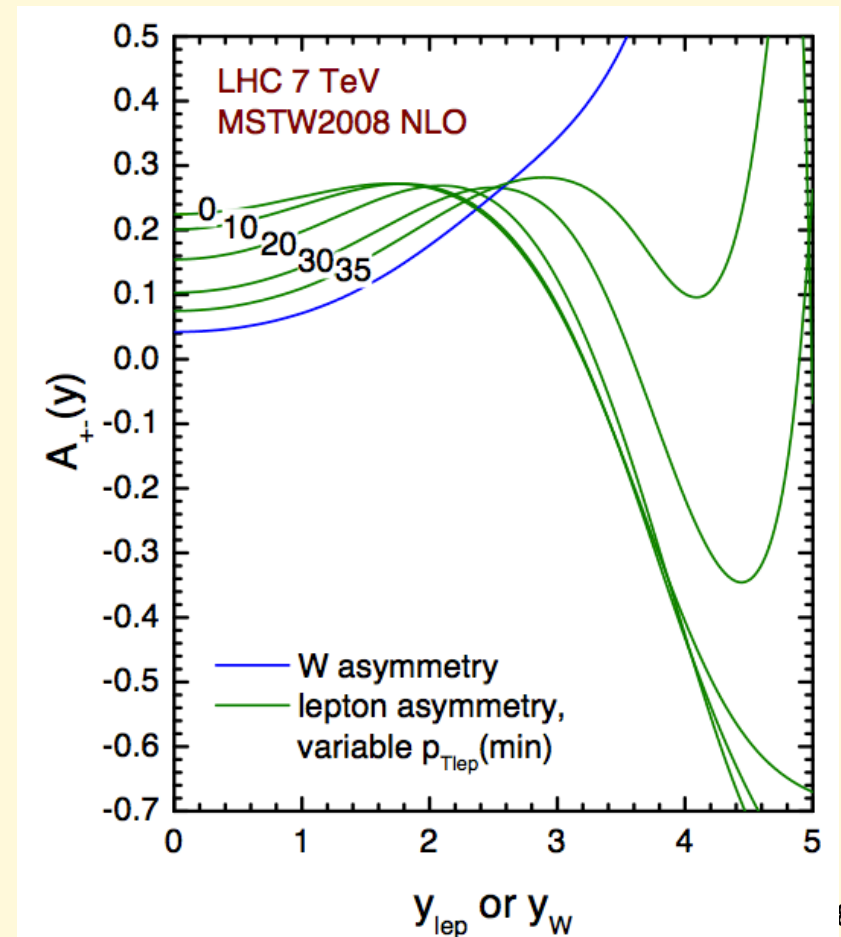


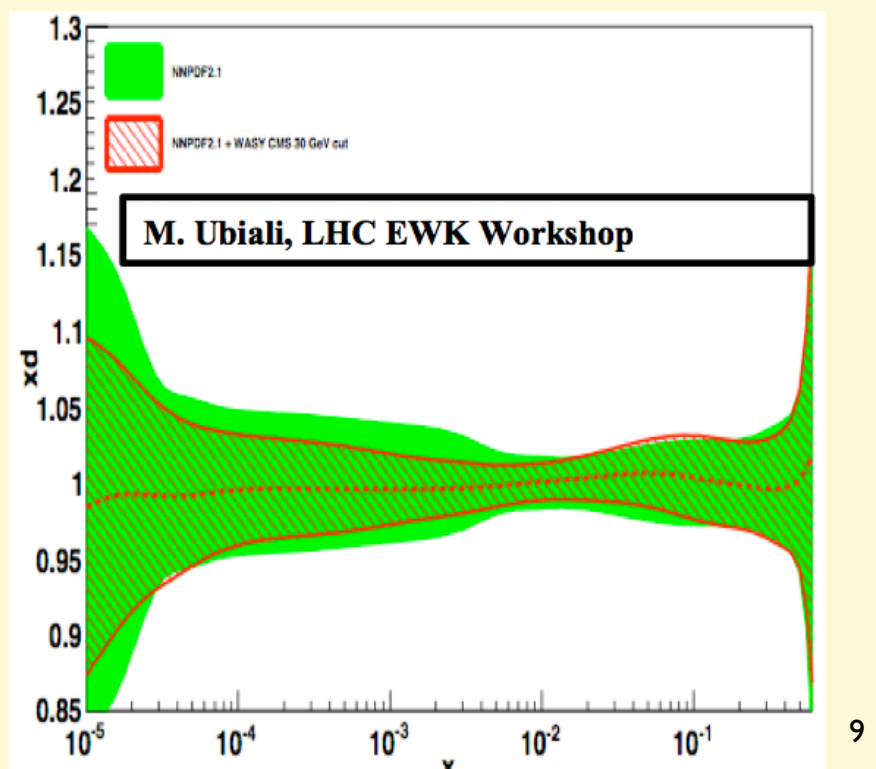
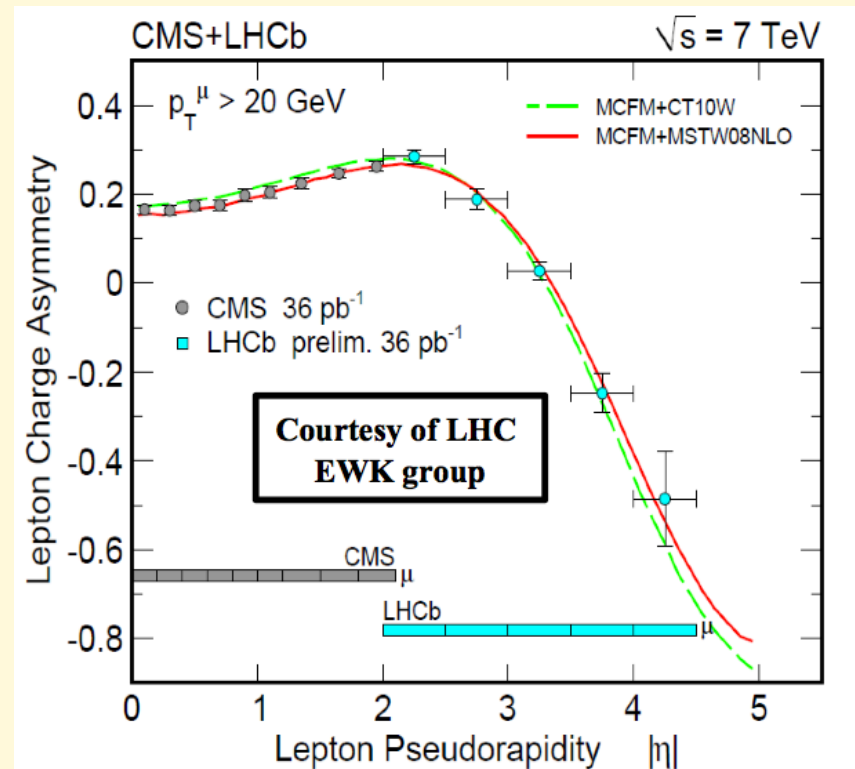
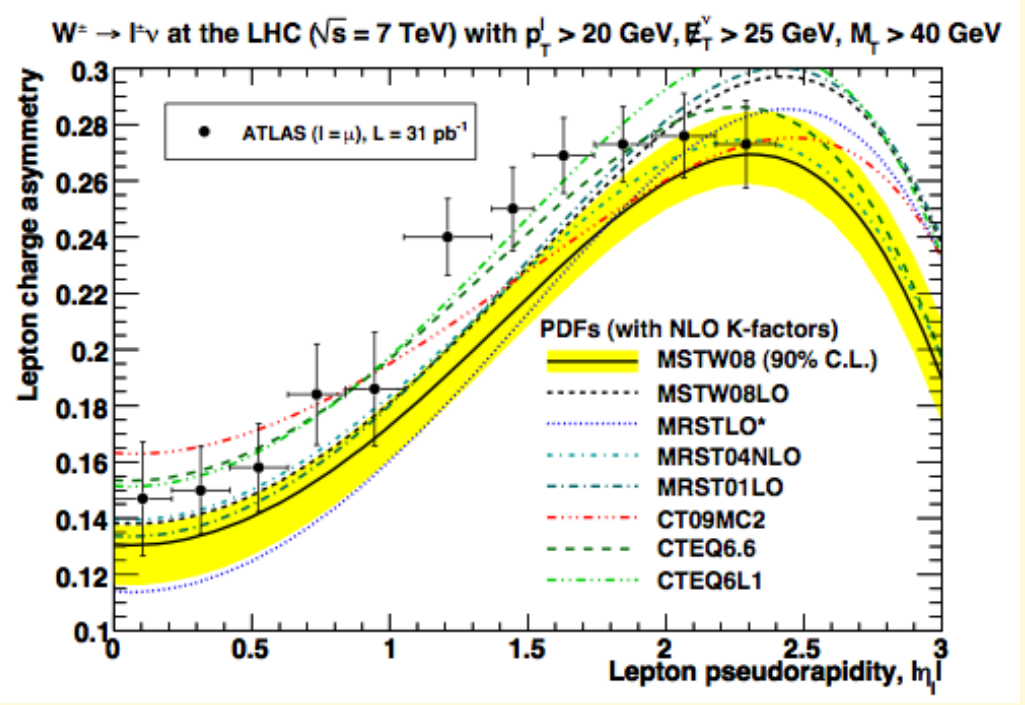
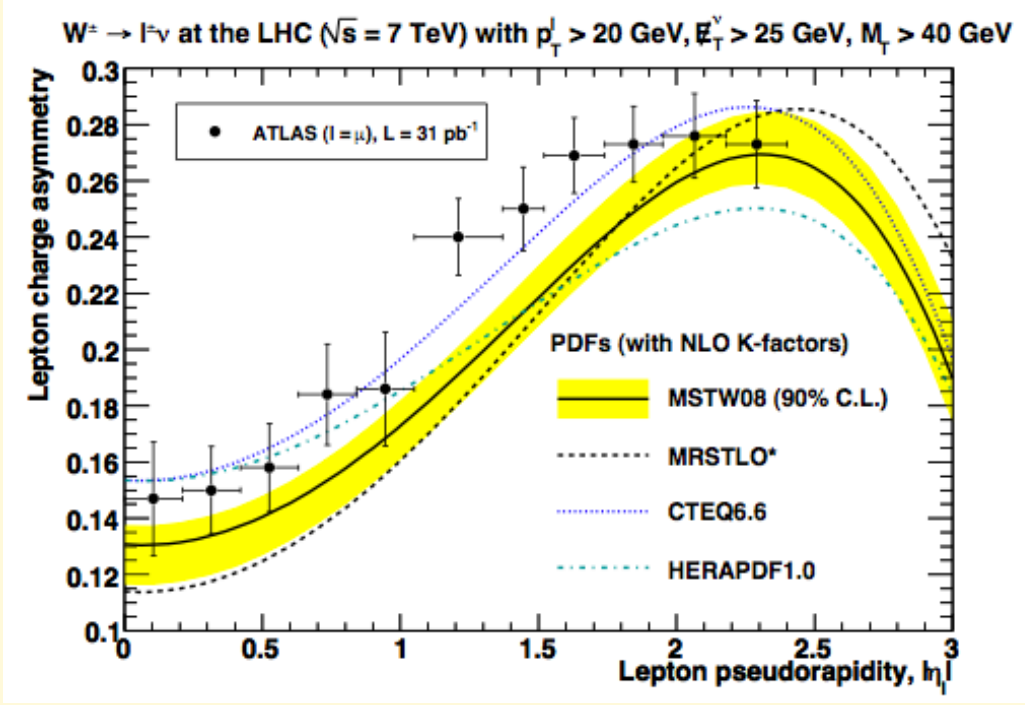
W charge asymmetry at large lepton pt



At large p_t this diagram dominates.
 V-A does not align the lepton with the IS quark, so u/d asymmetry dominates over V-A effects, which cause the bend over of the asymmetry at small $p_t W$

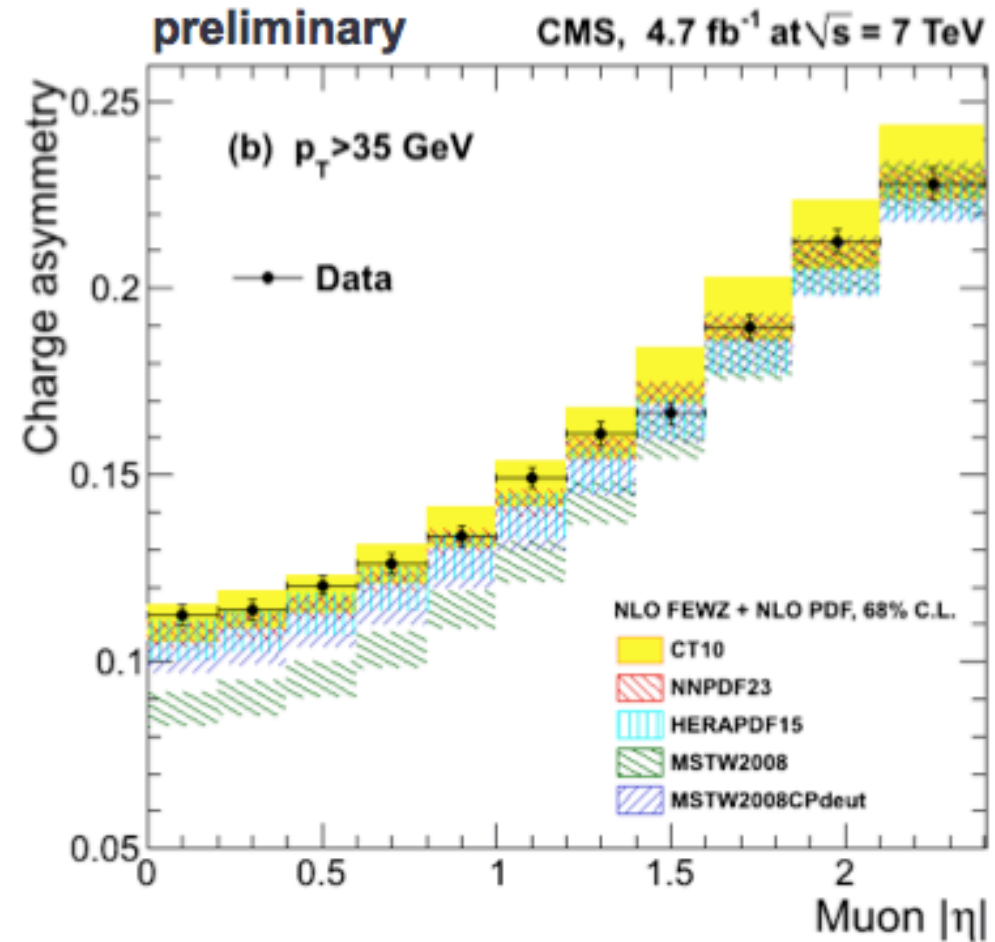
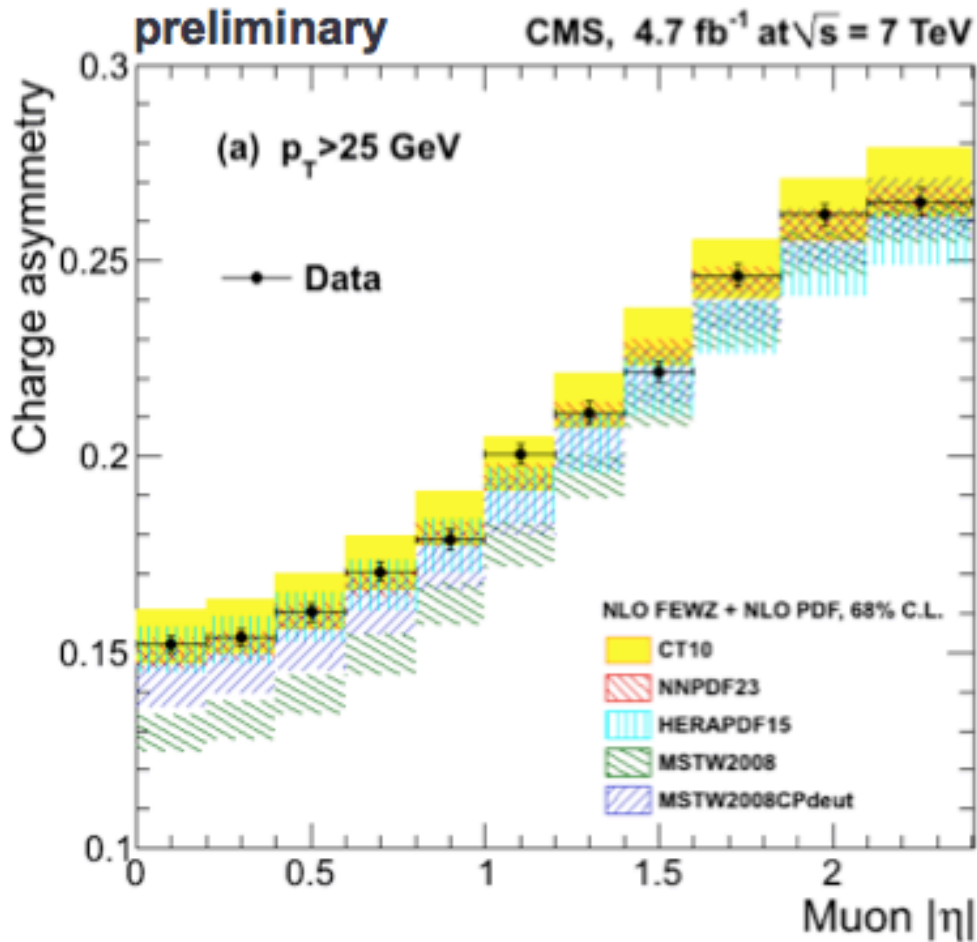
⇒ push the measurement to large p_t
 ⇒ also consider large- p_t and large-MET,
 to probe large x values





There is still room to further constrain PDF distributions relevant for W/Z production properties.

CMS-PAS-SMP-12-021



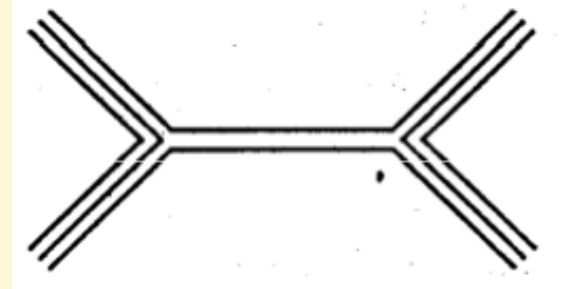
Questions:

- How do we convince ourselves that we are actually fitting the PDFs, and not missing higher-order QCD or EW effects in the matrix elements?

an example from the past ...

The presence of a quark substructure would manifest itself via contact interactions (as in Fermi's theory of weak interactions). On one side these new interactions would lead to an increase in cross-section, on the other they would affect the jets' angular distributions. In the dijet CMF, QCD implies Rutherford law, and extra point-like interactions can then be isolated using a fit.

Eichten, Lane, Peskin,
Phys.Rev.Lett. 50
 (1983) 811-814



From the supercollider-bible of the 80's,

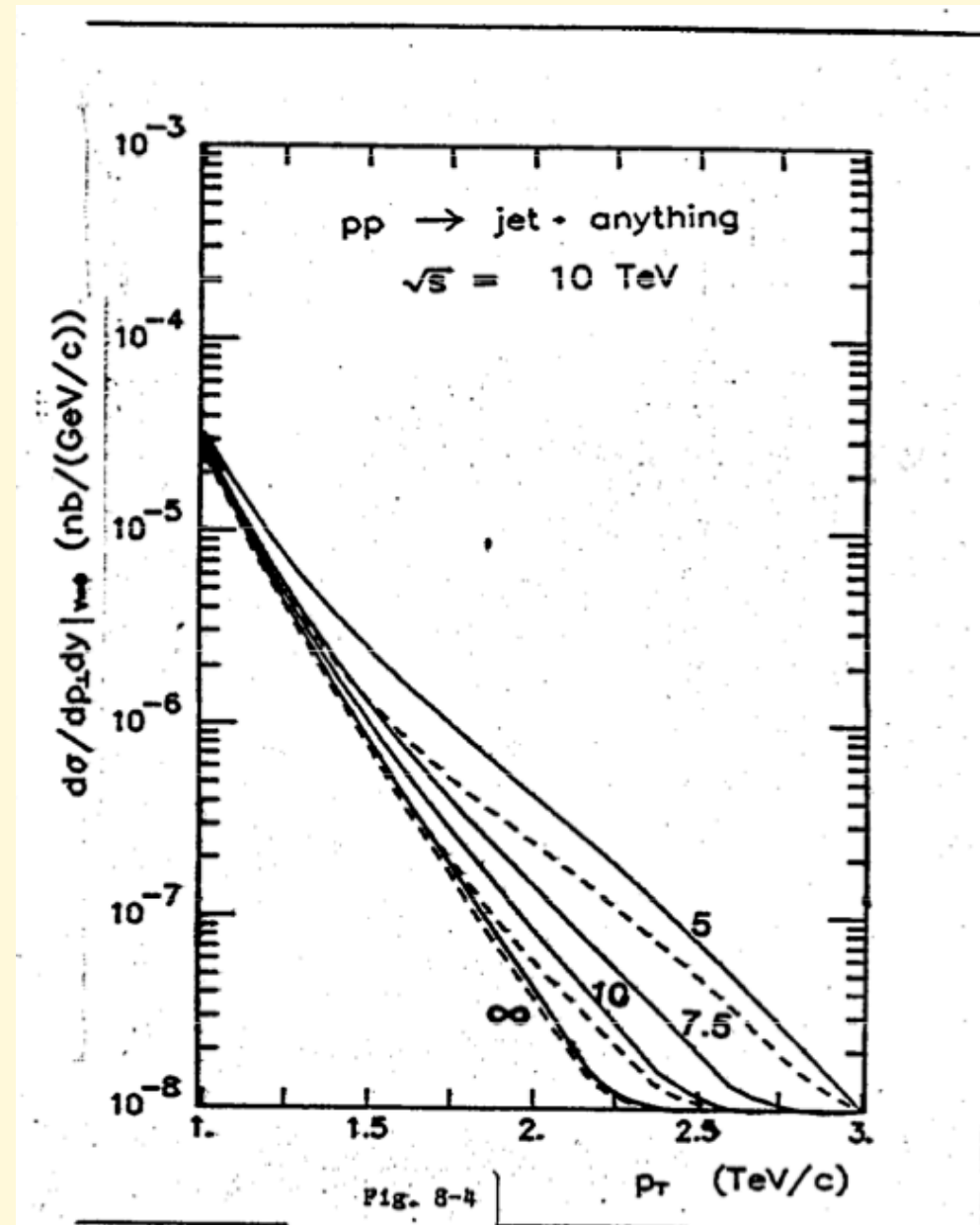
EHLQ (Eichten, Hinchliffe, Lane, Quigg):
 "Supercollider Physics", *Rev.Mod.Phys.* 56 (1984) 579-707

$$|A(u\bar{u} \rightarrow u\bar{u})|^2 = |A(d\bar{d} \rightarrow d\bar{d})|^2 =$$

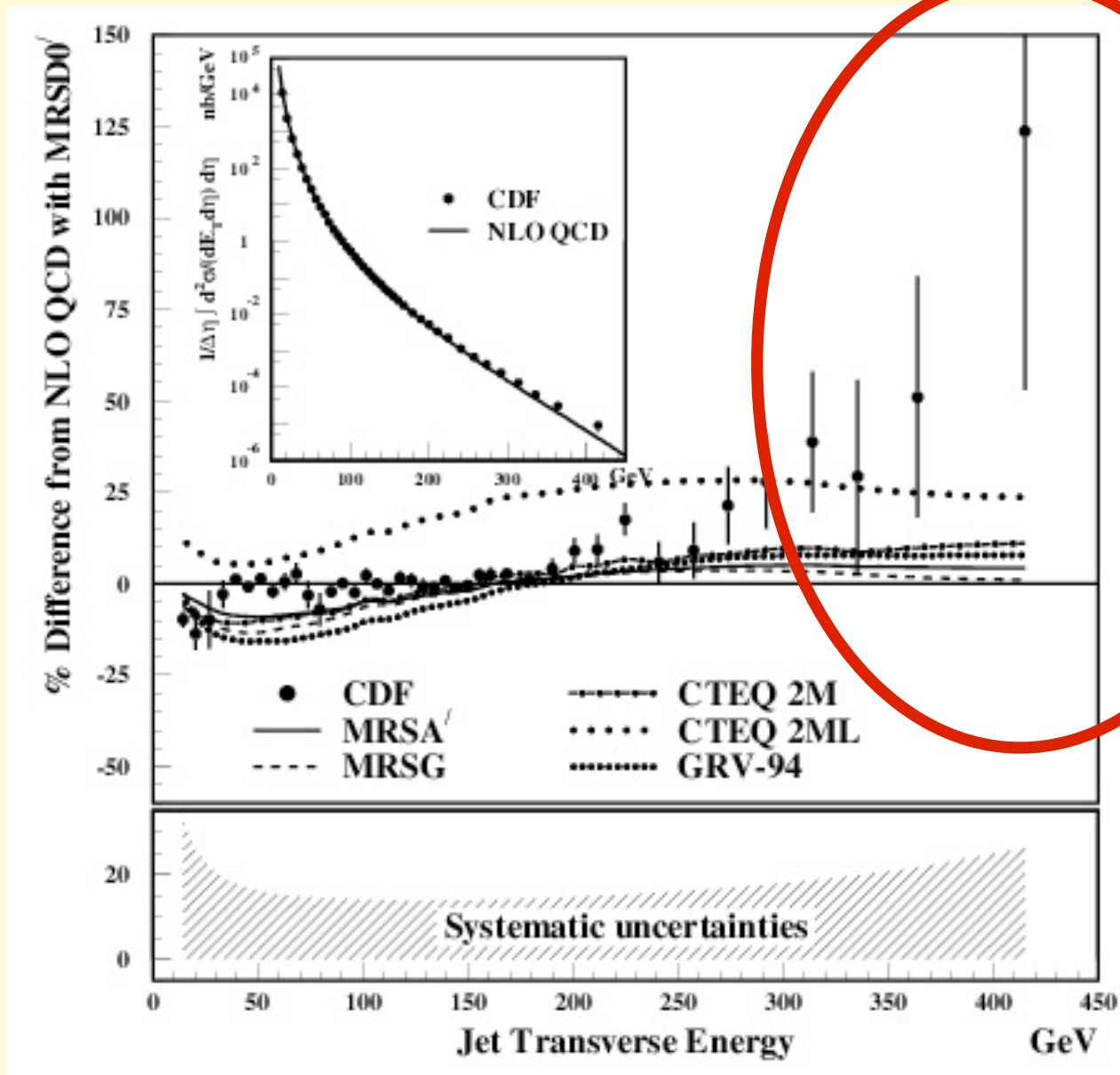
$$\frac{4}{9} \alpha_s^2(Q^2) \left[\frac{(\hat{u}^2 + \hat{s}^2)}{\hat{t}^2} + \frac{(\hat{u}^2 + \hat{t}^2)}{\hat{s}^2} - \frac{2}{3} \cdot \frac{\hat{u}^2}{\hat{s}\hat{t}} \right]$$

$$+ \frac{8}{9} \alpha_s(Q^2) \frac{\eta_0}{\Lambda^2} \left(\frac{\hat{u}^2}{\hat{t}} + \frac{\hat{u}^2}{\hat{s}} \right) + \frac{8}{3} \left(\frac{\eta_0 \hat{u}}{\Lambda^2} \right)^2;$$

At the LHC, with the anticipated statistics of 300 fb-1, limits on the scale of the new interactions in excess of 40 TeV should be reached (to increase to 60 TeV with 3000 fb-1)



Example, at the Tevatron, ~1995



Some more kinematics

Prove as an **exercise** that

$$x_{1,2} = \frac{p_T}{E_{beam}} \cosh y^* e^{\pm y_b}$$

where

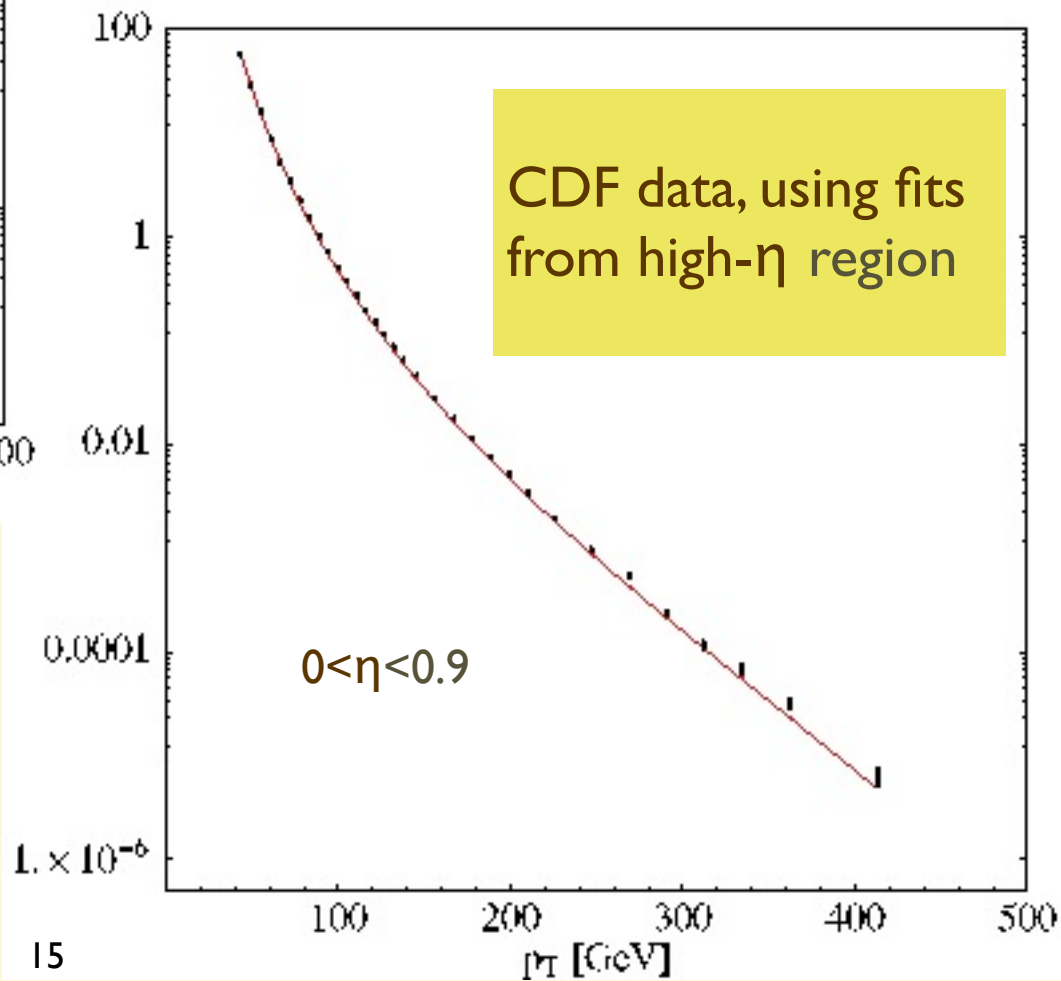
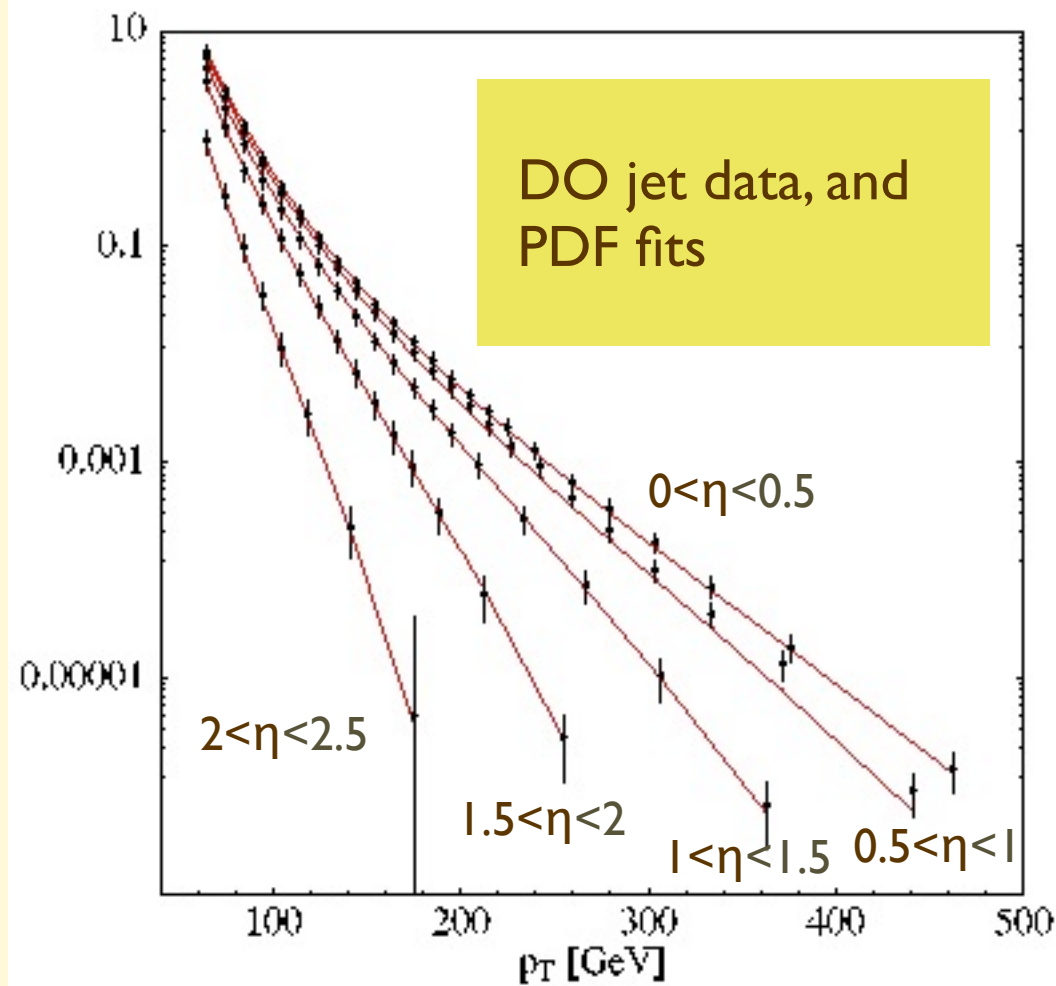
$$y^* = \frac{\eta_1 - \eta_2}{2}, \quad y_b = \frac{\eta_1 + \eta_2}{2}$$

We can therefore reach large values of x either by selecting large invariant mass events:

$$\frac{p_T}{E_{beam}} \cosh y^* \equiv \sqrt{\tau} \rightarrow 1$$

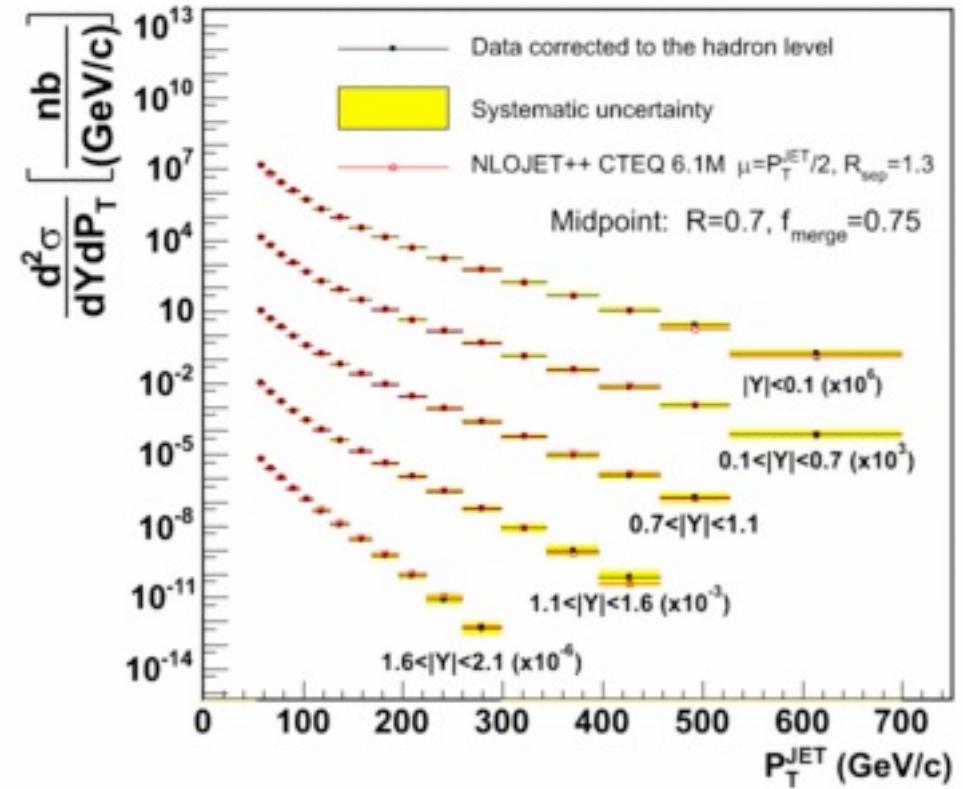
or by selecting low-mass events, but with large boosts (y_b large) in either positive or negative directions. In this case, we probe large- x with events where possible new physics is absent, thus setting consistent constraints on the behaviour of the cross-section in the high-mass region, which could hide new phenomena.

Follow-up analyses, spectra vs eta, PDF refitting,

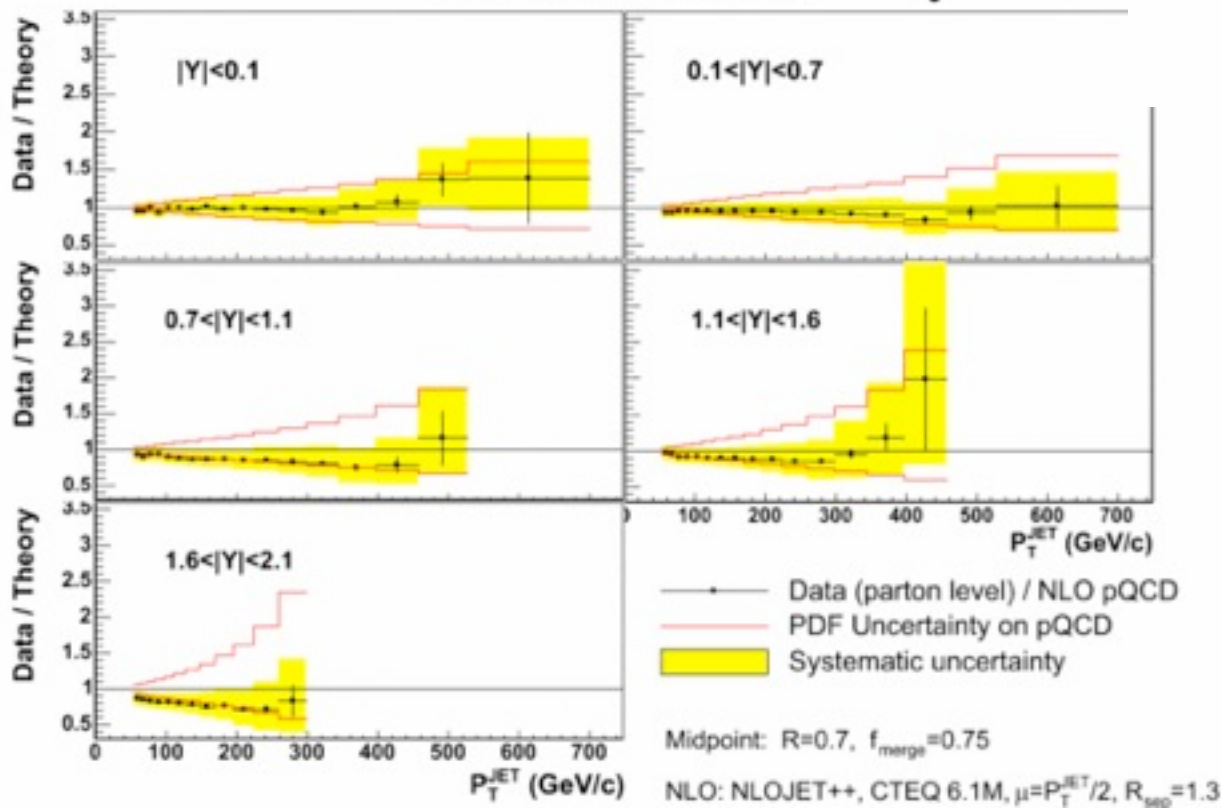


Tevatron, Run 2 results

CDF Run II Preliminary (L=1.13 fb⁻¹)



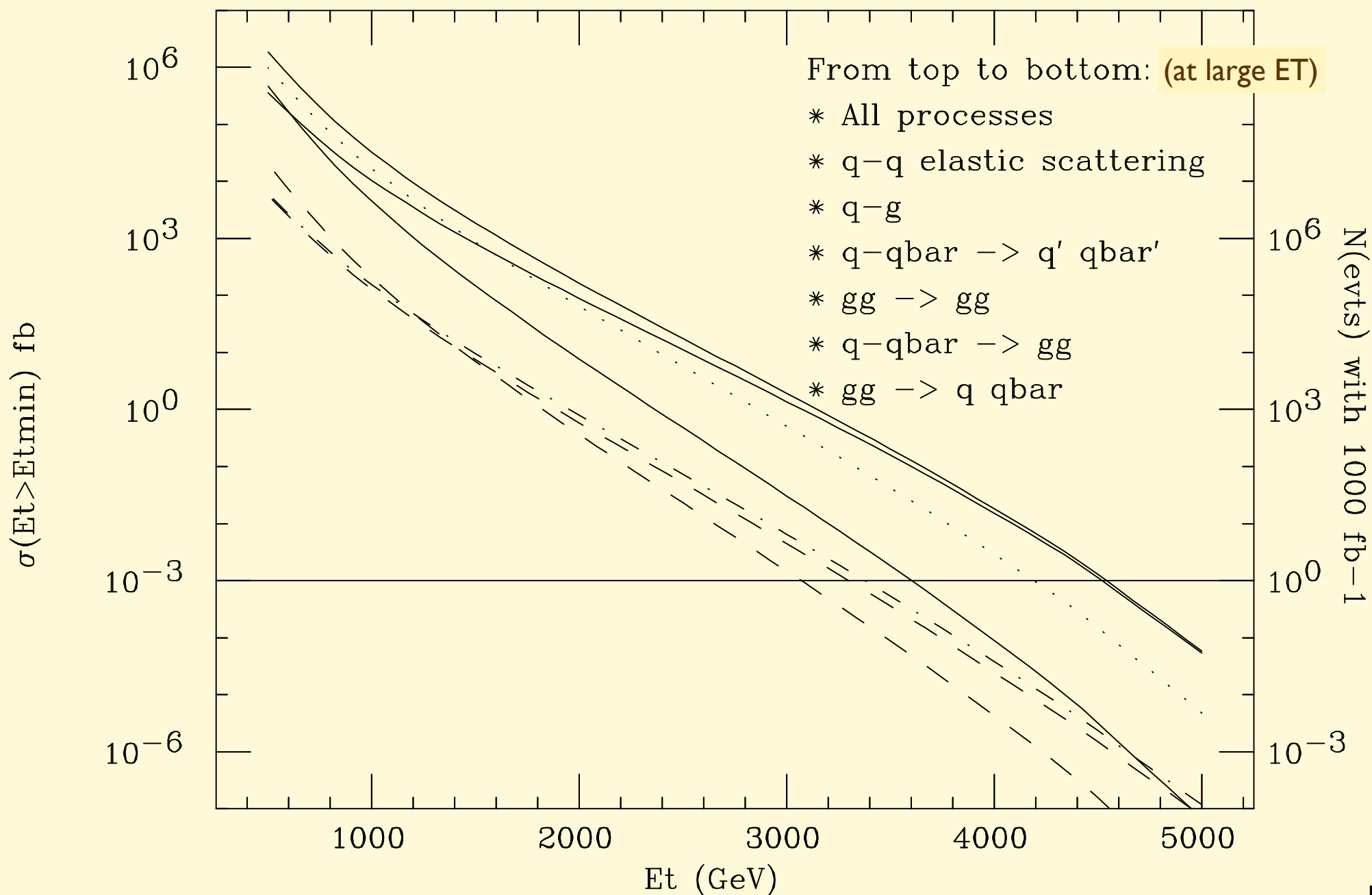
CDF Run II Preliminary $\int L=1.13 \text{ fb}^{-1}$



Selected jet physics results at the LHC

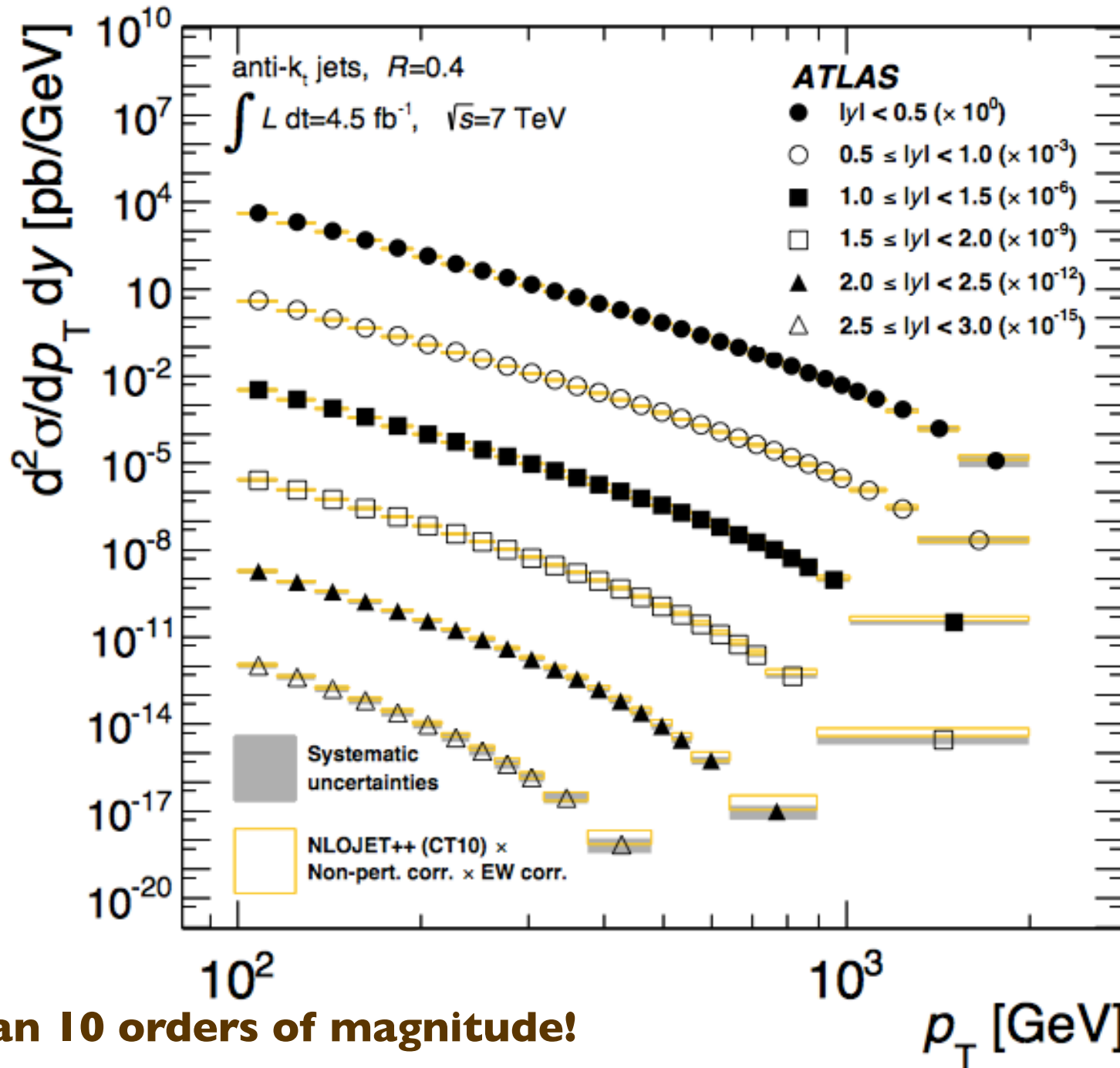
Jet production rates at the LHC, subprocess composition

(this is at 14 TeV: results at 7 TeV are ~obtained by rescaling ET by 0.5)



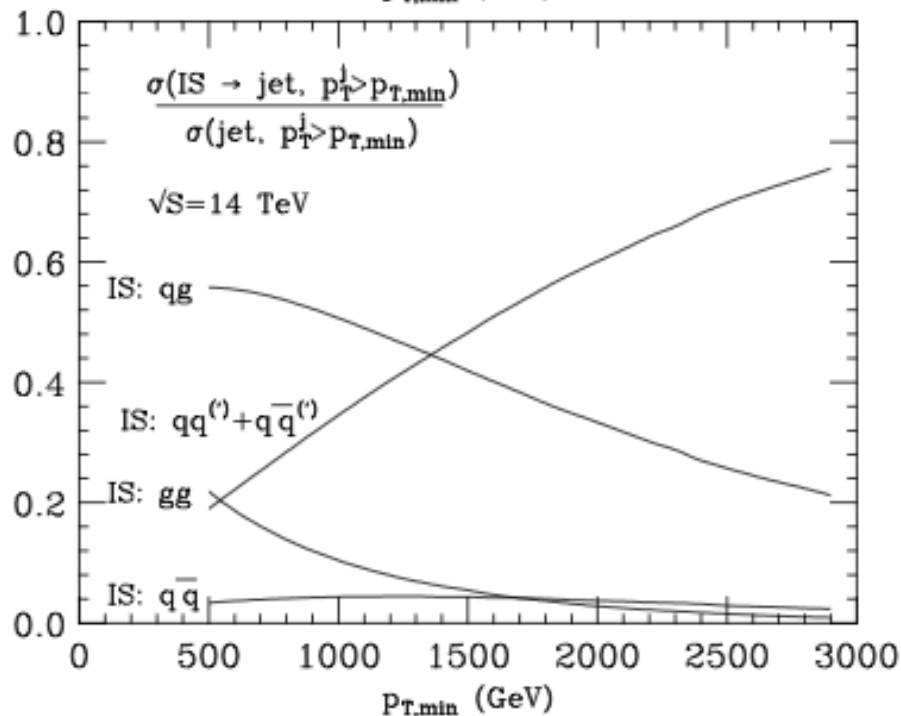
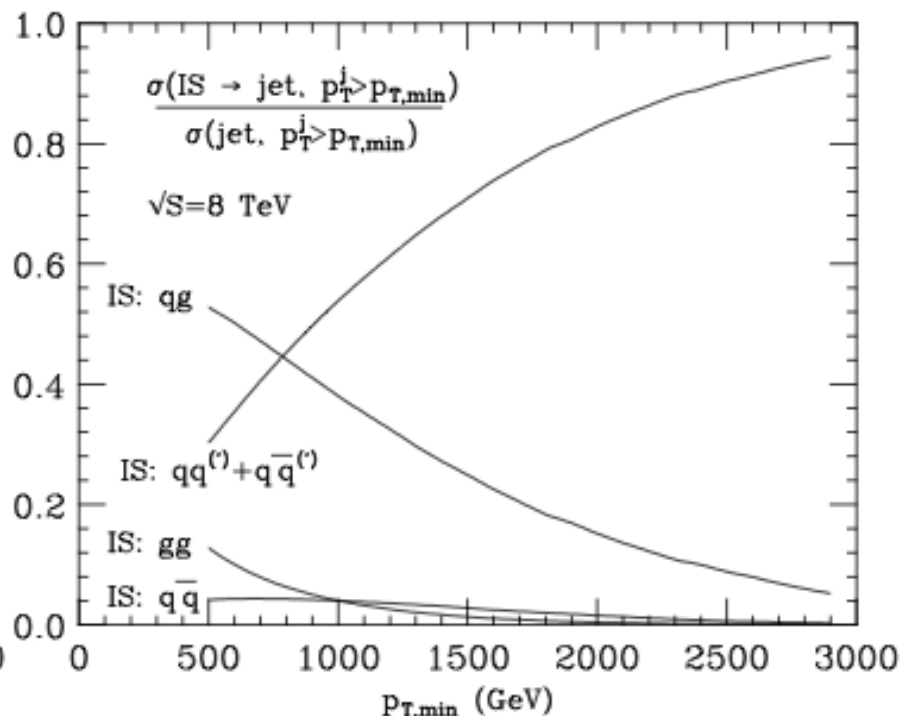
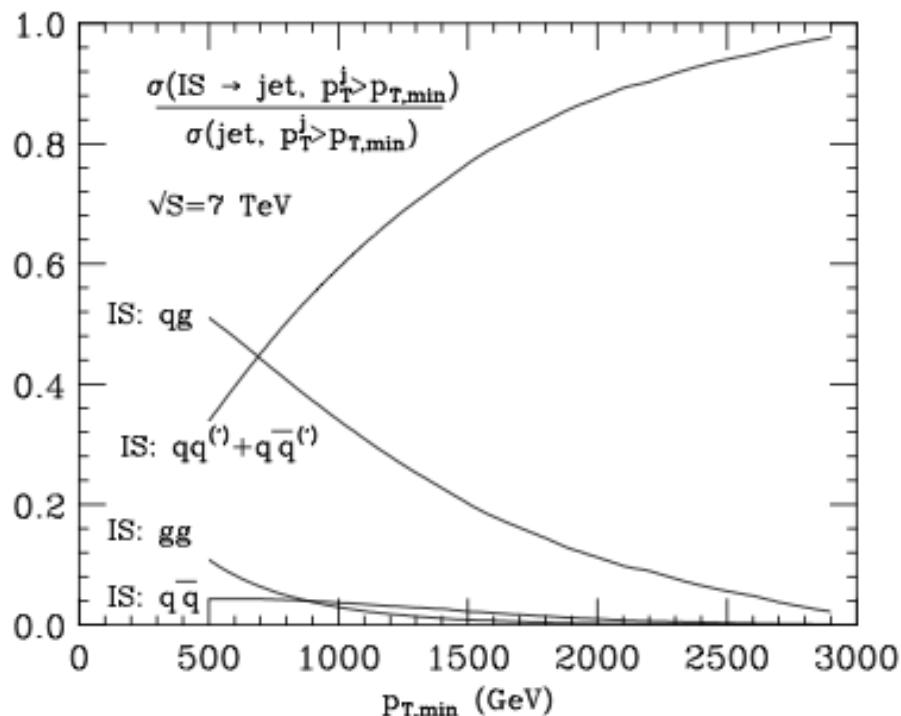
Example: Jet cross section

ATLAS, arXiv:1410.8857

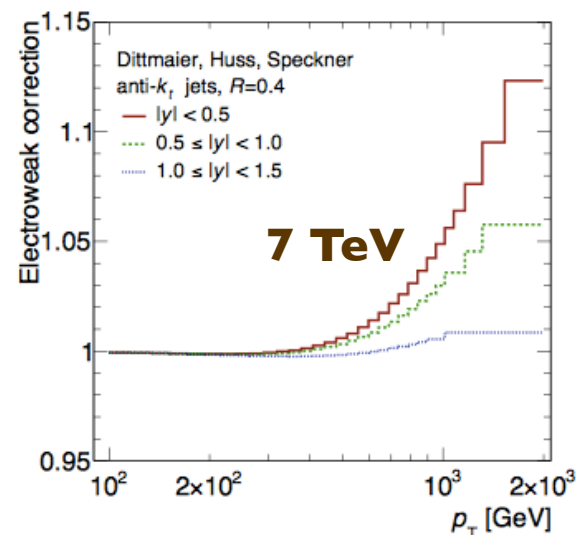


Rates span 10 orders of magnitude!

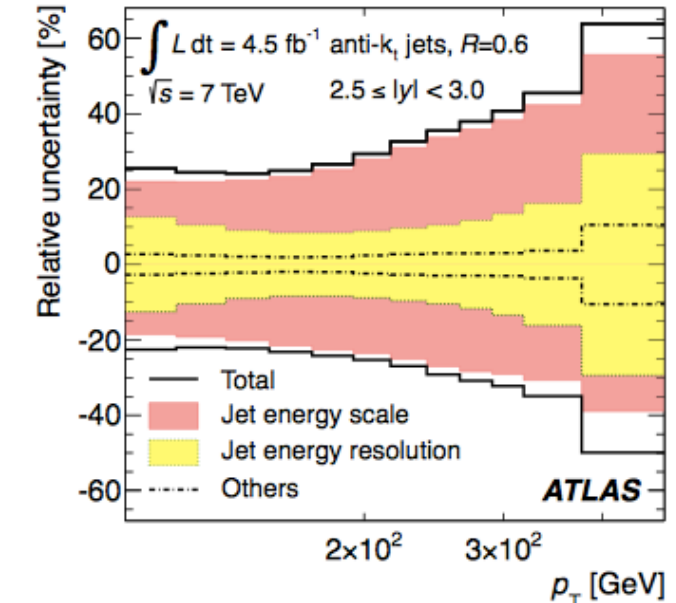
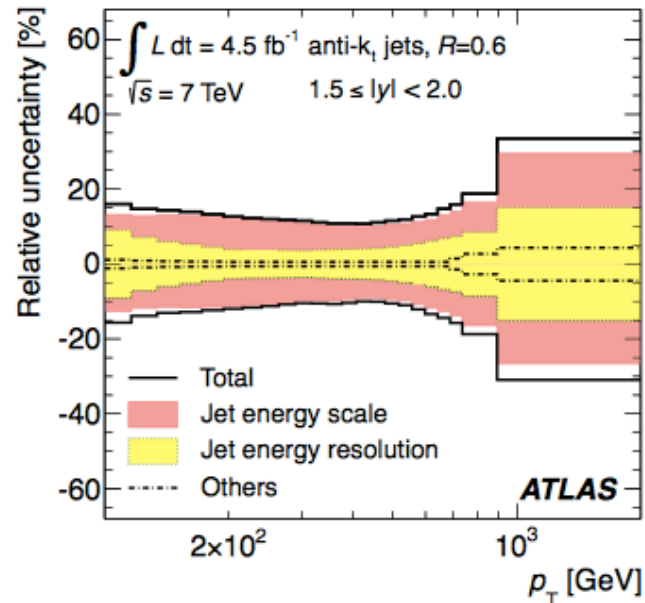
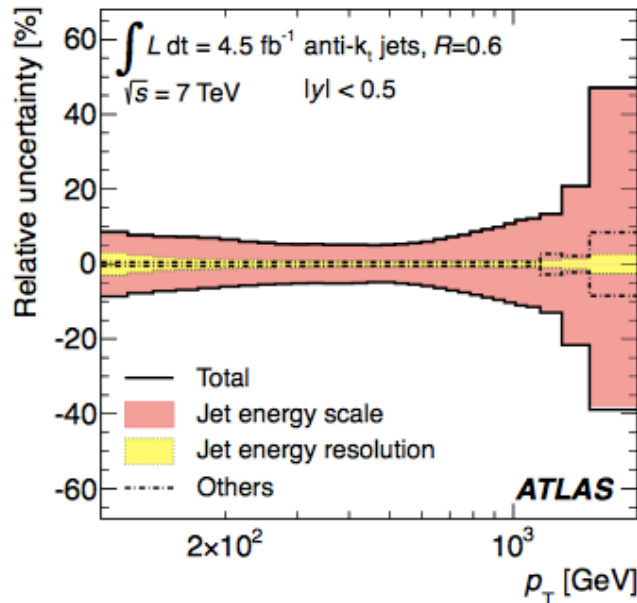
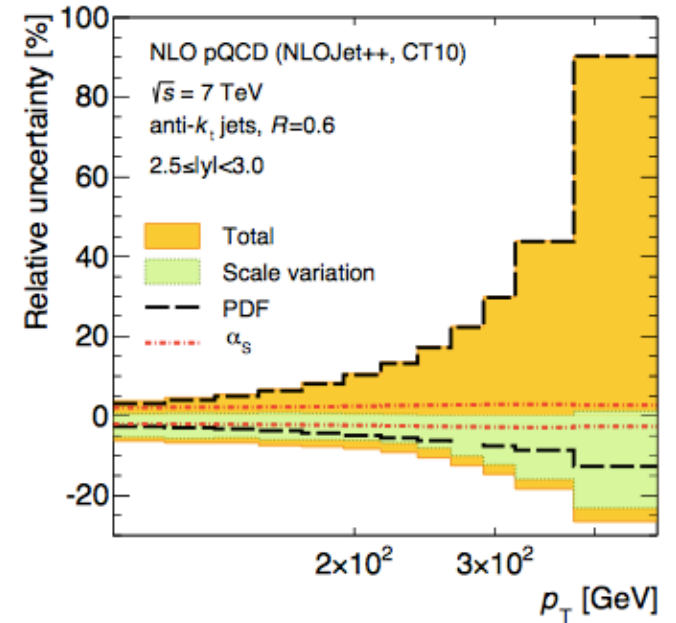
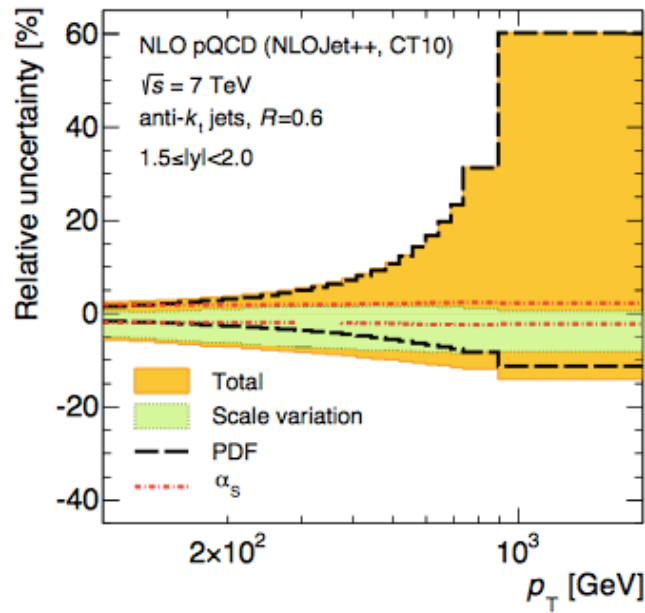
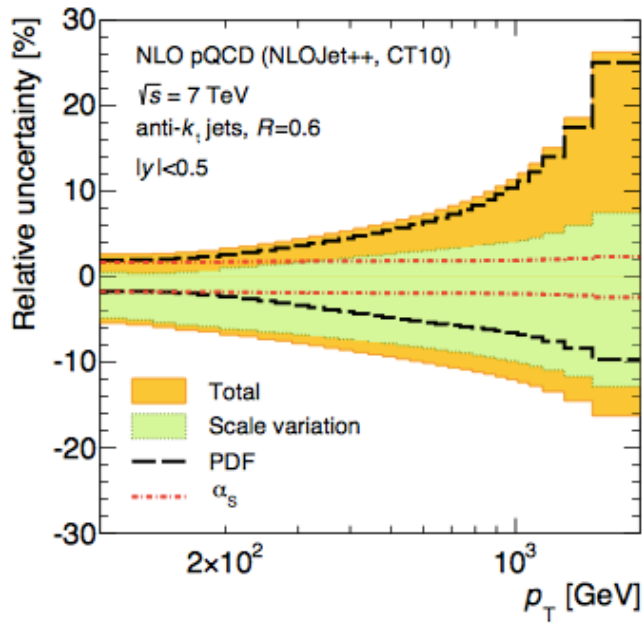
Initial state composition of inclusive jet events



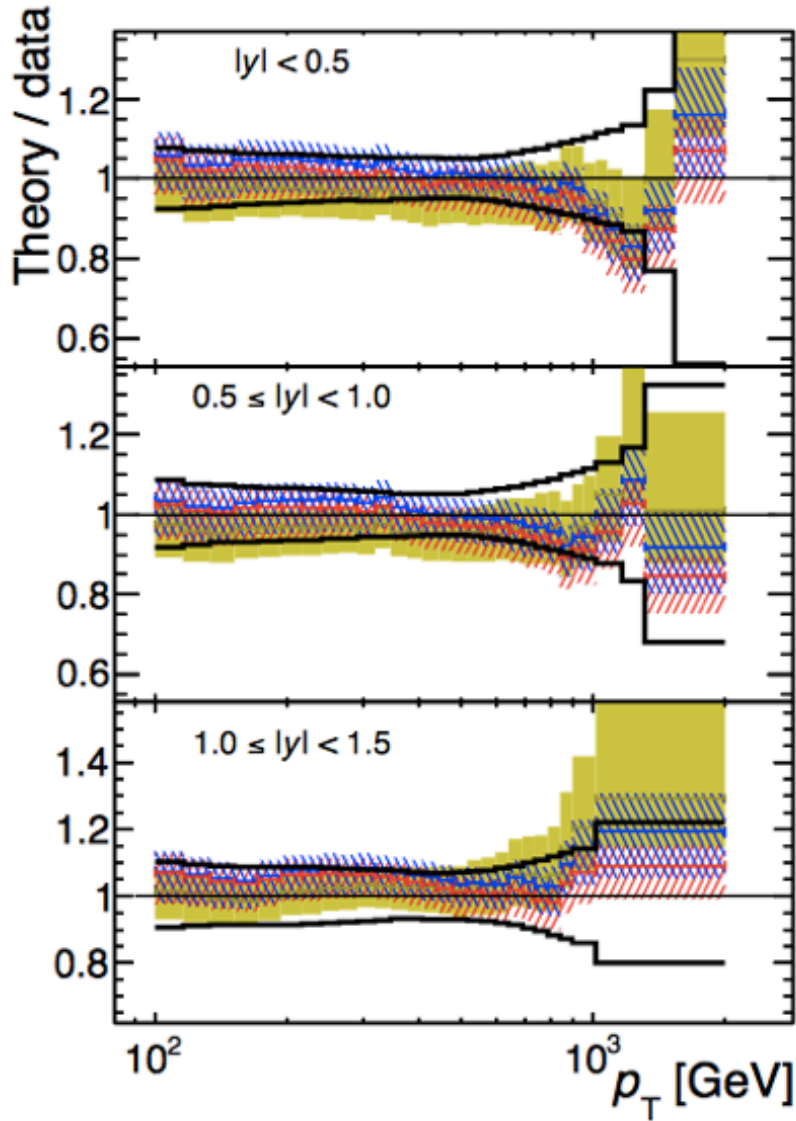
NB: Impact of virtual EW corrections:



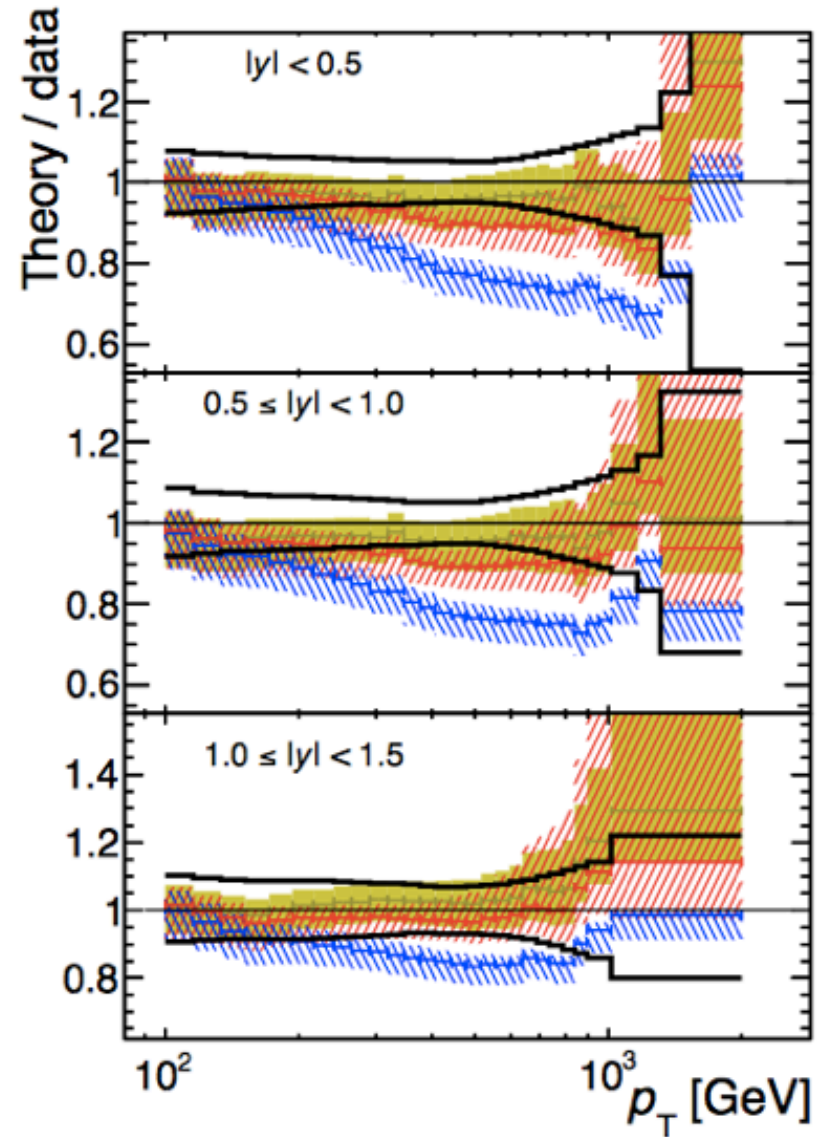
at $p_T \sim 2 \text{ TeV}$ it's larger than qg contribution



Central production, TH vs data
(TH: absolute prediction for both shape and normalization)



ATLAS
 $\int L dt = 4.5 \text{ fb}^{-1}$
 $\sqrt{s} = 7 \text{ TeV}$
 anti- k_r jets, $R=0.4$

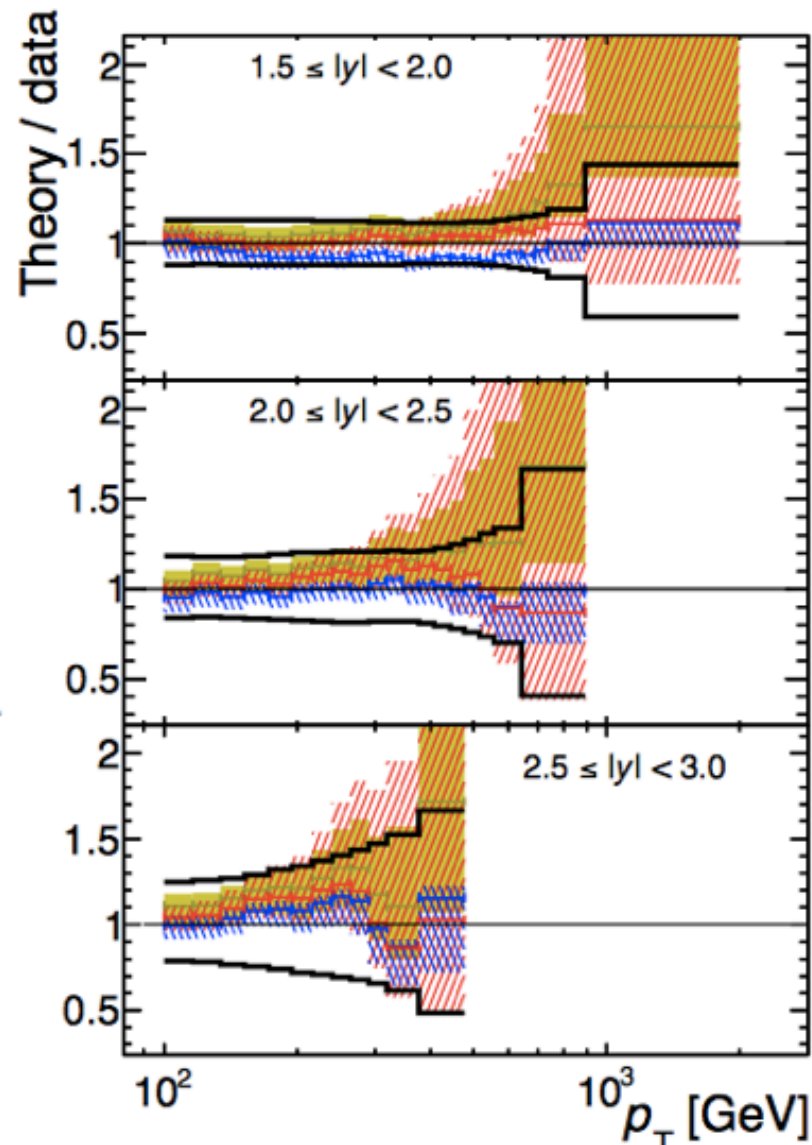
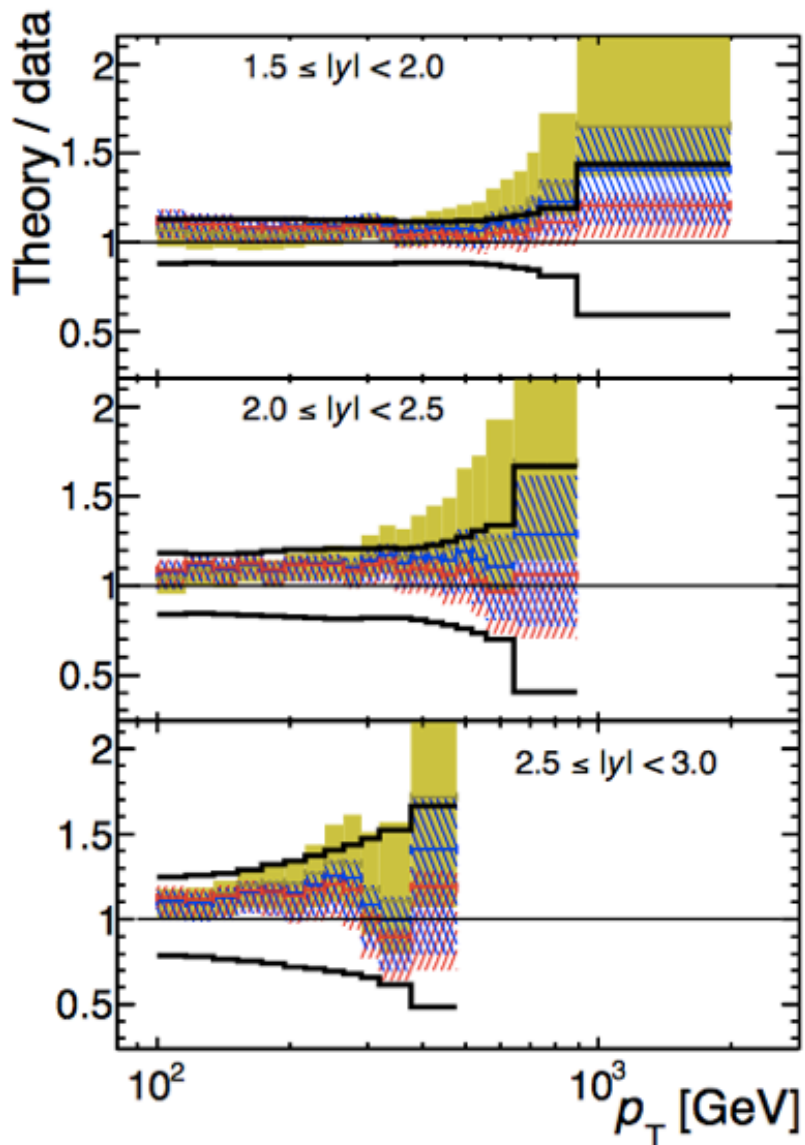


NLOJET++
 $\mu_F = \mu_R = p_T^{\text{max}}$
 Non-pert and
 EW corr.

CT10
 MSTW 2008
 NNPDF 2.1

CT10
 HERAPDF 1.5
 ABM11
 $n_f = 5$

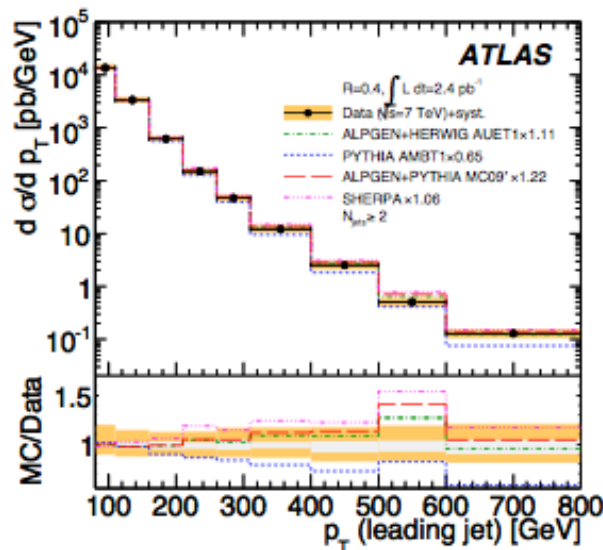
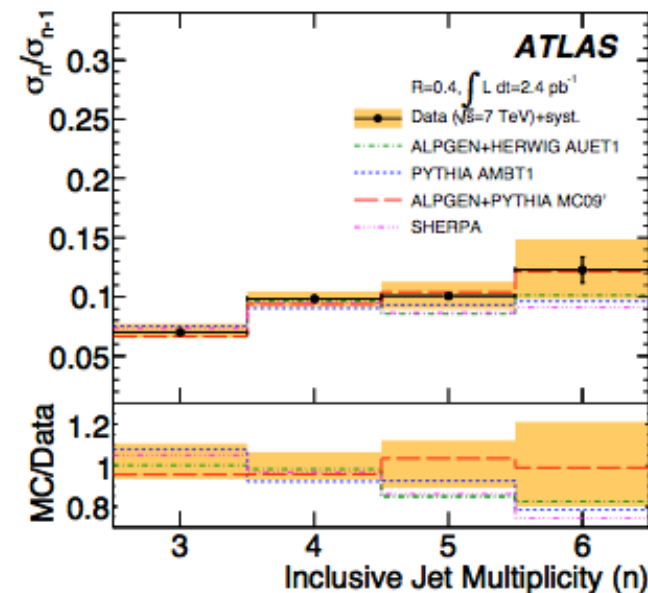
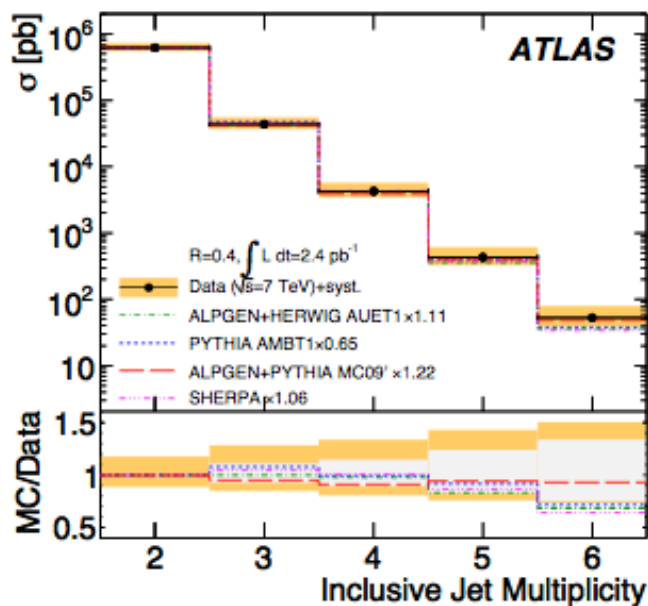
Forward production, TH vs data
(TH: absolute prediction for both shape and normalization)



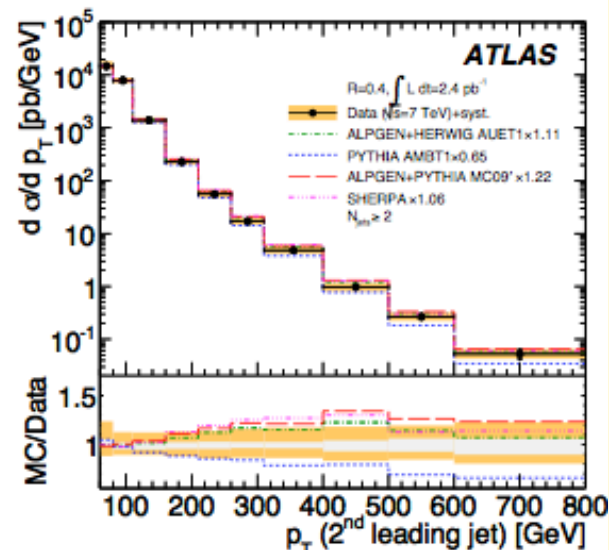
NLOJET++
 $\mu_F = \mu_R = p_T^{\max}$
 Non-pert and
 EW corr.

CT10
 MSTW 2008
 NNPDF 2.1

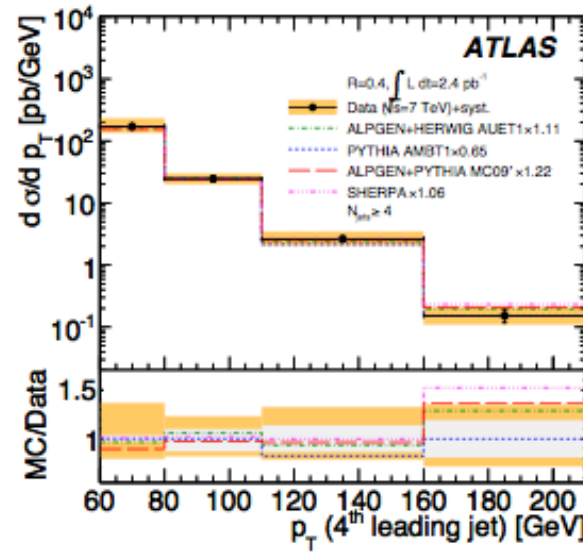
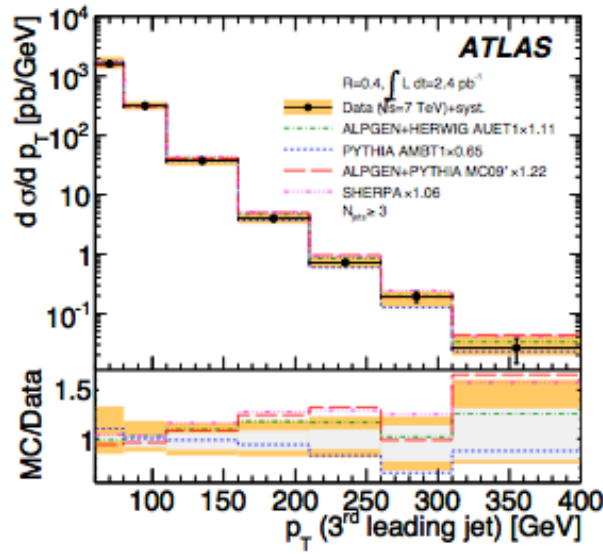
CT10
 HERAPDF
 1.5
 ABM11
 $n_f = 5$



(a)

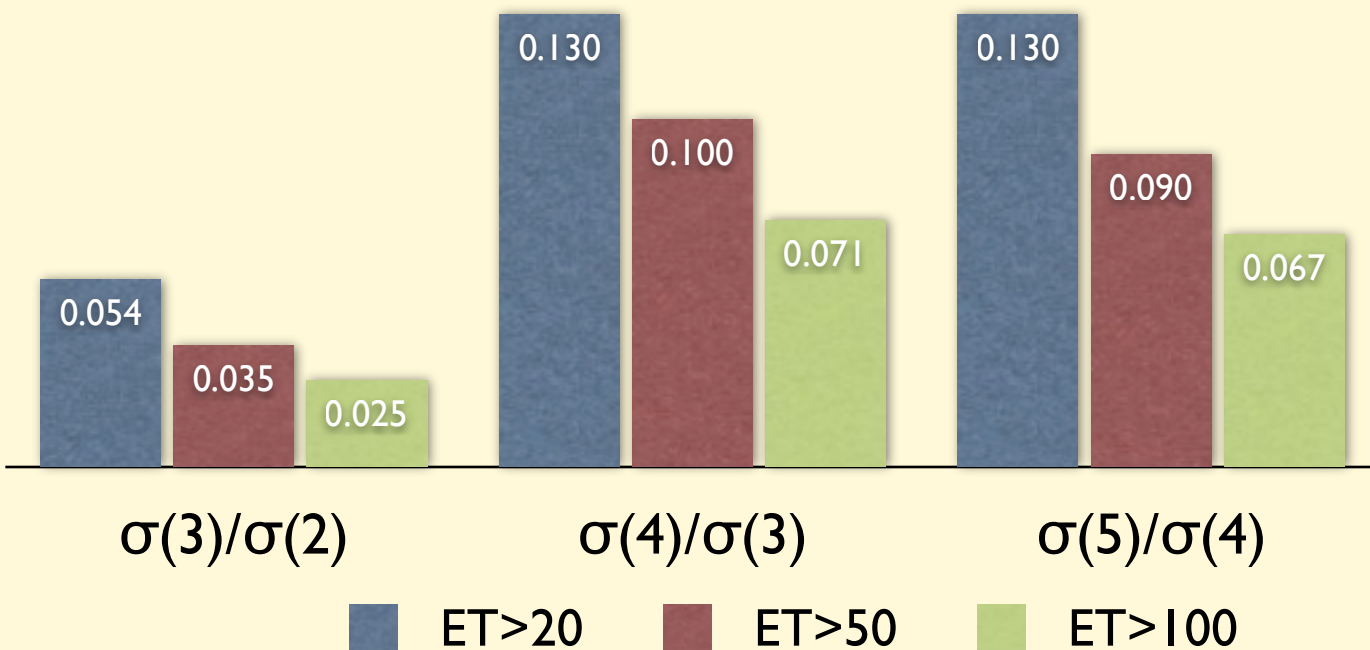


(b)



Multijet rates

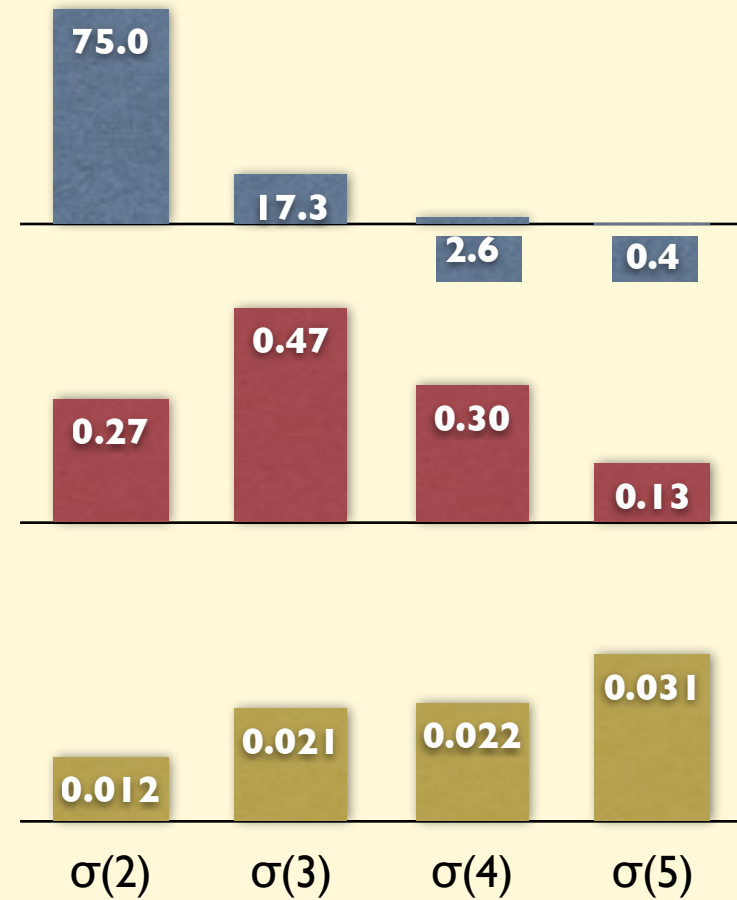
σ [μb]	N jet=2	N jet=3	N jet=4	N jet=5
$E_T^{\text{jet}} > 20$ GeV	350	19	2.6	0.35
$E_T^{\text{jet}} > 50$ GeV	12.7	0.45	0.045	0.004
$E_T^{\text{jet}} > 100$ GeV	0.85	0.021	0.0015	0.0001



- The higher the jet E_T threshold, the harder to emit an extra jet
- When several jets are already present, however, emission of an additional one is less suppressed

Multijet rates, vs \sqrt{s} , with $E_T^{\text{jet}} > 20 \text{ GeV}$

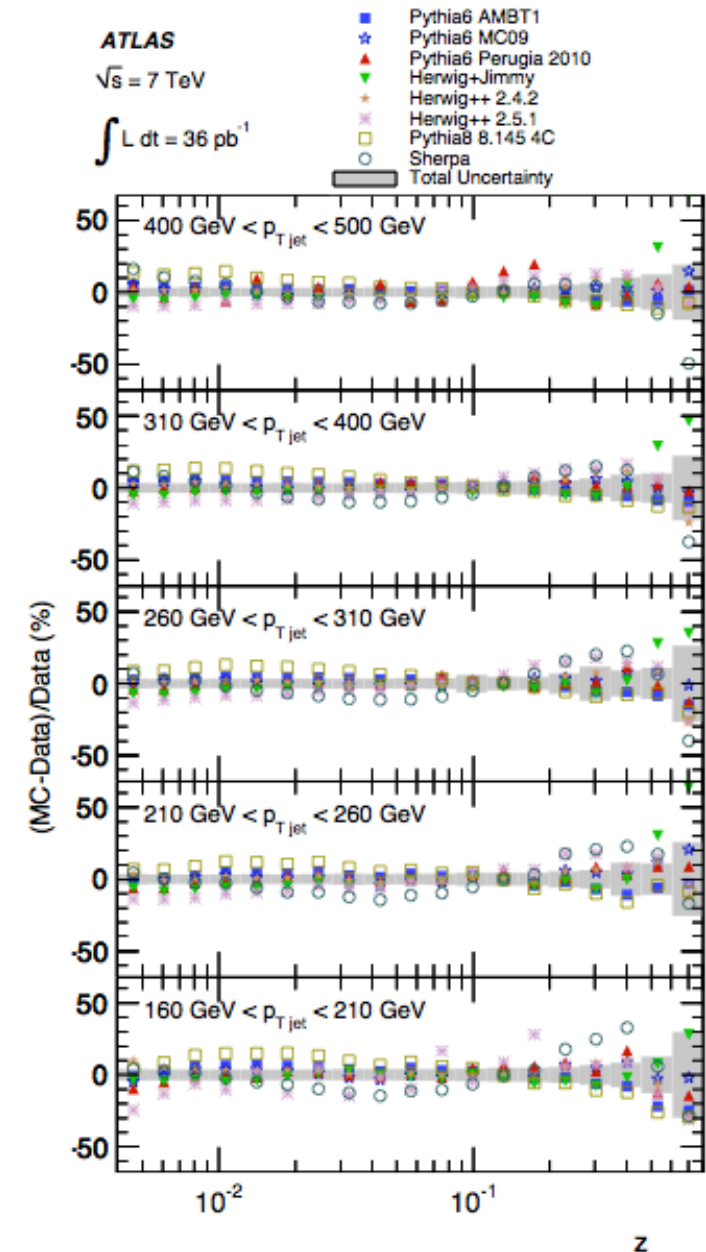
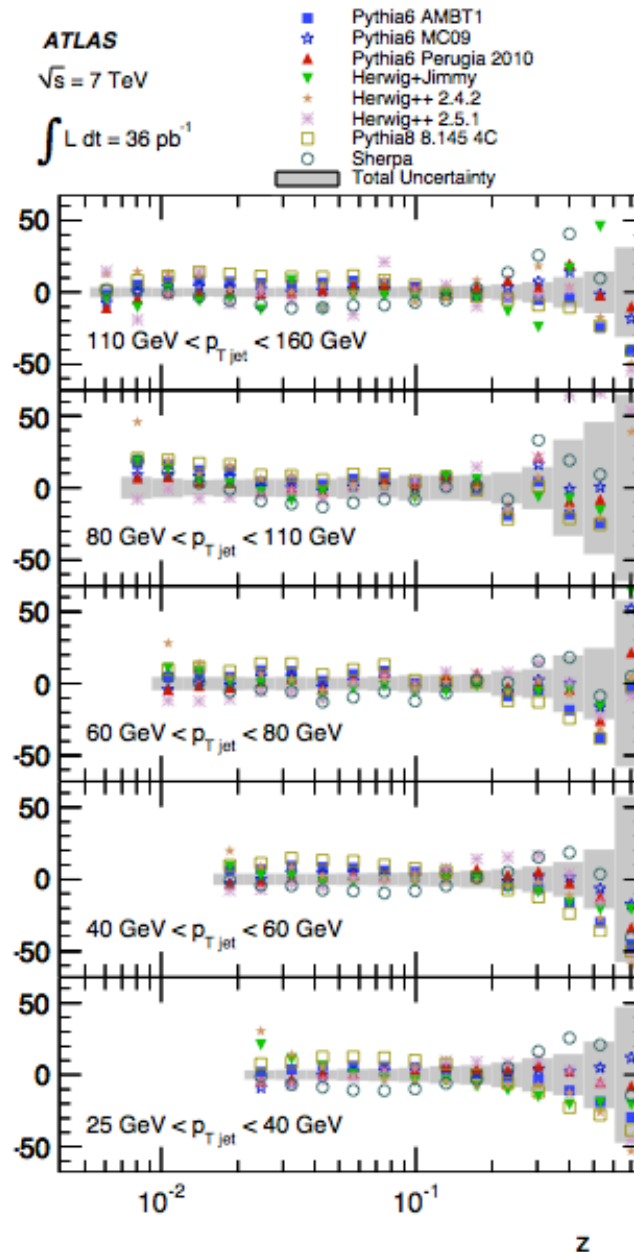
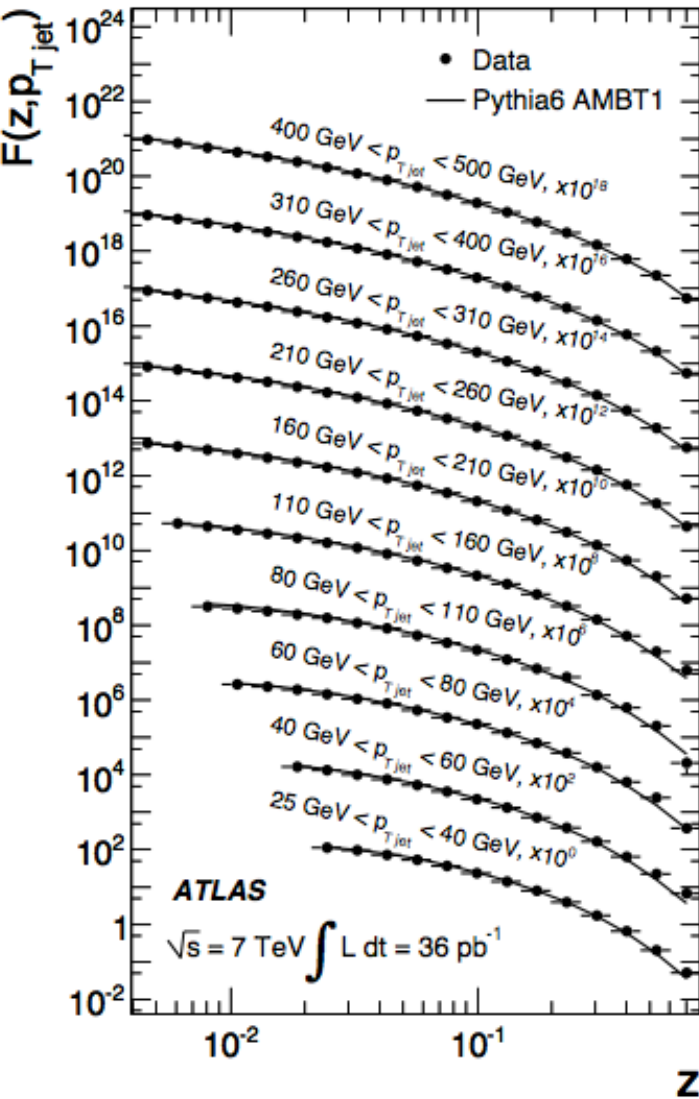
σ [μb]	N jet=2	N jet=3	N jet=4	N jet=5
$\sqrt{s} > 100 \text{ GeV}$	75	17.3	2.6	0.37
$\sqrt{s} > 500 \text{ GeV}$	0.27	0.47	0.30	0.13
$\sqrt{s} > 1000 \text{ GeV}$	0.012	0.021	0.022	0.031



High mass final states are dominated by multijet configurations

Jet fragmentation function

ATLAS, arXiv:1109.5816



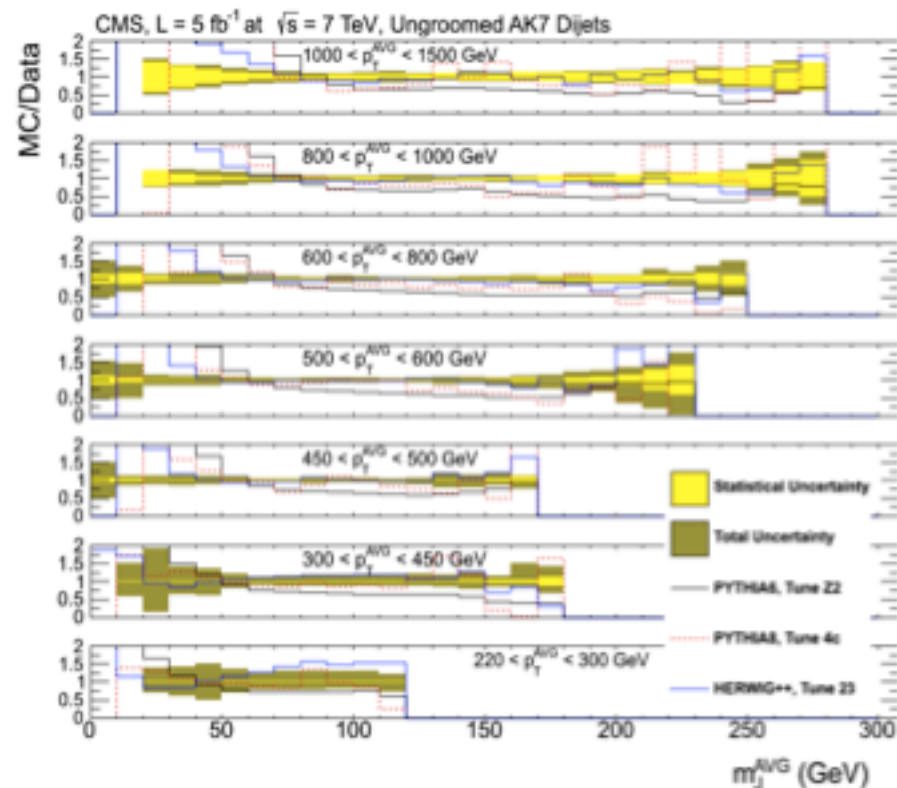
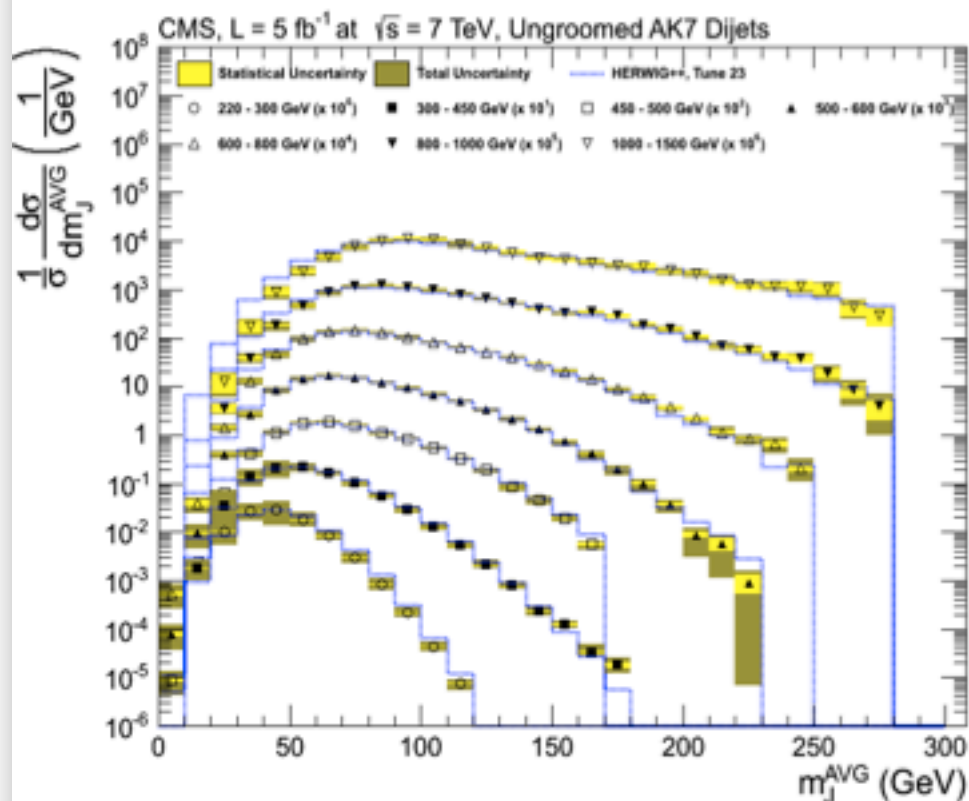
- plus
- jet shapes
- p_Trel spectra
- <N_{ch}> and <z> distributions,
-



QCD jet mass measurement



Processes with high mass jets (q/g initiated) are important backgrounds for many analyses in the boosted topology.

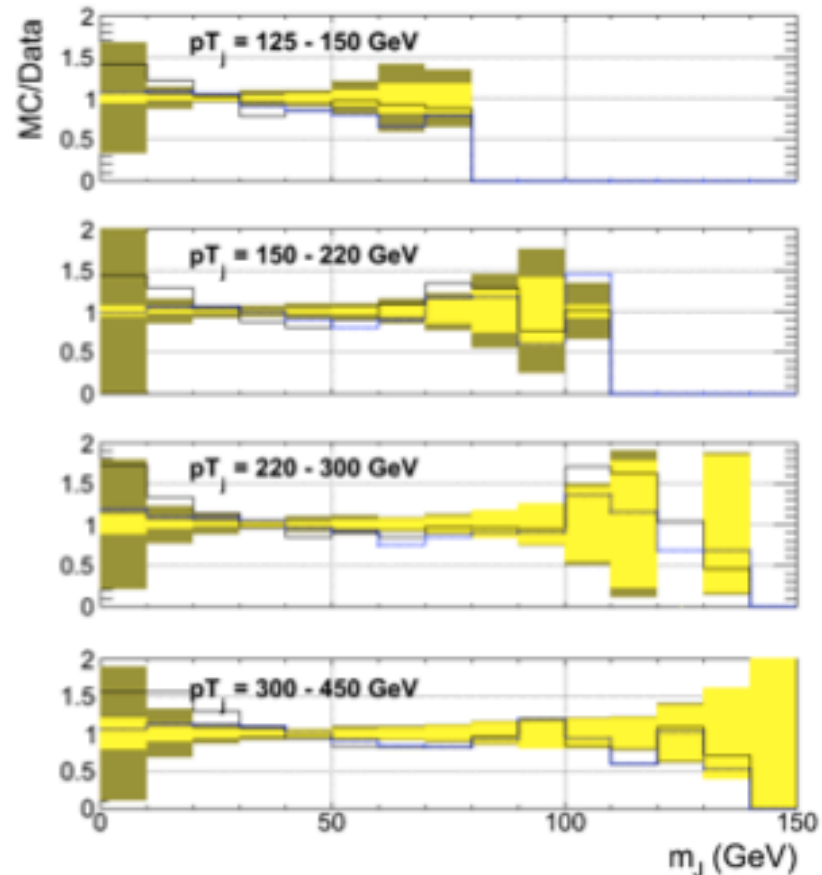
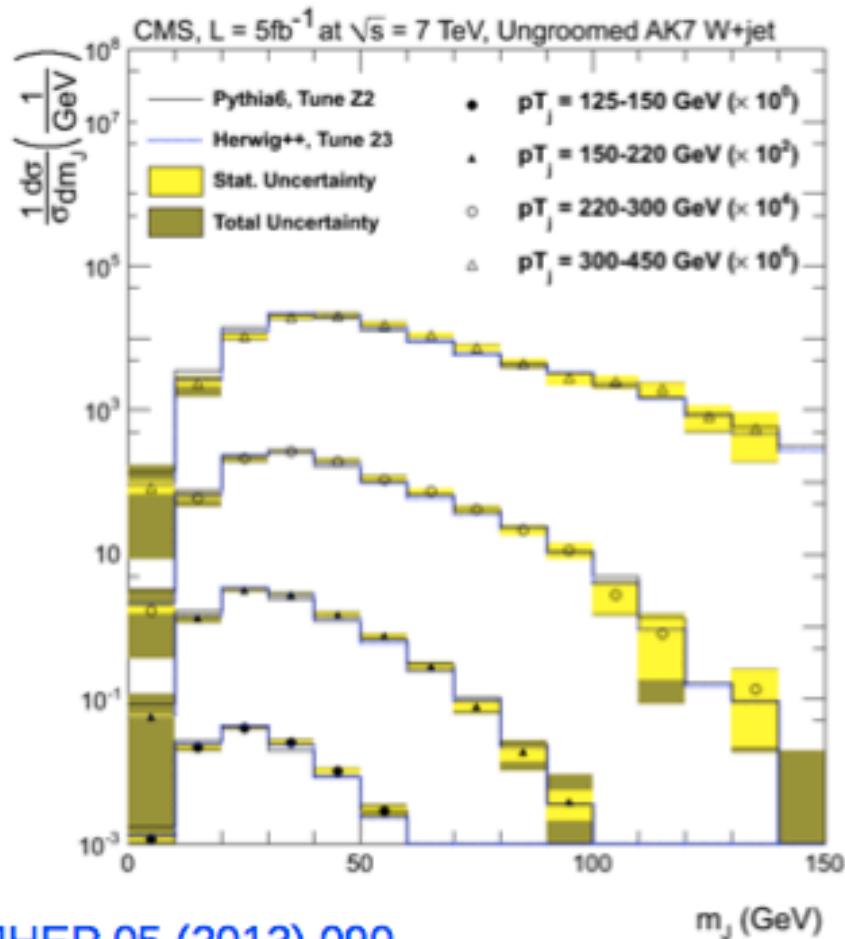


JHEP 05 (2013) 090
CMS-SMP-12-019

Dijet typology (gluon enriched)



QCD jet mass measurement



JHEP 05 (2013) 090
CMS-SMP-12-019

**V+jet typology (quark enriched):
agreement with data is slightly better**

Reconstruct $W/Z \rightarrow jj$ from broad jets at large p_T

Likelihood discriminant using (i) thrust minor (ii) sphericity (iii) aplanarity

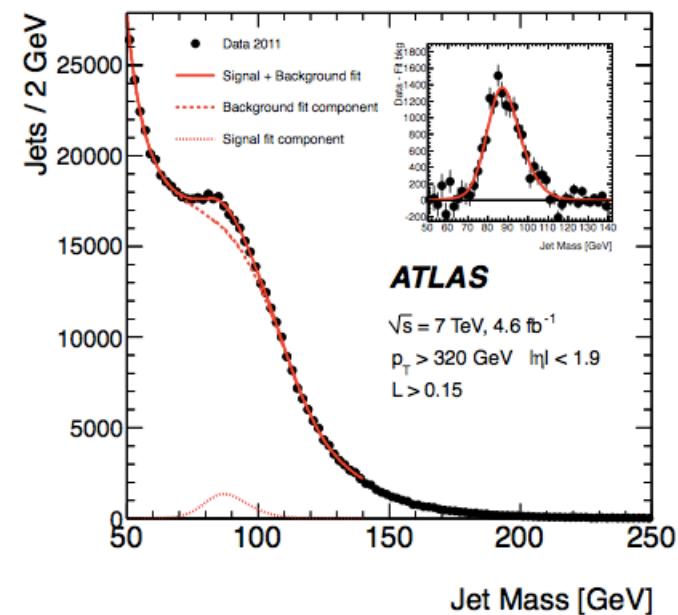
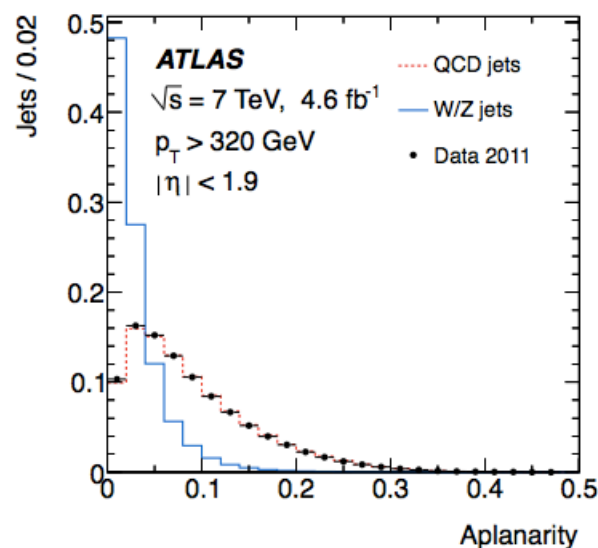
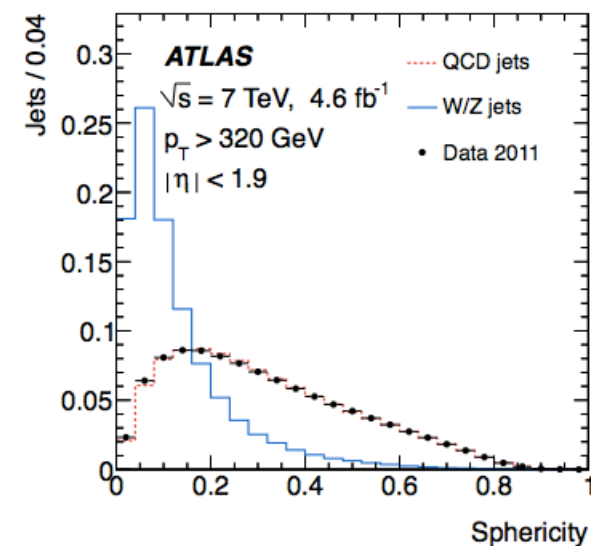
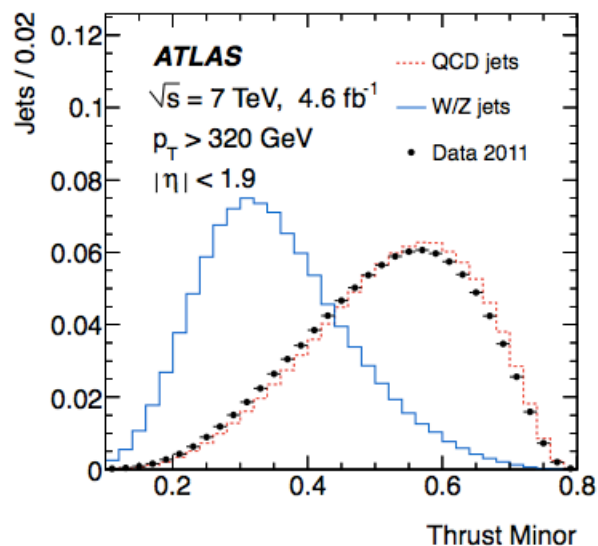
Extract

$$\sigma_{W+Z} = 8.5 \pm 0.8(\text{stat}) \pm 1.5(\text{syst}) \text{ pb}$$

ATLAS, *J.Phys.* **16** (2014) 113013

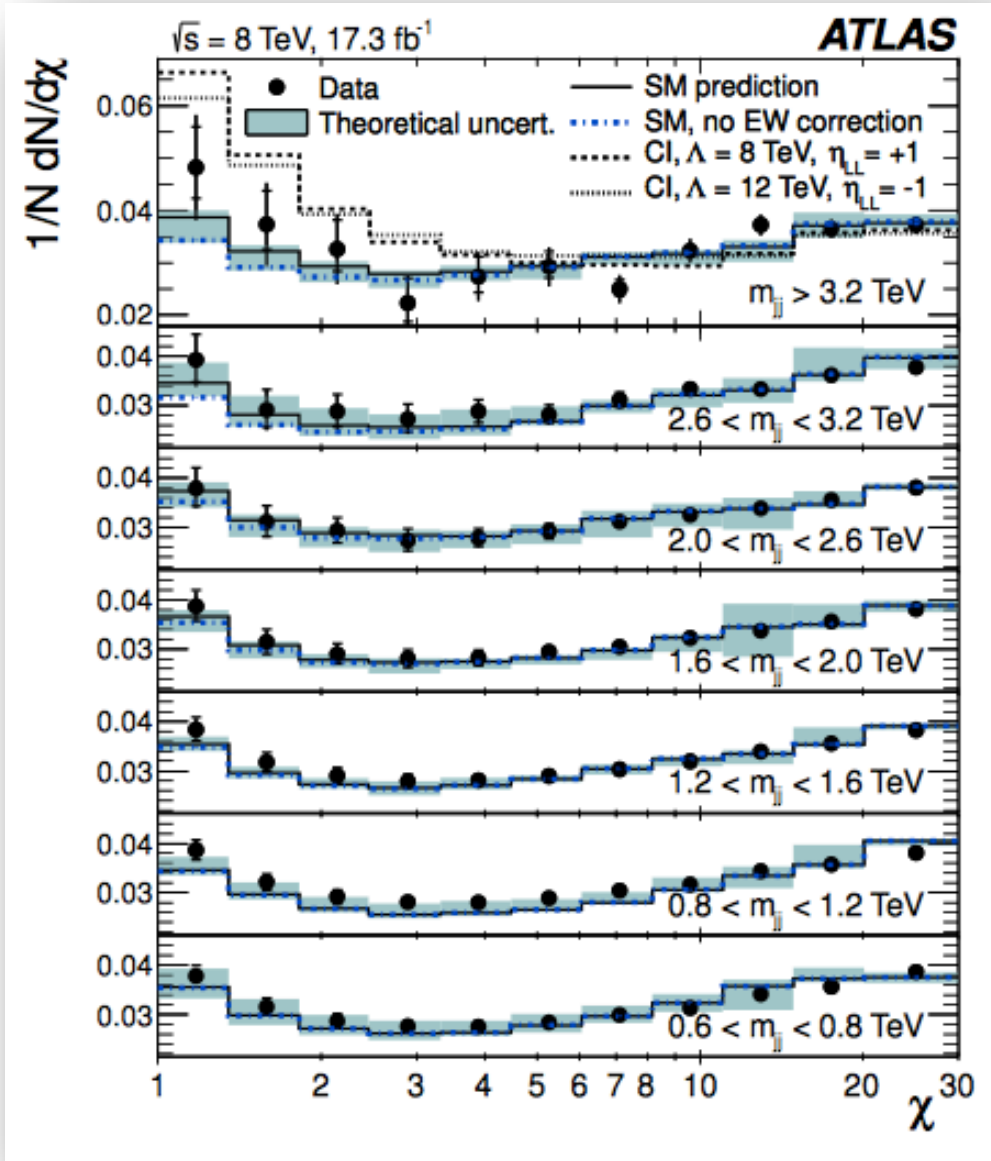
NLO:

$$\sigma_{W+Z} = 5.1 \pm 0.5 \text{ pb}$$

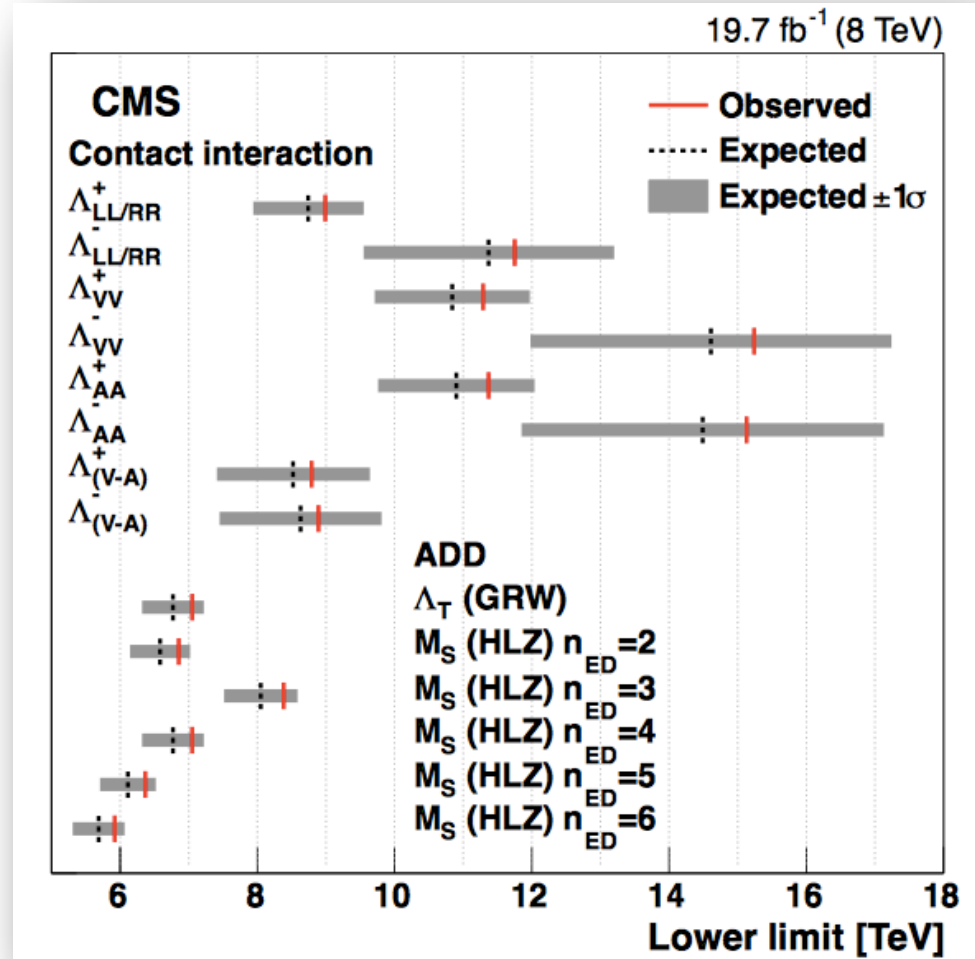


Constraints on quark contact interactions

ATLAS, <http://arxiv.org/abs/1504.00357>



CMS, <http://arxiv.org/abs/1411.2646>

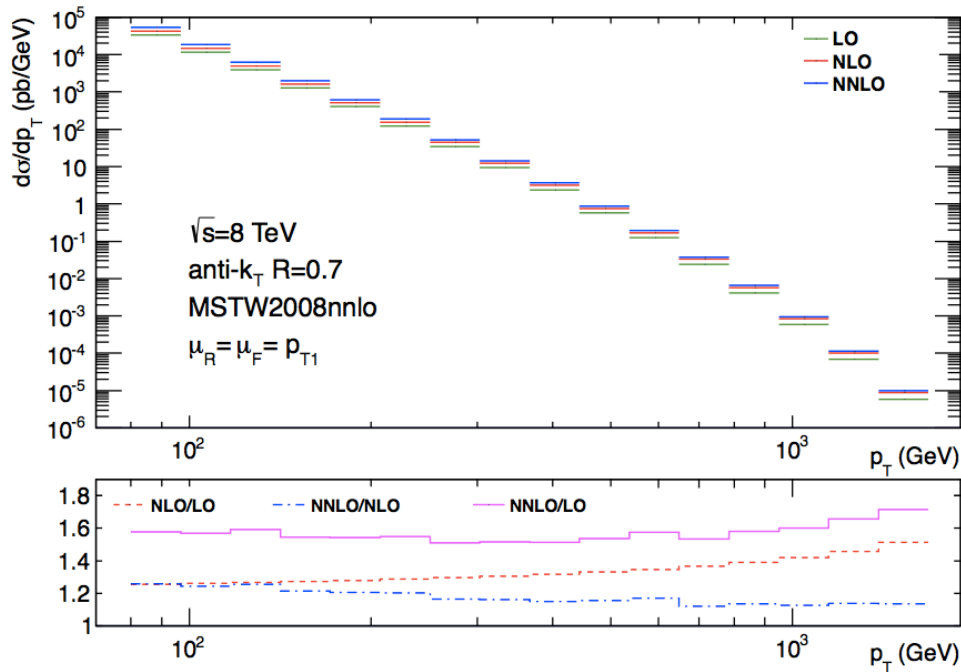


$$\chi = \frac{1 + |\cos \theta^*|}{1 - |\cos \theta^*|} \quad \text{NB: } d\chi = 2 \frac{d \cos \theta}{\sin^4(\theta/2)}$$

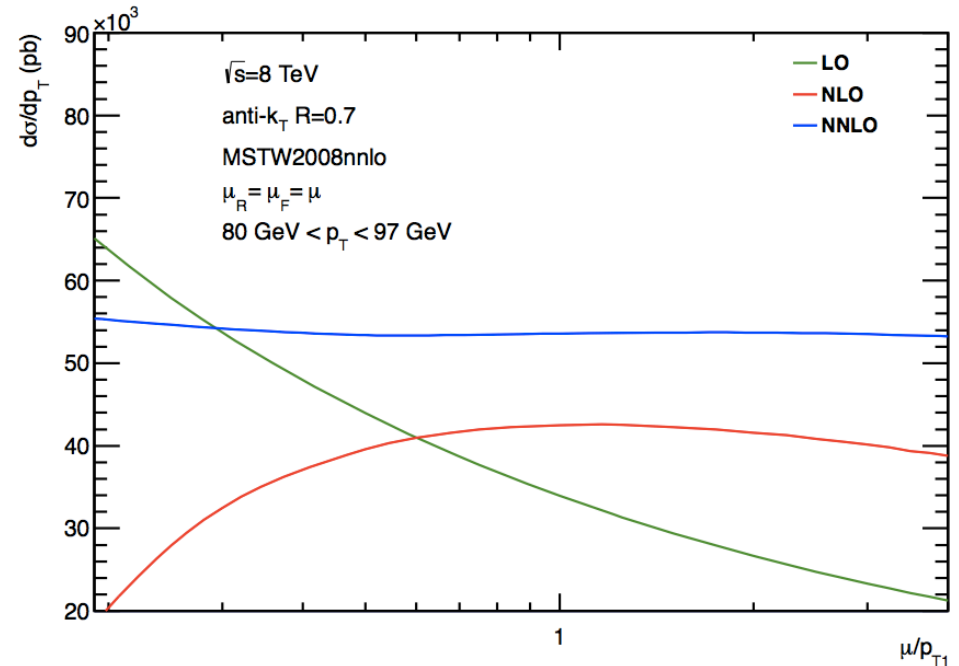
Quarks appear pointlike even at the distances probed by the LHC, up to scales in the range of (10 TeV)⁻¹

Inclusive jet cross section at NNLO

“Second order QCD corrections to jet production at hadron colliders: the all-gluon contribution”, A. Gehrmann-De Ridder, T. Gehrmann, E.W.N. Glover, J. Pires, arXiv:1301.7310



NNLO/NLO ~ 1.2

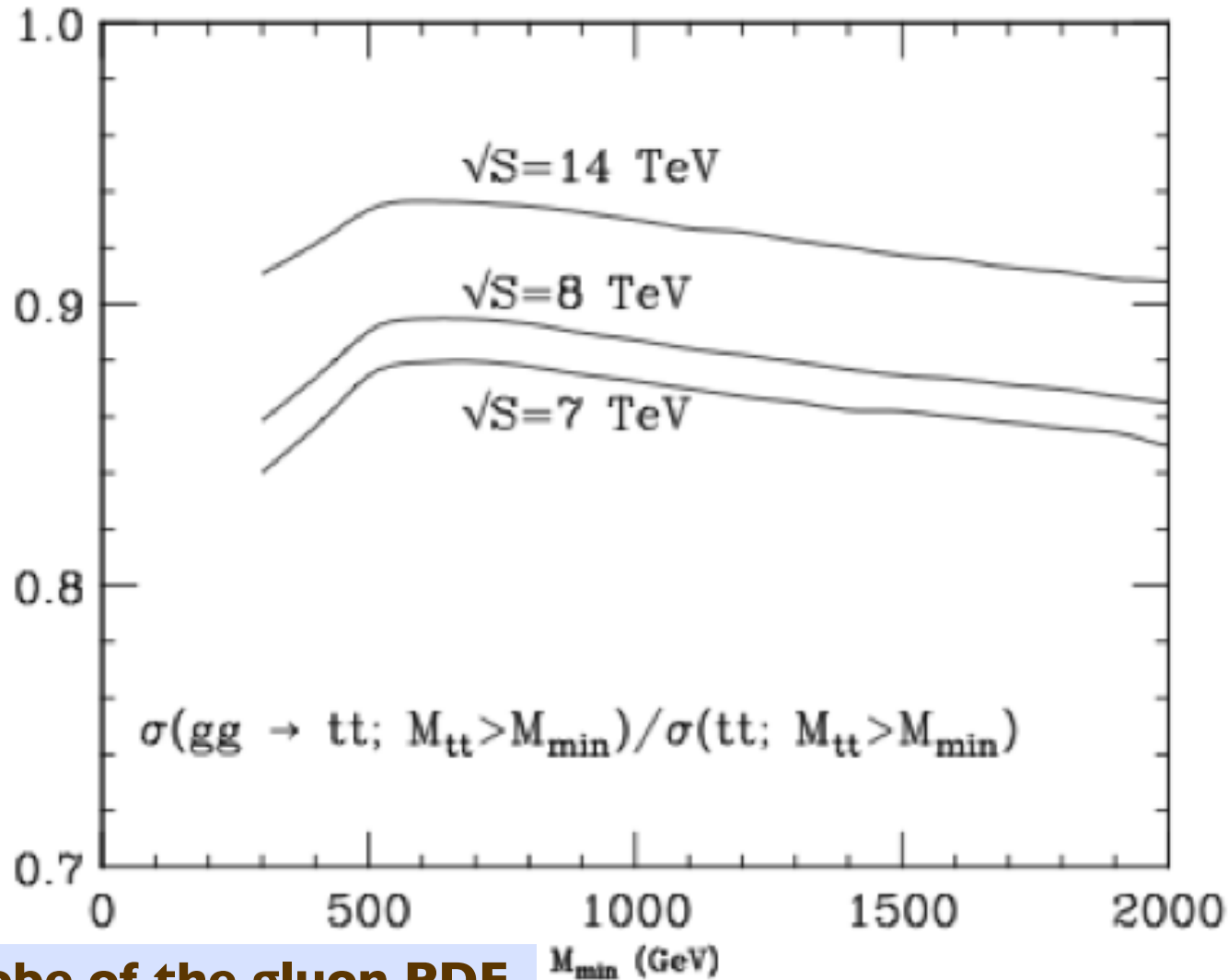
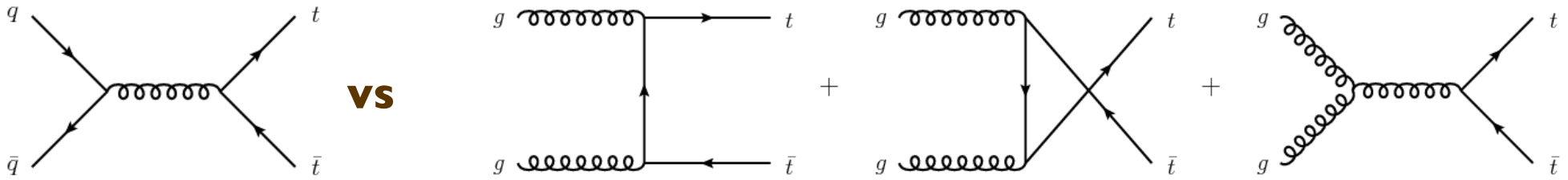


NNLO scale systematics ~ few % ...
- does this survive if $\mu_F \neq \mu_R$?

Notice that NNLO outside the NLO scale-variation band

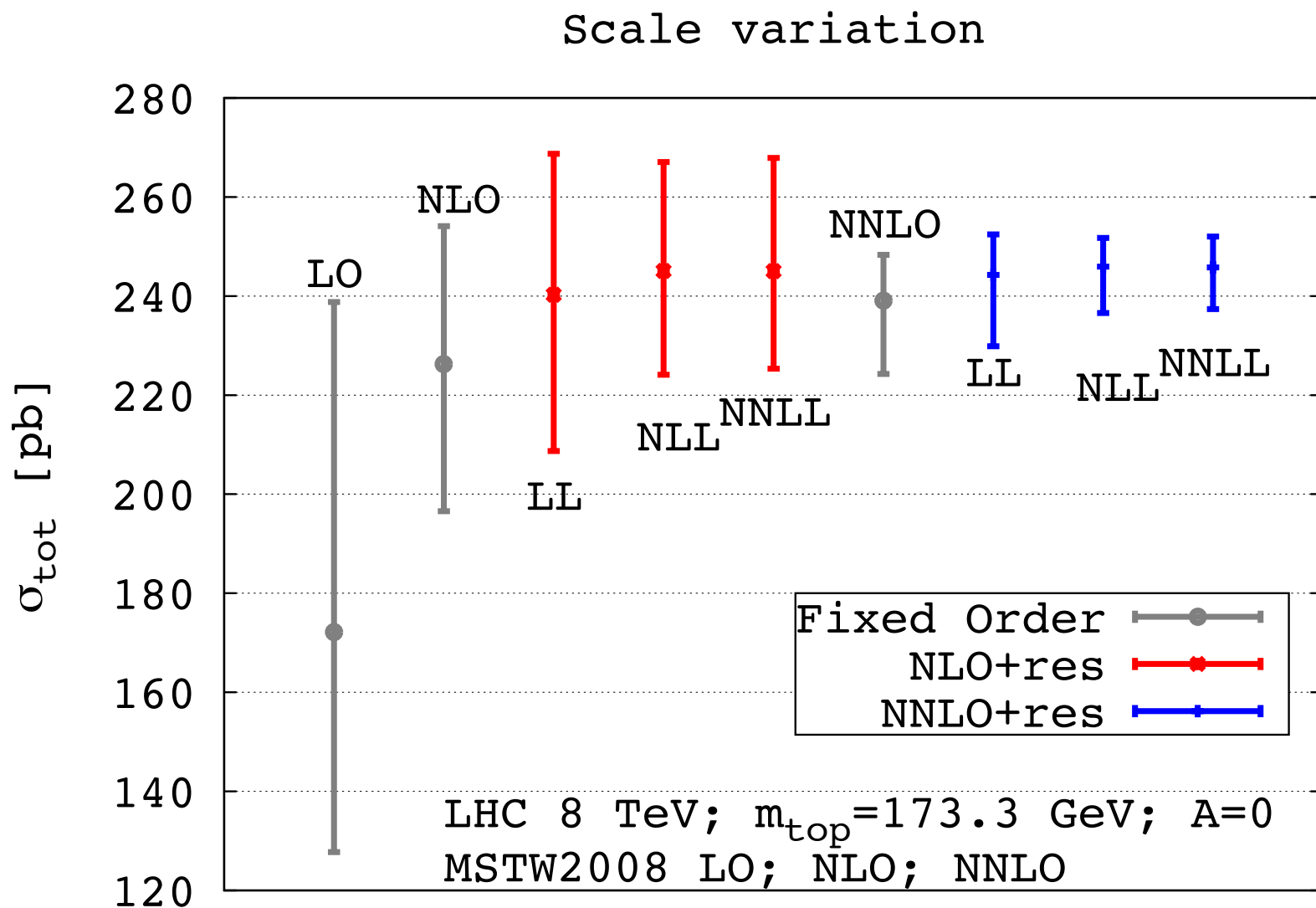
Top quark production

Production dominated by gg initial state up to very large p_T



⇒ sensitive probe of the gluon PDF

Great precision reached with the completion of the NNLO calculation



Independent μ_R , μ_F variation, with $\mu_0 = m_{\text{top}}$,
 $0.5 \mu_0 < \mu_{R,F} < 2 \mu_0$ and
 $0.5 < \mu_R / \mu_F < 2$

Baernreuther, Czakon, Mitov arXiv:1204.5201
Czakon, Mitov arXiv:1207.0236
Czakon, Mitov arXiv:1210.6832
Czakon, Fiedler, Mitov arXiv:1303.6254

Phenomenological study of $t\bar{t}$ production at NNLO

M. Czakon, M. Mangano, A. Mitov, J. Rojo arXiv:1303.7215

LHC 8 TeV

PDF set	$\sigma_{t\bar{t}}$ (pb)	δ_{scale} (pb)	δ_{PDF} (pb)	δ_{α_s} (pb)	δ_{m_t} (pb)	δ_{tot} (pb)
ABM11	198.6	+5.0 (+2.5%) -6.2 (-3.1%)	+8.5 (+4.3%) -8.5 (-4.3%)	+0.0 (+0.0%) -0.0 (-0.0%)	+6.1 (+3.1%) -5.9 (-3.0%)	+15.5 (+7.8%) -16.6 (-8.4%)
CT10	246.3	+6.4 (+2.6%) -8.6 (-3.5%)	+10.1 (+4.1%) -8.2 (-3.3%)	+4.9 (+2.0%) -4.9 (-2.0%)	+7.4 (+3.0%) -7.1 (-2.9%)	+19.8 (+8.1%) -20.5 (-8.3%)
HERA1.5	252.7	+6.5 (+2.6%) -5.9 (-2.3%)	+5.4 (+2.1%) -8.6 (-3.4%)	+4.0 (+1.6%) -4.0 (-1.6%)	+7.5 (+3.0%) -7.3 (-2.9%)	+16.6 (+6.6%) -17.8 (-7.1%)
MSTW08	245.8	+6.2 (+2.5%) -8.4 (-3.4%)	+6.2 (+2.5%) -6.2 (-2.5%)	+4.0 (+1.6%) -4.0 (-1.6%)	+7.4 (+3.0%) -7.1 (-2.9%)	+16.6 (+6.8%) -18.7 (-7.6%)
NNPDF2.3	248.1	+6.4 (+2.6%) -8.7 (-3.5%)	+6.6 (+2.7%) -6.6 (-2.7%)	+3.7 (+1.5%) -3.7 (-1.5%)	+7.5 (+3.0%) -7.2 (-2.9%)	+17.1 (+6.9%) -19.1 (-7.7%)
ATLAS	241.0					± 32.0 (13.3%)
CMS	227.0					± 15.0 (6.6%)

TH and parametric uncertainties are all of similar size:

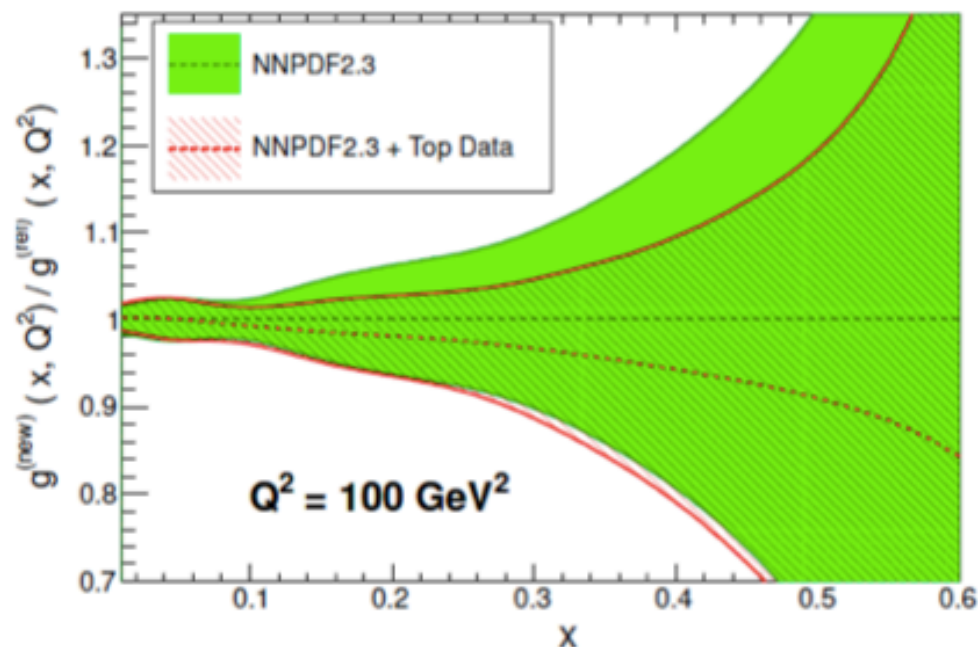
	scales (i.e. missing yet-higher order corrections)	$\sim 3\%$
	pdf (at 68%cl)	$\sim 2\text{-}3\%$
$\Delta\alpha_s = \pm 0.0007$ <input type="checkbox"/>	α_s (parametric)	$\sim 1.5\%$
$\Delta m_{\text{top}} = \pm 1 \text{ GeV}$ <input type="checkbox"/>	m_{top} (parametric)	$\sim 3\%$

Constraining the gluon PDF with $\sigma(t\bar{t})$

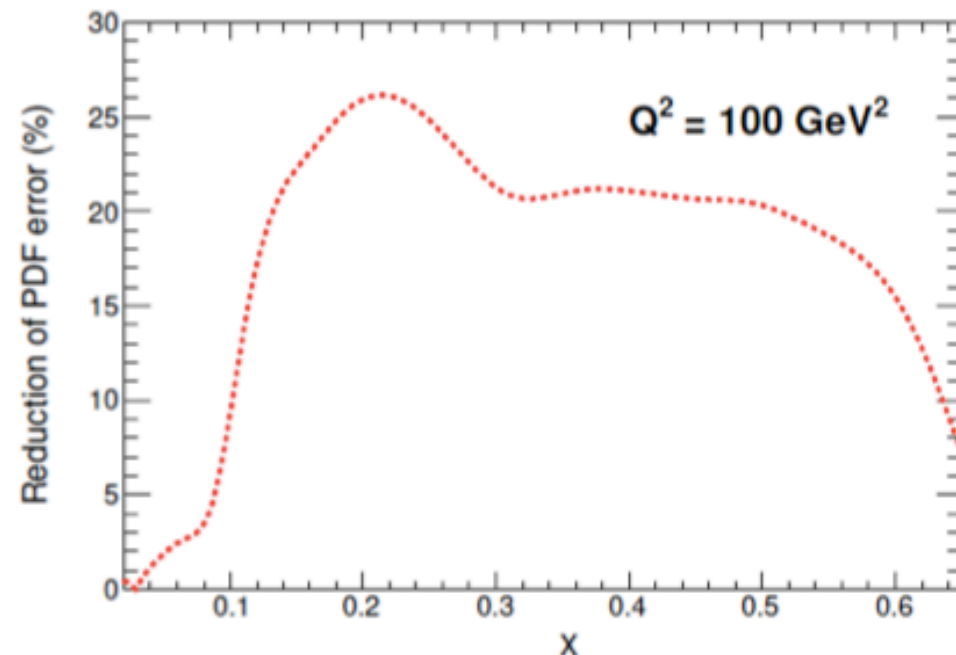
M. Czakon et al arXiv:1303.7215

- Top quark cross-section data **discriminates between PDF sets**
- In addition, it can also be used to **reduce the PDF uncertainties** within a single PDF set
- We included the most precise top quark data into the **NNPDF2.3** global PDF analysis

Ratio to NNPDF2.3 NNLO, $\alpha_s = 0.118$



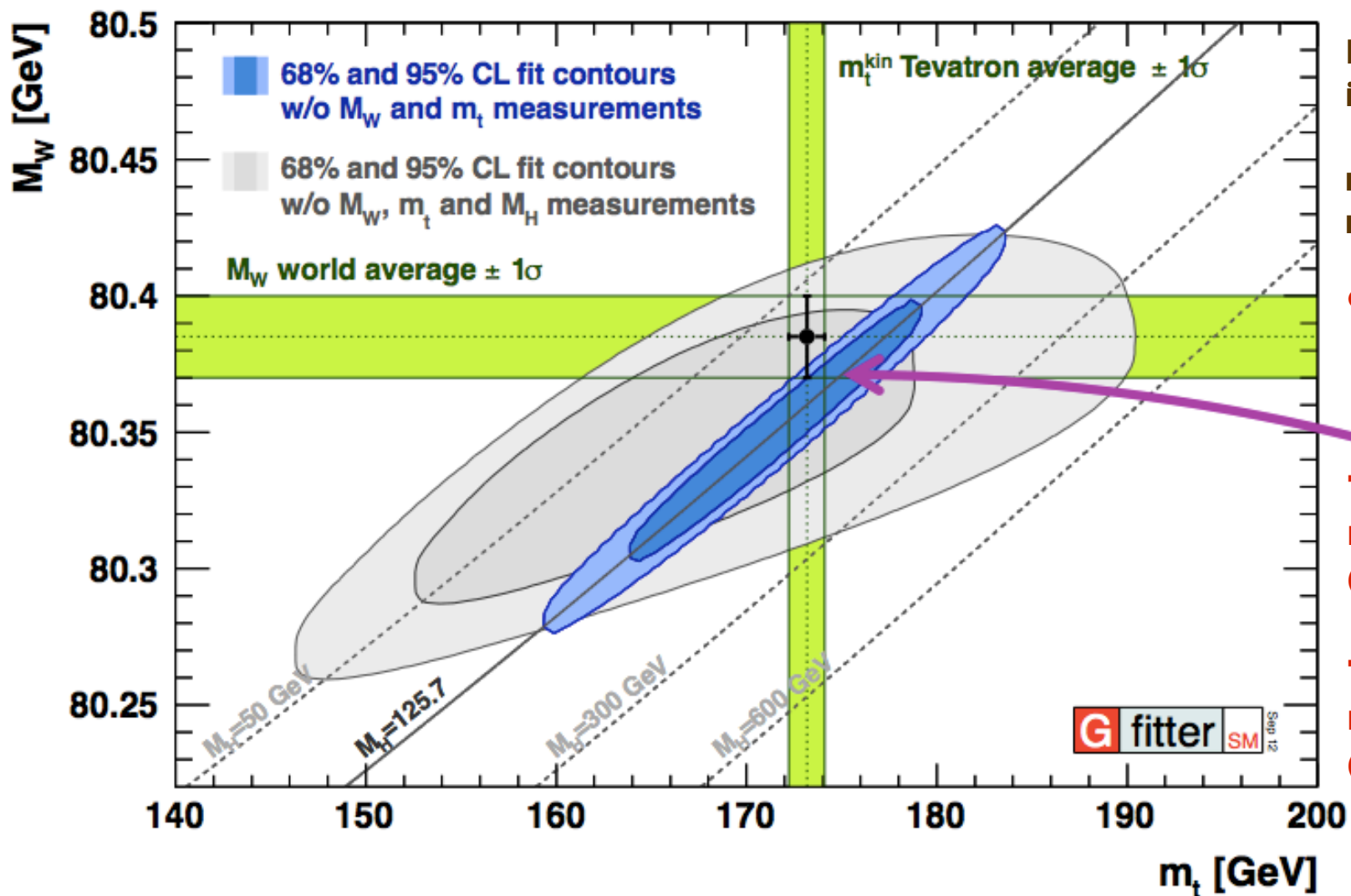
NNPDF2.3 NNLO + TeV, LHC Top Quark Data



Collider	Ref	Ref+TeV	Ref +TeV+LHC7	Ref+TeV+LHC7+8
Tevatron	7.26 ± 0.12	-	-	-
LHC 7 TeV	172.5 ± 5.2	172.7 ± 5.1	-	-
LHC 8 TeV	247.8 ± 6.6	248.0 ± 6.5	245.0 ± 4.6	-
LHC 14 TeV	976.5 ± 16.4	976.2 ± 16.3	969.8 ± 12.0	969.6 ± 11.6

Top quark and W mass

Inclusion of m_H in EW fits greatly tightens correlation between m_W and m_{top}
introducing perhaps a slight tension ?



New EW fit results, including m_{Higgs} :

**$m_{top} = 175.8^{+2.7}_{-2.4} \text{ GeV}$
 $m_W = 80359 \pm 11 \text{ MeV}$**

cfr:

**Tevatron+LEP2:
 $M_W = 80385 \pm 15 \text{ MeV}$**

**Tevatron+LHC:
 $m_t = 173.34 \pm 0.76 \text{ GeV}$
 (Mar 2014)**

**Tevatron:
 $m_t = 174.34 \pm 0.64 \text{ GeV}$
 (Jul 2014)**

Continued improvement in the direct determination of m_W and m_{top} remains a high priority

Tevatron combined W mass: $M_W = 80387 \pm 16$ MeV

Tevatron+LEP2 combined W mass: $M_W = 80385 \pm 15$ MeV

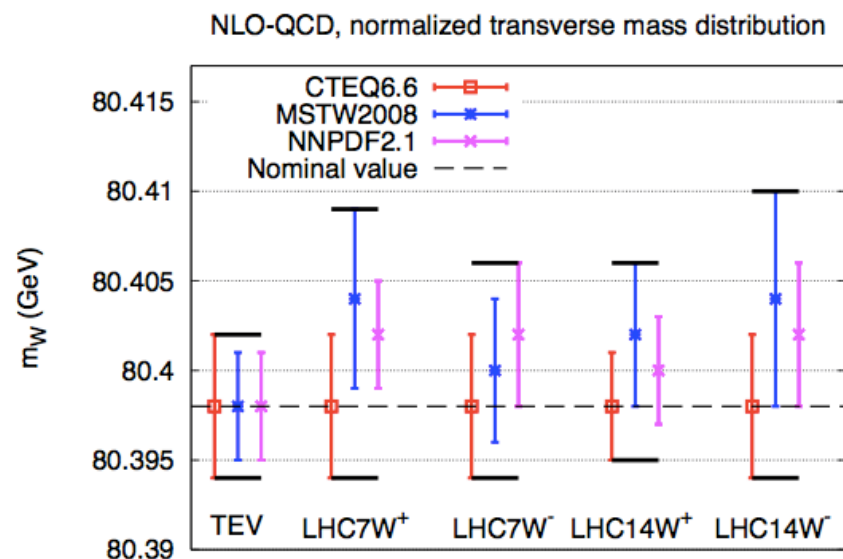
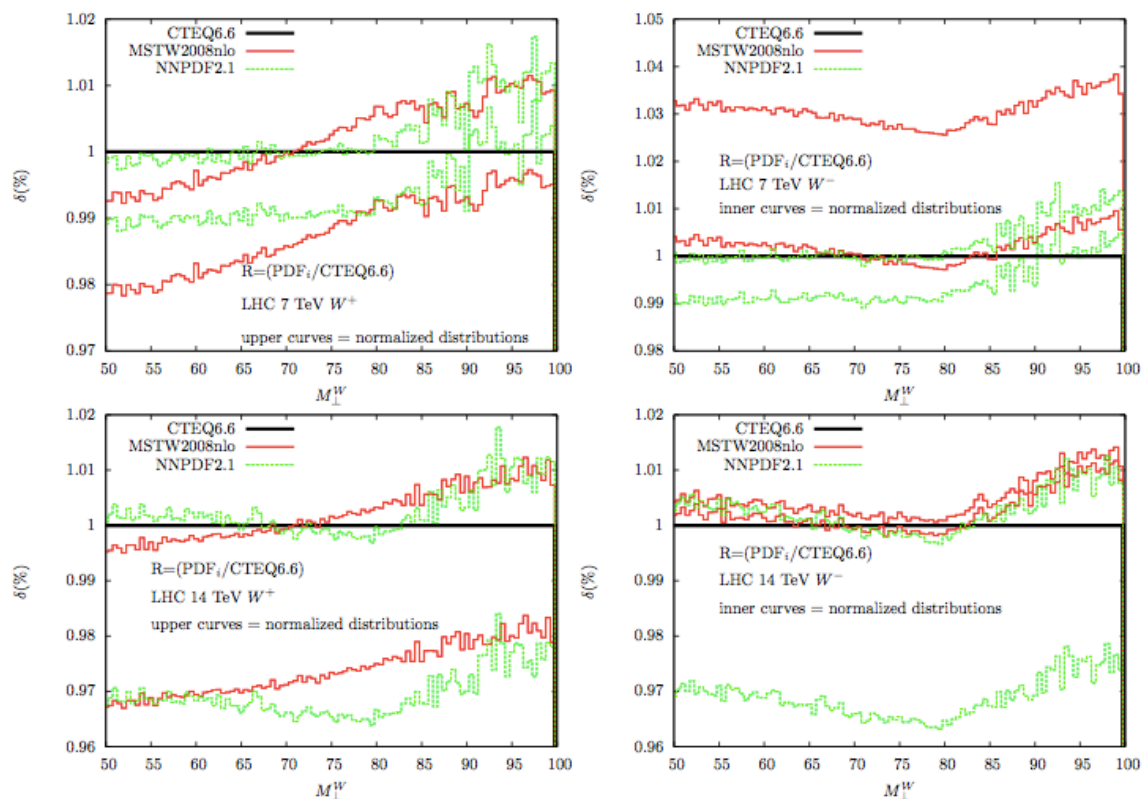
Uncertainties

Uncertainty	D0	CDF	
Lepton energy scale/resn/modelling	17	7	<i>Largely stat. in origin</i> 10 MeV
Hadronic recoil energy scale and resolution	5	6	
Backgrounds	2	3	
Parton distributions	11	10	<i>Largely theory in origin</i> 12 MeV
QED radiation	7	4	
$p_T(W)$ model	2	5	
Total systematic uncertainty	22	15	
W-boson statistics	13	12	
Total uncertainty	26 MeV	19 MeV	

90% of M_W information is in transverse mass

Predictions for PDF-induced TH syst at the LHC

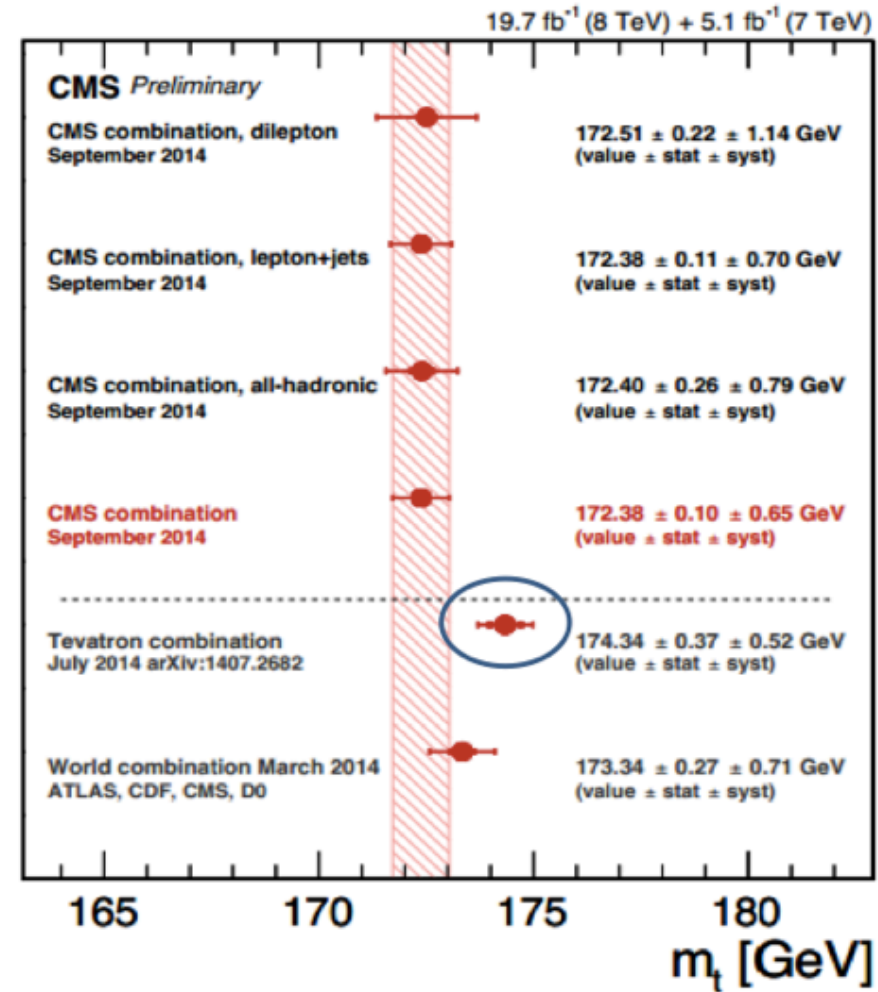
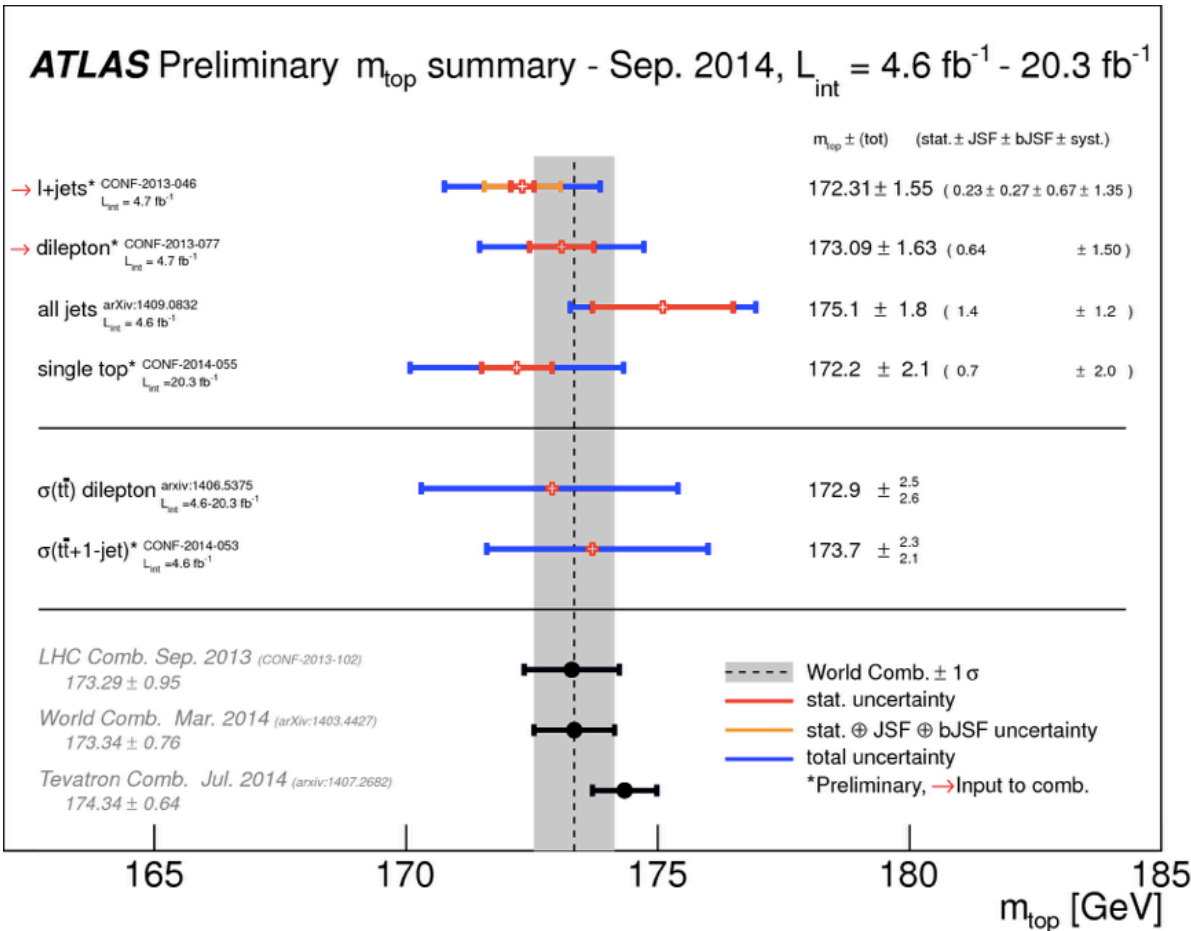
Bozzi, Rojo, Vicini, arXiv:1104.2056, updated in arXiv:1309.1311



Theory syst:
 $\Delta m_w \approx \pm 8 \text{ MeV}$

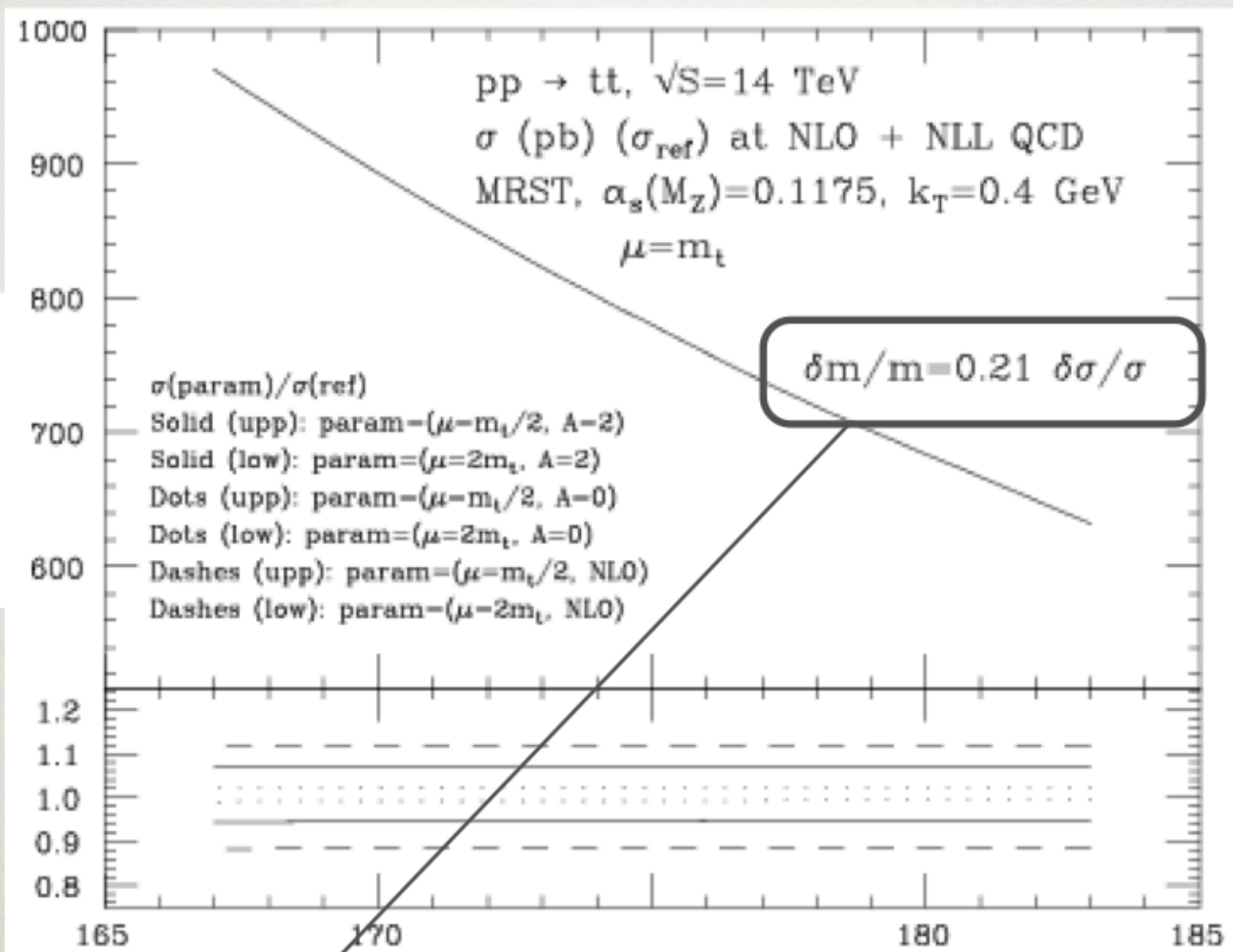
- This uncertainty should be further reduced, to be confident that it's negligible in the context of a measurement with a total systematics of less than $\pm 20 \text{ MeV}$
- These systematics should be validated through dedicated measurements: can one extract at the same time PDF and m_w from the fit of the relevant distributions (e.g. $pt(e)$)?
- there remain issues raised by Krasny et al, Eur. Phys. J. C 69, 379 (2010) which are not fully addressed by this study (e.g. the impact of the charm mass in using $pt(Z)$ to model $pt(W)$)

Top quark mass



m_{top} from t-tbar cross section at the LHC

$\sigma(tt)$ [pb]



m_{top}

$\Delta\sigma/\sigma = \pm 5\% \Leftrightarrow \Delta m/m = \pm 1\% \lesssim 2 \text{ GeV}$, comparable to Δm_{direct}
 ~ 2 larger than

Top decay

Exercise

t → bW

$$\frac{m_t}{16\pi} y_t^2$$

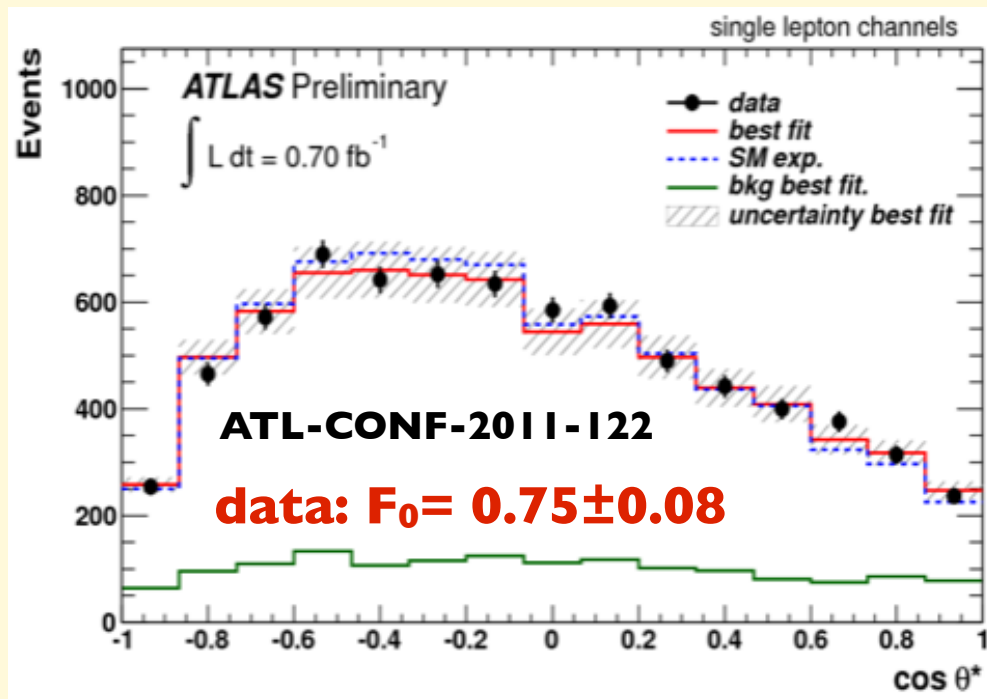
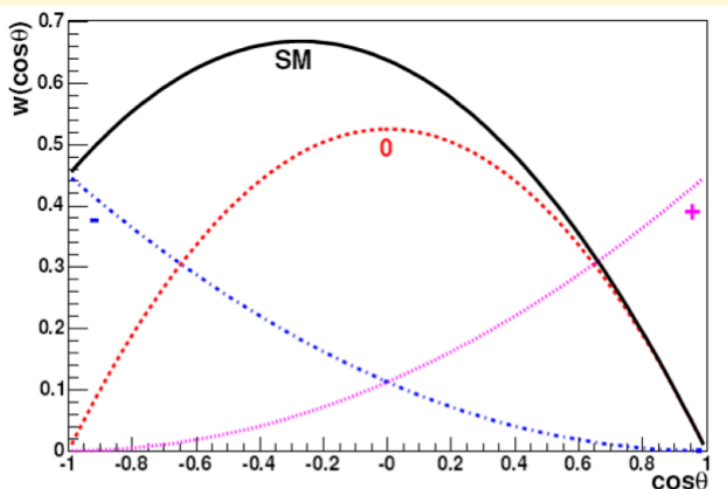
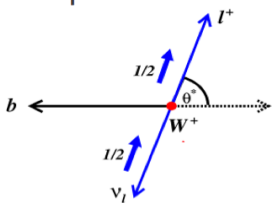
Coupling to longitudinal W, i.e. Goldstone boson

Coupling to transverse W d.o.f.

$$\Gamma_t = \frac{G_F m_t^3}{8\pi\sqrt{2}} \left(1 - \frac{M_W^2}{m_t^2}\right)^2 \left(1 + 2\frac{M_W^2}{m_t^2}\right) \left[1 - \frac{2\alpha_s}{3\pi} \left(\frac{2\pi^2}{3} - \frac{5}{2}\right)\right]$$

1) $\#(W_{\text{longitudinal}}) = m_t^2 / (m_t^2 + 2M_W^2) = 0.687 \pm 0.005$

Cos θ* = angle between charged lepton and top direction in W rest-frame



Top decay

Exercise

t → bW

$$\frac{m_t}{16\pi} y_t^2$$

Coupling to longitudinal W, i.e. Goldstone boson

Coupling to transverse W d.o.f.

$$\Gamma_t = \frac{G_F m_t^3}{8\pi\sqrt{2}} \left(1 - \frac{M_W^2}{m_t^2}\right)^2 \left(1 + 2\frac{M_W^2}{m_t^2}\right) \left[1 - \frac{2\alpha_s}{3\pi} \left(\frac{2\pi^2}{3} - \frac{5}{2}\right)\right]$$

2) $\Gamma_{\text{top}} \sim 1.34 \text{ GeV} > \tau_{\text{had}}^{-1} \sim \Lambda_{\text{QCD}}$

t-quark DECAY WIDTH

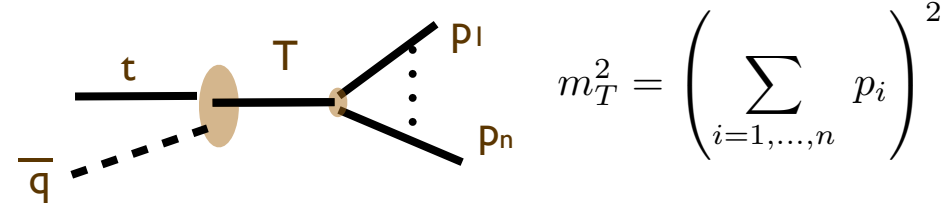
VALUE (GeV)	CL%	DOCUMENT ID	TECN	COMMENT
$1.99^{+0.69}_{-0.55}$		¹ ABAZOV	11B D0	$\Gamma(t \rightarrow Wb)/B(t \rightarrow Wb)$

¹ Based on 2.3 fb^{-1} in $p\bar{p}$ collisions at $\sqrt{s} = 1.96 \text{ TeV}$. ABAZOV 11B extracted Γ_t from the partial width $\Gamma(t \rightarrow Wb) = 1.92^{+0.58}_{-0.51} \text{ GeV}$ measured using the t-channel single top production cross section, and the branching fraction $\text{br}(t \rightarrow Wb) = 0.962^{+0.068}_{-0.066}(\text{stat})^{+0.064}_{-0.052}(\text{syst})$. The $\Gamma(t \rightarrow Wb)$ measurement gives the 95% CL lowerbound of $\Gamma(t \rightarrow Wb)$ and hence that of Γ_t .

⇒ Top quark decays before hadronizing: there are no top-hadrons

Why is it hard to measure/define m_{top} at the LHC ?

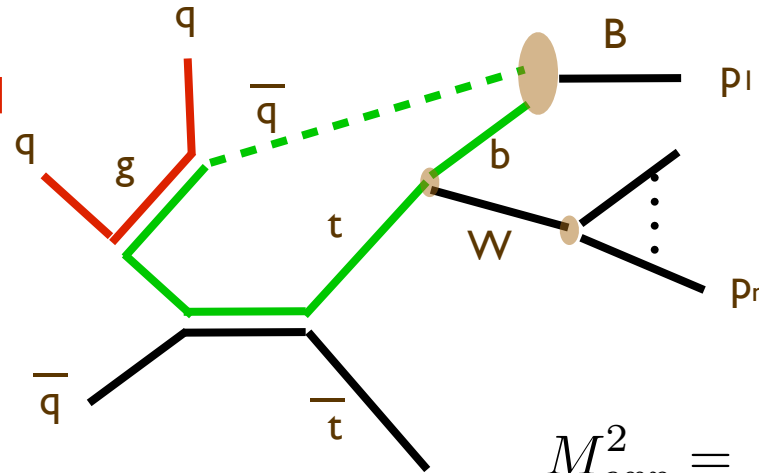
If $\Gamma_{top} < 1 \text{ GeV}$, top would hadronize before decaying. Same as b-quark



$$m_T^2 = \left(\sum_{i=1, \dots, n} p_i \right)^2$$

$$m_t = F_{\text{lattice/potential models}}(m_T, \alpha_{\text{QCD}})$$

But $\Gamma_{top} > 1 \text{ GeV}$, top decays before hadronizing. Extra antiquarks must be added to the top-quark decay final state in order to produce the physical state whose mass will be measured



$$M_{exp}^2 = \left(\sum_{i=1, \dots, n} p_i \right)^2$$

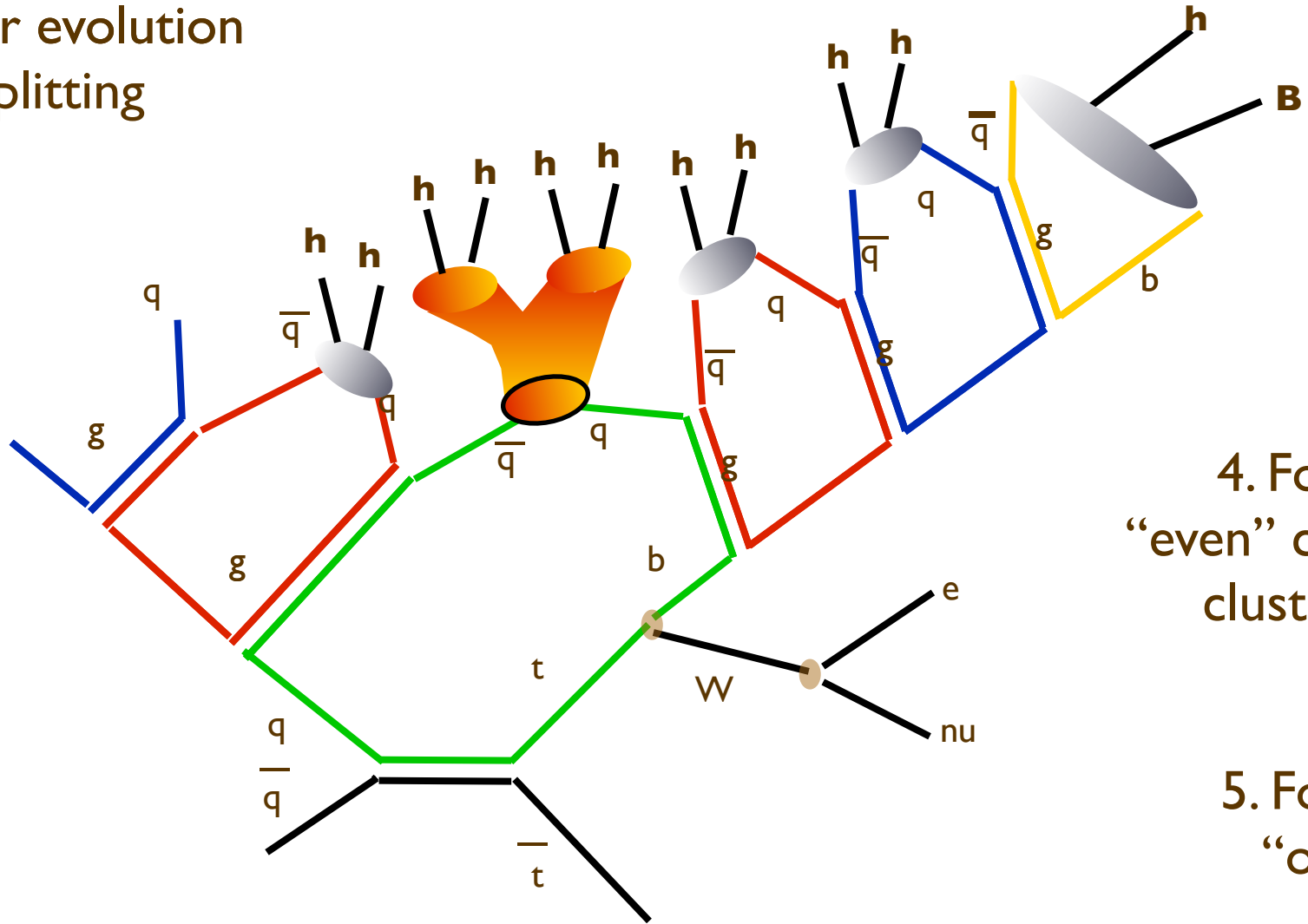
As a result, M_{exp} is not equal to $m_{pole_{top}}$, and will vary in each event, depending on the way the event has evolved.

The top mass extracted in hadron collisions is not well defined below a precision of $O(\Gamma_{top}) \sim 1 \text{ GeV}$

Goal:

- correctly quantify the systematic uncertainty
- identify observables that allow to validate the theoretical modeling of hadronization in top decays
- identify observables less sensitive to these effects

1. Hard Process
2. Shower evolution
3. Gluon splitting



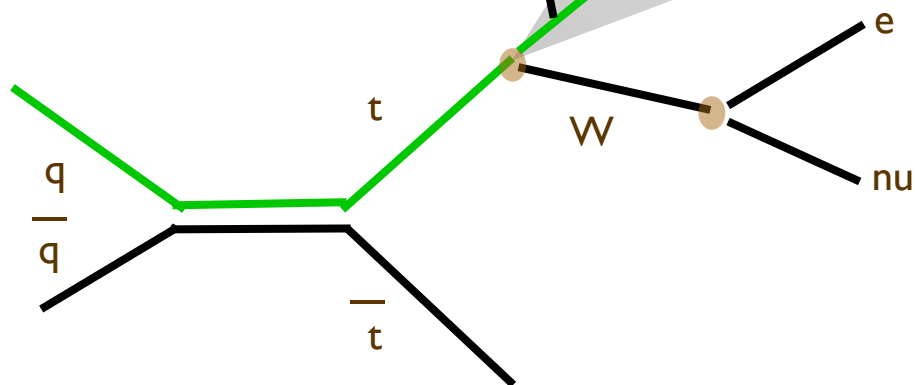
4. Formation of “even” clusters and cluster decay to hadrons

5. Formation of “odd” cluster

6. Decay of “odd” clusters, if large cluster mass, and decays to hadrons

Controlled by perturbative shower evolution, mostly insensitive to hadronization modeling

Partly shower evolution, partly color reconnection, ambiguous paternity



Out-of-cone radiation, controlled by perturbative shower evolution, minimally sensitive to hadronization modeling

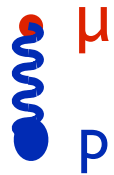
m_{MC} VS m_{pole}

Consider a simplified example

Take $\mu \rightarrow e\nu\nu$.

$$m_\mu = m_{pole} \text{ and } m_\mu^2 = [p(e)+p(\nu)+p(\nu)]^2$$

Take μ interacting with an external field, e.g. bound with a proton in an atom:



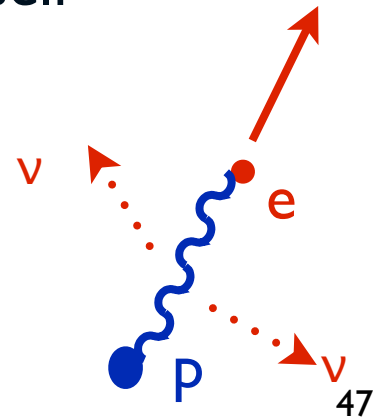
$$E = m_p + m_\mu + (K + V)_\mu = m_p + m_\mu - m_\mu \alpha^2/2 = m_p + m_\mu^*$$

$m_\mu^* = m_\mu (1 - \alpha^2/2)$ absorbs part of the potential energy into itself

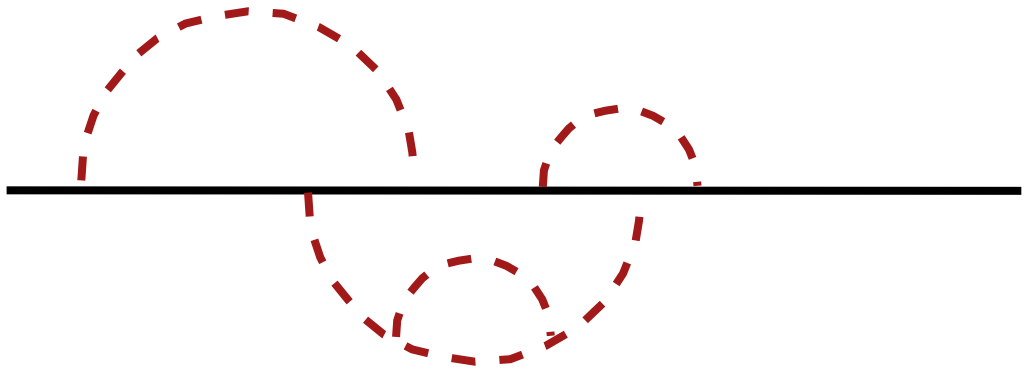
It is a “useful” mass, since, once the muon decays,

$$[p(e)+p(\nu)+p(\nu)]^2 = m_\mu^{*2}, \text{ which } \neq m_\mu^2 \text{ by } O(\alpha^2)$$

The reason is that the electron, to escape, must overcome the Coulomb potential, and its energy will be shifted by $V = -m_\mu\alpha^2$

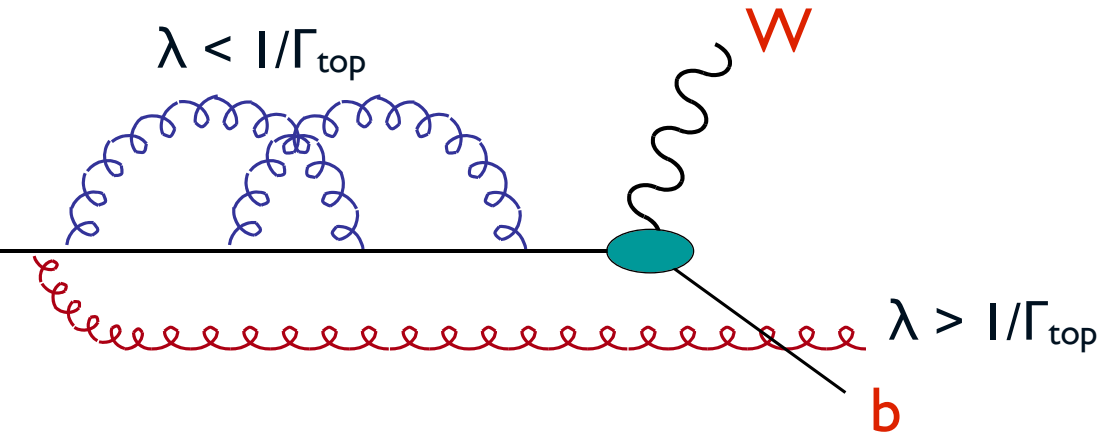


In the case of a quark, the potential is due to the interaction with its own gluon field



The pole mass is defined by resumming the effects of all these diagrams, absorbing all divergences. However, we know that we find problems if we integrate the loop momenta below the scale Λ_{QCD} , where perturbation theory breaks down. If we do it, to define m_{pole} , the perturbative series can only be resummed up to a (“renormalon”) ambiguity. If we stop before, at some scale, we dump into a m^* mass the self-energy potential due to modes with wavelength above that scale.

This is further justified for the top, which anyway only lives $1/\Gamma_{\text{top}}$, so gluons with wavelength $> 1/\Gamma_{\text{top}}$ are cutoff:

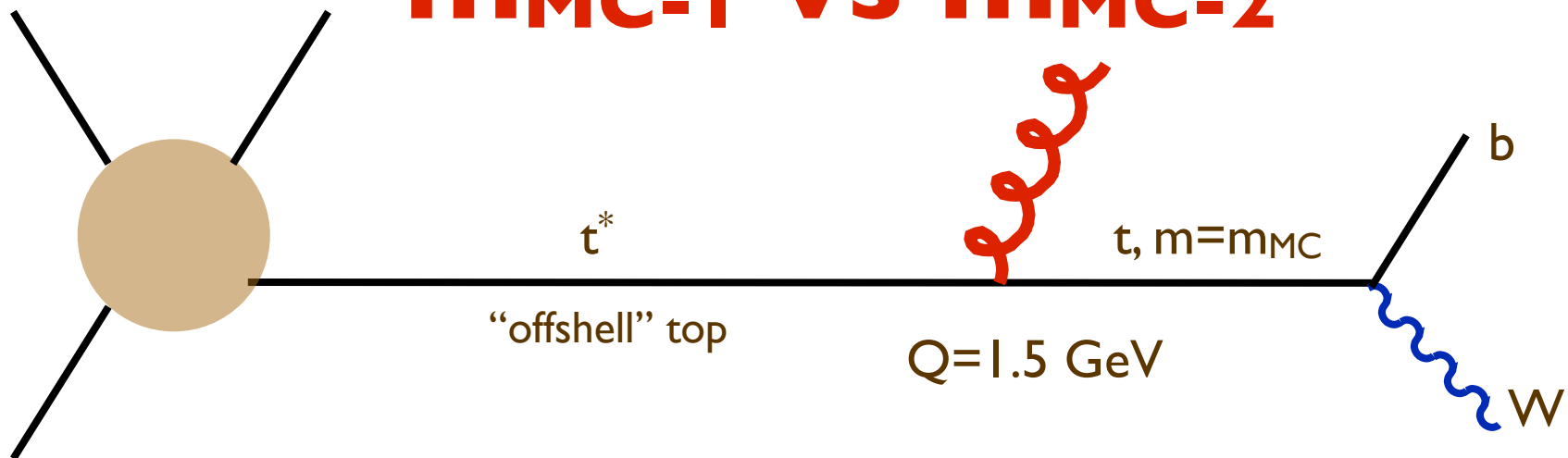


In this case,

$$\delta m \sim \alpha_s \Gamma_{\text{top}}$$

what is the coefficient ? 48

m_{MC-1} VS m_{MC-2}



This emission at scale $Q=1.5$ GeV may or may not be present in the MC, depending on the IR cutoff scale of the shower (e.g. 1 GeV vs 2 GeV). One may consider this is as using m_{MSR} defined at different scales, or as using different top-mass definitions.

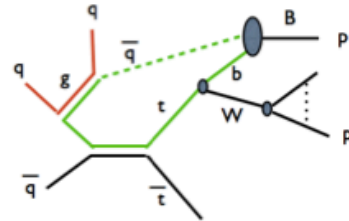
The question is whether the emission of the extra gluons in the region ($\text{cutoff}_{MC-1} - \text{cutoff}_{MC-2}$) affects the observables used to measure m_{MC} and change the measured value

Typically we consider these possible differences as part of the shower/hadronization systematics. There is no evidence that they exceed the 100 MeV level.

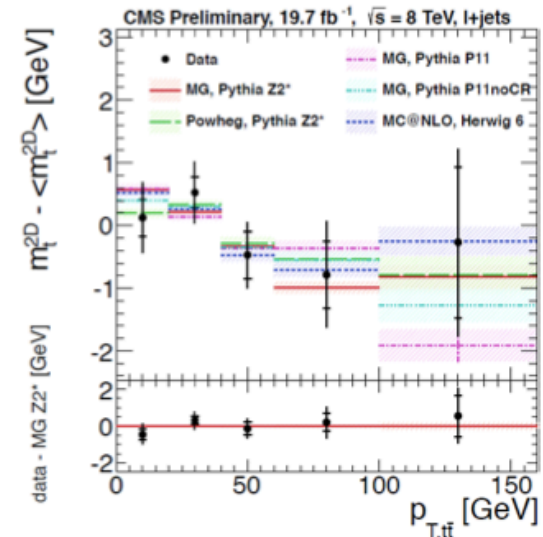
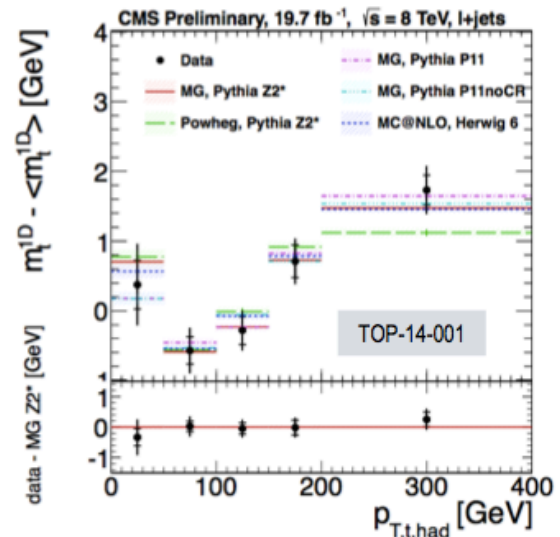
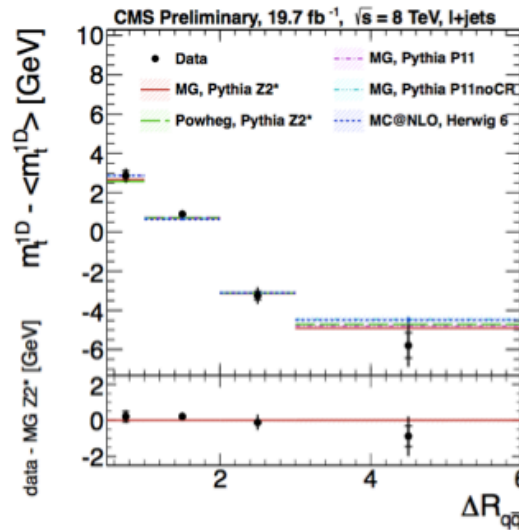
Studies like those shown by CMS (m_{top} vs different production configurations) are crucial to understand the sensitivity to these effects, the consistency of the modeling in different MC, with data and with themselves

Top Mass: Kinematic Dependence

- Probe for issues with QCD modeling or Mass Definition by looking for kinematic dependence in extracted top mass
- Investigate distributions with sensitivity to
 - Color reconnection
 - ISR/FSR
 - b-quark kinematics
- Figures: $m_{top} - \langle m_{top} \rangle$
- Check 14 variables; ≈ 50 total bins



Observable	$m_t^{1D} \chi^2$	JSF χ^2	$m_t^{2D} \chi^2$	Ndf
$\Delta R_{q\bar{q}}$	2.87	3.66	0.83	3
$p_{T,t, had}$	0.89	12.03	5.76	4
$ \eta_{t, had} $	5.56	1.22	1.14	3
H_T^4	6.19	9.18	7.54	4
$m_{t\bar{t}}$	2.16	4.69	4.22	5
$p_{T,t\bar{t}}$	1.02	1.22	1.33	4
Jet multiplicity	4.24	0.10	1.16	2
$p_{T,b, had}$	2.57	5.80	2.17	4
$ \eta_{b, had} $	1.15	0.08	0.72	2
$\Delta R_{b\bar{b}}$	0.37	1.63	1.77	3
$p_{T,q, had}^1$	4.04	8.39	1.28	4
$ \eta_{q, had}^1 $	3.36	3.79	6.27	2
$p_{T,W, had}$	1.59	8.06	1.60	4
$ \eta_{W, had} $	1.41	1.09	1.35	3
Total	37.43	60.94	37.15	47



No significant deviations between data and various models w.r.t their kinematic dependence

17

$$\Delta m_t = m_t^{had} - m_{\bar{t}}^{had} = -272 \pm 196 (stat) \pm 122 (syst.) MeV$$

remarks

QCD effects depend on how long the top actually lives. Should one change m_{MC} as a function of lifetime, event by event ?

When a top lives longer than $1/\Lambda_{QCD}$ (prob $\sim \exp(-\Gamma_{top}/\Lambda_{QCD})$) it likely hadronizes

8TeV/7TeV and 14TeV/8TeV cross section ratios: the ultimate precision

MLM and J.Rojo, arXiv:1206.3557

E_{1,2}: different beam energies

X,Y: different hard processes

$$R_{E_2/E_1}(X) \equiv \frac{\sigma(X, E_2)}{\sigma(X, E_1)} \longrightarrow$$

- TH: reduce “scale uncertainties”
- TH: reduce parameters’ systematics: PDF, m_{top} , α_S , ... at E_1 and E_2 are fully correlated
- TH: reduce MC modeling uncertainties
- EXP: reduce syst’s from acceptance, efficiency, JES, ...

$$R_{E_2/E_1}(X, Y) \equiv \frac{\sigma(X, E_2)/\sigma(Y, E_2)}{\sigma(X, E_1)/\sigma(Y, E_1)} \equiv \frac{R_{E_2/E_1}(X)}{R_{E_2/E_1}(Y)} \longrightarrow$$

- TH: possible further reduction in scale and PDF syst’s
- EXP: no luminosity uncertainty
- EXP: possible further reduction in acc, eff, JES syst’s (e.g. X,Y=W⁺,W⁻)

14 TeV / 8 TeV: NNPDF results

CrossSection	$r^{\text{th,nnpdf}}$	$\delta_{\text{PDF}}(\%)$	$\delta_{\alpha_s}(\%)$	$\delta_{\text{scales}}(\%)$
$t\bar{t}/Z$	2.121	1.01	-0.84 - 0.75	0.42 - 1.10
$t\bar{t}$	3.901	0.84	-0.51 - 0.66	0.38 - 1.07
Z	1.839	0.37	-0.10 - 0.34	0.28 - 0.18
W^+	1.749	0.41	-0.03 - 0.27	0.31 - 0.18
W^-	1.859	0.39	-0.08 - 0.26	0.32 - 0.13
W^+/W^-	0.941	0.28	0.00 - 0.05	0.00 - 0.04
W/Z	0.976	0.09	-0.07 - 0.04	0.04 - 0.02
ggH	2.564	0.36	-0.10 - 0.09	0.89 - 0.98
$ggH/t\bar{t}$	0.657	0.75	-0.56 - 0.41	1.38 - 1.05
$t\bar{t}(M_{t\bar{t}} \geq 1\text{TeV})$	8.215	2.09	0.00 - 0.00	1.61 - 2.06
$t\bar{t}(M_{t\bar{t}} \geq 2\text{TeV})$	24.776	6.07	0.00 - 0.00	3.05 - 1.07
$\sigma_{\text{jet}}(p_T \geq 1\text{TeV})$	15.235	1.72	0.00 - 0.00	2.31 - 2.19
$\sigma_{\text{jet}}(p_T \geq 2\text{TeV})$	181.193	6.75	0.00 - 0.00	3.66 - 5.76

- $\delta < 10^{-2}$ in W^\pm ratios: absolute calibration of 14 vs 8 TeV lumi
- $\delta \sim 10^{-2}$ in $\sigma(t\bar{t})$ ratios
- $\delta_{\text{scale}} < \delta_{\text{PDF}}$ at large p_T^{jet} and $M_{t\bar{t}}$: constraints on PDFs

14 TeV / 8 TeV: NNPDF vs MSTW vs ABKM

Ratio	$r^{\text{th,nnpdf}}$	$\delta_{\text{PDF}}(\%)$	$r^{\text{th,mstw}}$	$\delta_{\text{PDF}}(\%)$	$\Delta^{\text{mstw}}(\%)$	$r^{\text{th,abkm}}$	$\delta_{\text{ABKM}}(\%)$	$\Delta^{\text{abkm}}(\%)$
$t\bar{t}/Z$	2.121	1.01	2.108	0.95	0.93	2.213	1.87	-3.99
$t\bar{t}$	3.901	0.84	3.874	0.91	0.97	4.103	1.87	-4.90
Z	1.839	0.37	1.838	0.41	0.04	1.855	0.34	-0.87
W^+	1.749	0.41	1.749	0.49	0.03	1.767	0.30	-0.98
W^-	1.859	0.39	1.854	0.42	0.21	1.879	0.32	-1.11
W^+/W^-	0.941	0.28	0.943	0.19	-0.19	0.940	0.13	0.13
W/Z	0.976	0.09	0.976	0.10	0.03	0.977	0.10	-0.14
ggH	2.564	0.36	2.572	0.57	-0.30	2.644	0.66	-3.12
$ggH/t\bar{t}$	0.657	0.75	0.000	0.00	0.00	0.000	0.00	0.00
$t\bar{t}(M_{t\bar{t}} \geq 1\text{TeV})$	8.215	2.09	7.985	2.02	3.12	8.970	3.58	-8.83
$t\bar{t}(M_{t\bar{t}} \geq 2\text{TeV})$	24.776	6.07	23.328	4.32	6.05	23.328	4.93	6.05
$\sigma_{\text{jet}}(p_T \geq 1\text{TeV})$	15.235	1.72	15.193	1.62	-1.33	14.823	1.84	1.13
$\sigma_{\text{jet}}(p_T \geq 2\text{TeV})$	181.193	6.75	191.208	3.34	-6.52	174.672	4.94	2.69

- Several examples of $3\text{-}4\sigma$ discrepancies between predictions of different PDF sets, even in the case of W and Z rates

Xsection ratios as probes of BSM contributions

Assume the final state **X** receives both SM and BSM contributions:

$$\sigma^{exp}(pp \rightarrow X) = \sigma^{SM}(pp \rightarrow X) + \sigma^{BSM}(pp \rightarrow X)$$

Define the ratio:

$$R_{7/8}^X = \frac{\sigma^{exp}(pp \rightarrow X; 7 \text{ TeV})}{\sigma^{exp}(pp \rightarrow X; 8 \text{ TeV})} = \frac{\sigma_X^{exp}(7)}{\sigma_X^{exp}(8)}$$

We easily get:

$$R_{7/8}^X \sim \frac{\sigma_X^{SM}(7)}{\sigma_X^{SM}(8)} \times \left\{ 1 + \frac{\sigma_X^{BSM}(7)}{\sigma_X^{SM}(7)} \Delta_{7/8} \left[\frac{\sigma_X^{BSM}}{\sigma_X^{SM}} \right] \right\}$$

where:

$$\Delta_{7/8} \left[\frac{\sigma_X^{BSM}}{\sigma_X^{SM}} \right] = 1 - \frac{\sigma_X^{BSM}(8)/\sigma_X^{SM}(8)}{\sigma_X^{BSM}(7)/\sigma_X^{SM}(7)} \sim 1 - \frac{\mathcal{L}_X^{BSM}(8)/\mathcal{L}_X^{BSM}(7)}{\mathcal{L}_X^{SM}(8)/\mathcal{L}_X^{SM}(7)} = \Delta_{7/8} \left[\frac{\mathcal{L}_X^{BSM}}{\mathcal{L}_X^{SM}} \right]$$

Therefore:

$$\frac{\delta R_{7/8}^X}{R_{7/8}^X} = \frac{\delta R_{7/8}^{SM}}{R_{7/8}^{SM}} + \frac{\sigma_X^{BSM}(7)}{\sigma_X^{SM}(7)} \times \Delta_{7/8} \left[\frac{\mathcal{L}_X^{BSM}}{\mathcal{L}_X^{SM}} \right]$$

↑
relative BSM contamination
↓

↑
Energy dependence of the relative BSM contamination
↑

theory systematics in 7→8 TeV extrapolation

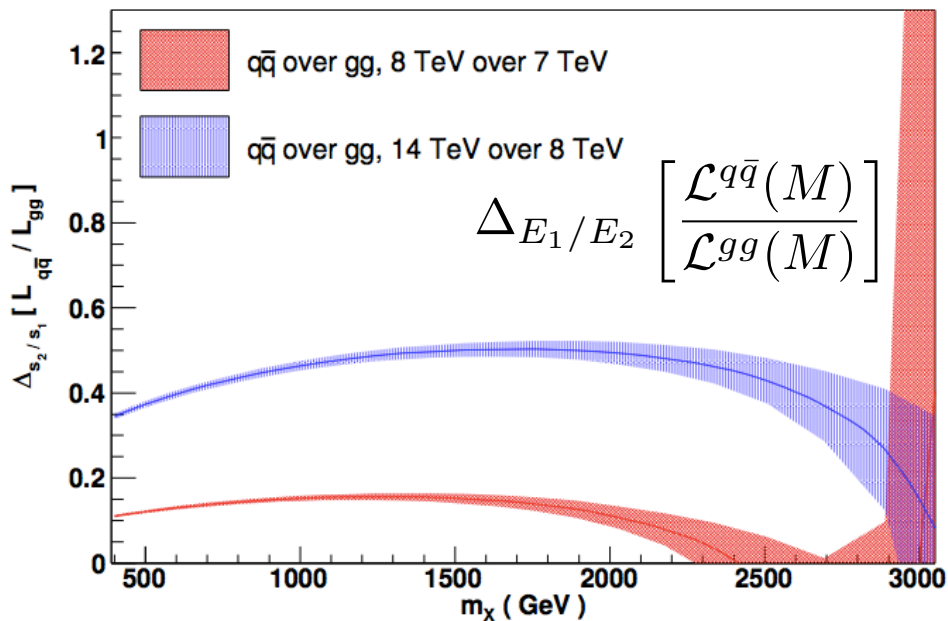
E.g., assuming $\sigma_{SM}(pp \rightarrow X) = \sigma(gg \rightarrow X)$ and $\sigma_{BSM}(pp \rightarrow X) = \sigma(qq \rightarrow X)$ (*)

$$\Delta_{7/8} \left[\frac{\mathcal{L}_X^{BSM}}{\mathcal{L}_X^{SM}} \right] = \Delta_{7/8} \left[\frac{\mathcal{L}^{q\bar{q}}(M)}{\mathcal{L}^{gg}(M)} \right]$$

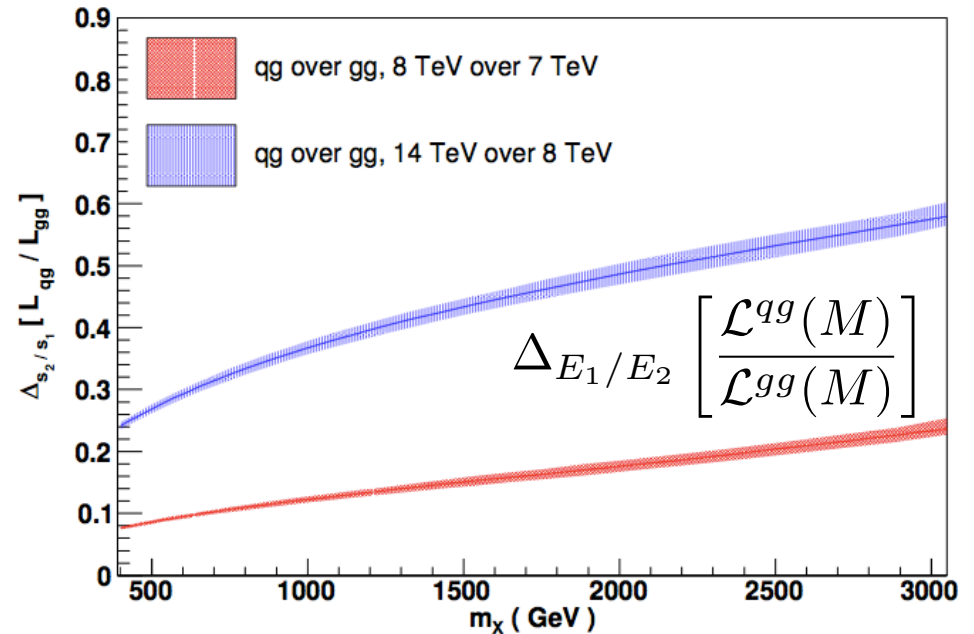
(*) e.g. SM: $gg \rightarrow tt$ and BSM: $qq\bar{q} \rightarrow Z' \rightarrow tt$

Examples of E-dependence of luminosity ratios

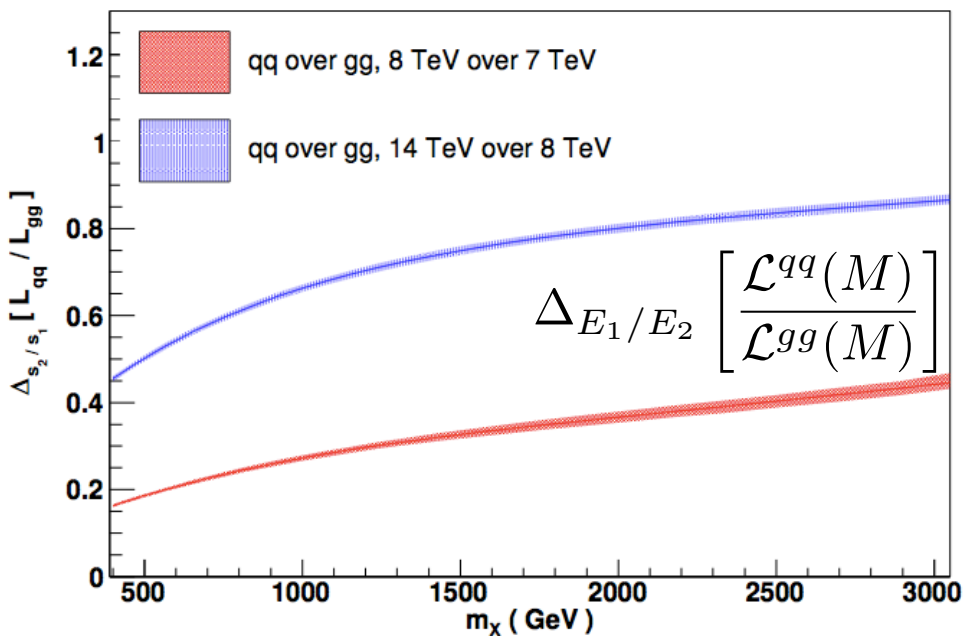
Parton Luminosities, NNPDF2.1 NNLO



Parton Luminosities, NNPDF2.1 NNLO



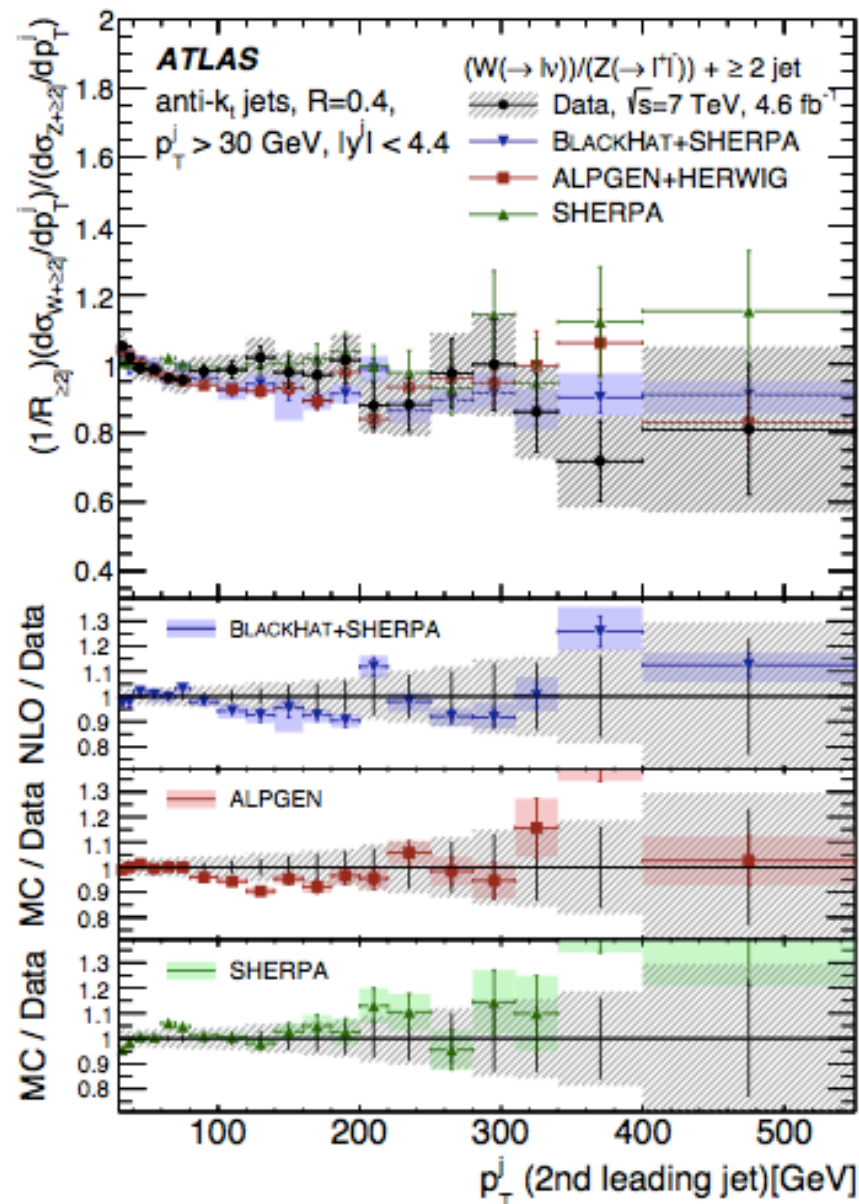
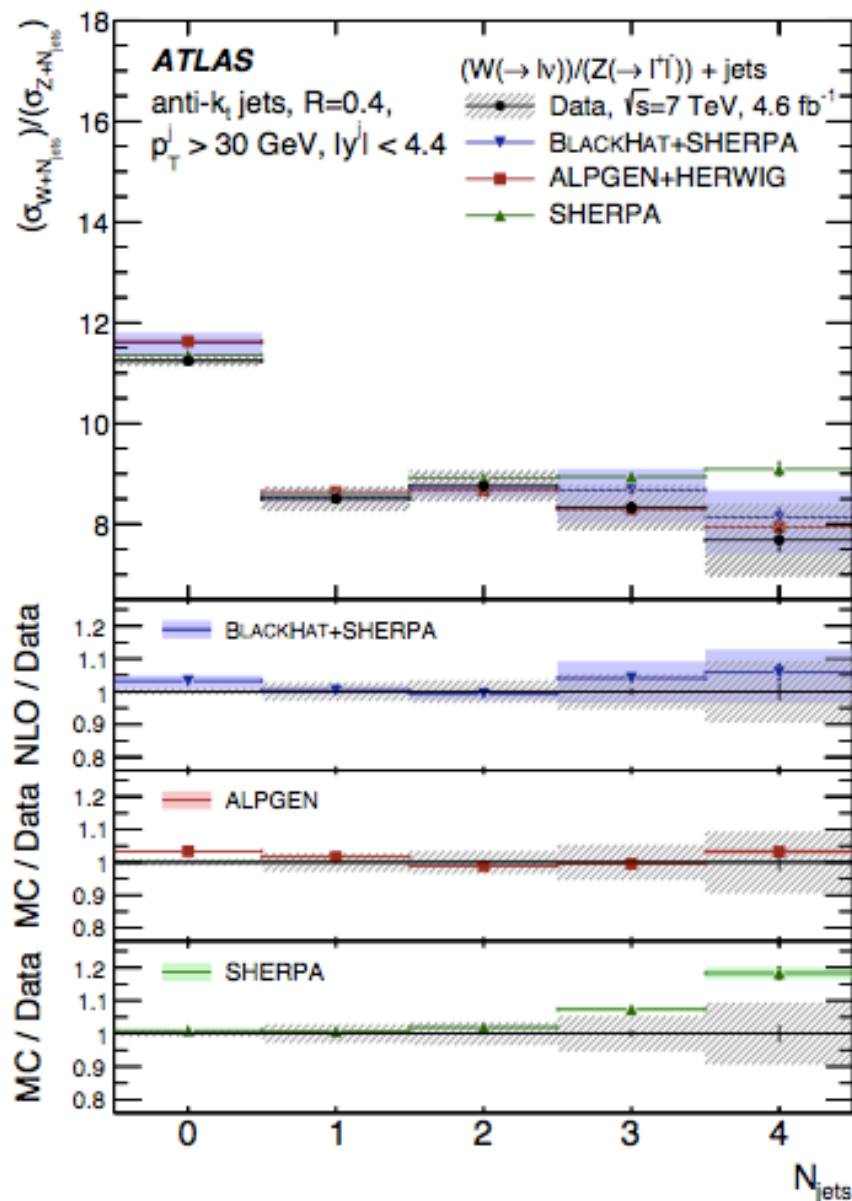
Parton Luminosities, NNPDF2.1 NNLO



Given the sub-% precision of the SM ratio predictions, there is sensitivity to BSM rate contributions at the level of few% (to be improved with better PDF constraints, especially for 8/14 ratios)

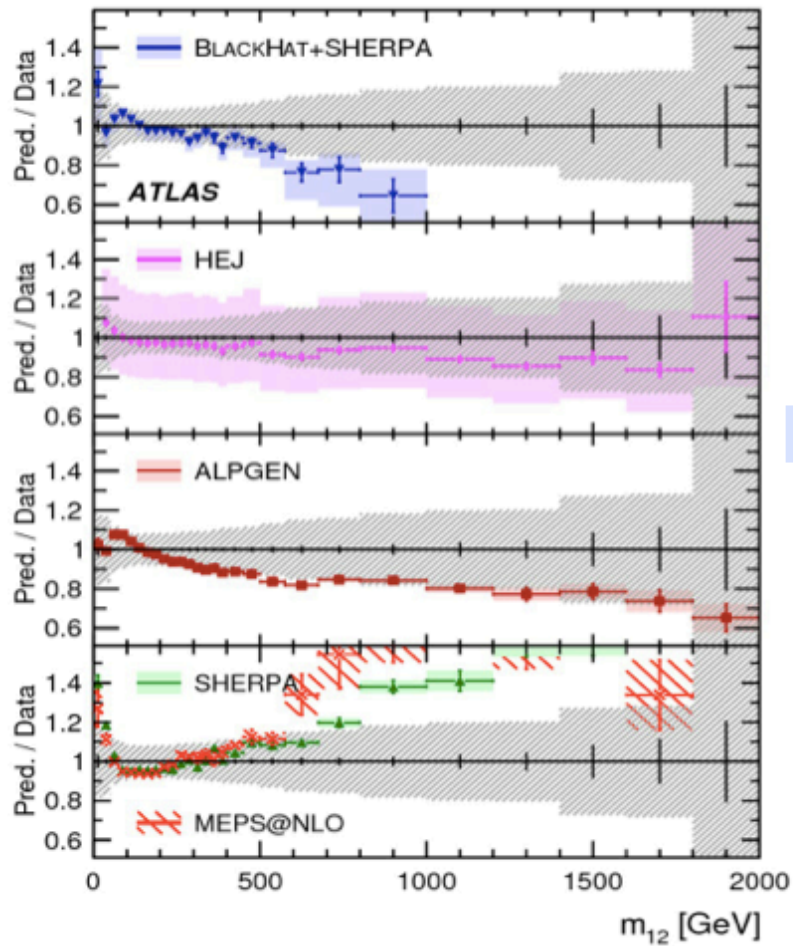
(W+jets)/(Z+jets) ratios

ATLAS, Eur. Phys. J. C (2014) 74:3168

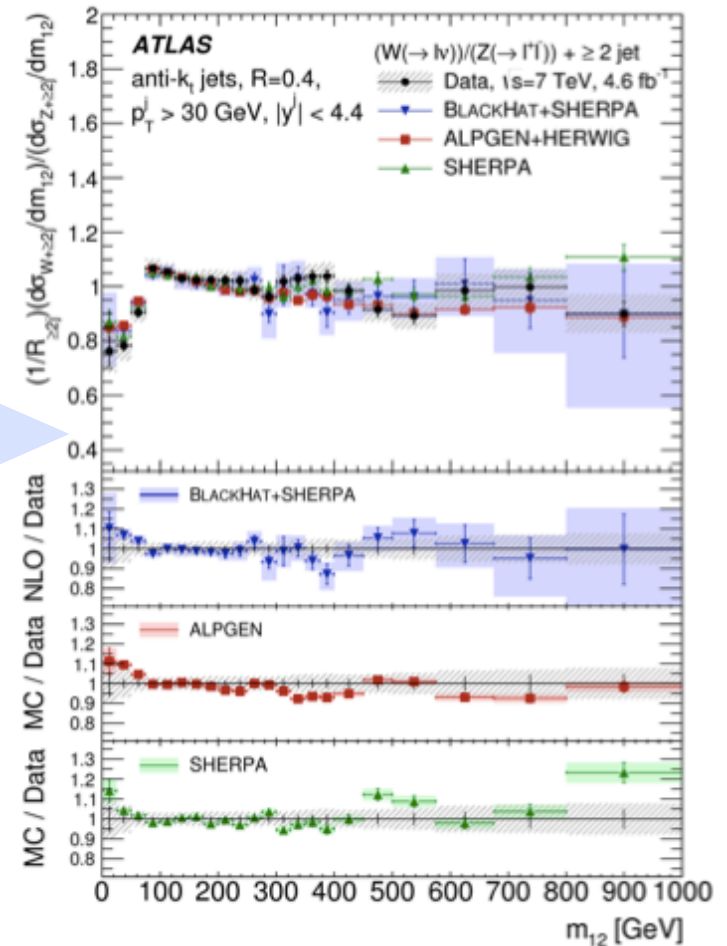


Potential for %-level precision comparisons between TH and data

W+jets



W+jets / Z+jets



Possible mis-modeling of individual processes cancels in the ratios. Ratios are more robust. Ratios can therefore be affected by BSM physics, feeding only the W or the Z channel